AN ABSTRACT OF THE DISSERTATION OF

Pamela R. Beilby for the degree of Doctor of Philosophy in Biochemistry and Biophysics presented on May 5, 2017.

Title: Oxidative Stress in Amyotrophic Lateral Sclerosis: The Role of Cellular Senescence and Glutathione.

Abstract approved:

Joseph S. Beckman

Amyotrophic lateral sclerosis (ALS) is a devastating neurological disorder characterized by neuromuscular junction decay, motor neuron death, progressive paralysis, and eventually death of the individual, usually by respiratory failure. Oxidative stress is a prominent hallmark of the disease and is often accompanied and exacerbated by mitochondrial dysfunction and neuroinflammation. This dissertation examines the role of glial cell senescence, a potential mechanism underlying oxidative stress in ALS. Microglia play a prominent role in ALS pathology. The data presented here provide the first evidence that microglia of transgenic rats bearing an ALS phenotype undergo senescence, which becomes more pronounced as the disease progresses, and is also associated with aberrant glial cell phenotypes.

The dissertation also highlights the importance of glutathione in the disease process and how alterations in glutathione metabolism eventually fail to compensate for accumulating oxidative damage. This revelation informed development of a novel glutathione derivative as a potential therapeutic for ALS and other diseases, where oxidative stress and glutathione loss combine to impair proper cellular function. The new derivative was created by altering glutathione disulfide through esterification of the carboxylic acid groups, followed by conjugation of 4-(Carboxybutyl)triphenylphosphonium bromide (TPP), a mitochondrial targeting moiety, to the amino groups. A further modification exchanged the bromide counterion for a mesylate group to enhance the water solubility of the glutathione derivative.

Finally, as a first step in the characterization of this new therapeutic, nuclear magnetic resonance (NMR) was used to study the dynamics of the derivatives in solution. Glutathione is a relatively flexible molecule in solution. This study demonstrated that the esterification of glutathione carboxylic acids and amino group coupling with TPP significantly reduce the motion of mitochondrially-targeted glutathione.

Oxidative Stress in Amyotrophic Lateral Sclerosis: The Role of Cellular Senescence and Glutathione

by

Pamela R. Beilby

A DISSERTATION

submitted to

Oregon State University

in partial fulfillment of
the requirements for the
degree of

Doctor of Philosophy

Presented May 5, 2017

Commencement June 2017

Doctor of Philosophy dissertation of Pamela R. Beilby presented on May 5, 2017.

APPROVED:

Major Professor, representing Biochemistry and Biophysics

Chair of the Department of Biochemistry and Biophysics

Dean of the Graduate School

I understand that my dissertation will become part of the permanent collection of Oregon State University libraries. My signature below authorizes release of my dissertation to any reader upon request.

Pamela R. Beilby, Author

ACKNOWLEDGEMENTS

So many people have impacted my work over the last five years. First and foremost is my advisor, Joe Beckman. It has been a privilege to work with you. Thank you for taking a huge risk and granting me an opportunity to work and learn in your lab. You have challenged and encouraged me throughout this experience, and your enthusiasm for and dedication to research are an inspiration.

To our lab manager, Nathan Lopez, without whom the lab would crumble and fall to the ground – thank you for not laughing at me when I pestered you with questions and for being patient and thorough in your explanations. I am grateful for the many times you have fixed what I have broken. When I grew frustrated with life in the lab, your cheerful sarcasm brightened the day for me.

Thank you to all the Beckman lab members who have made the laboratory an enjoyable place to conduct research: Sam Bradford, Ed Labut, Joseph Meeuwsen, and Jim Hurst. The quiet humor and helpfulness made laboratory life very pleasant. And thank you, too, to our Beckman “lab members” in Uruguay, especially Emiliano Trias, who is a gifted histologist and one of the brightest scientists I know.

I owe many thanks to friends here at OSU who have made this long journey a little bit easier: Nicole Hams, Nick Thomas, Amanda Kelley, Judy Butler, Bharath Sunchu, and Lillian Padgitt-Cobb. Thank you all for laughter and listening.

Thank you especially to my committee members, Viviana Pérez, Kathy Magnusson, Barb Taylor, and Tory Hagen, who have provided guidance and

encouragement over the years. Thank you for your investment in my education and growth as a scientist.

Many thanks to Patrick Reardon, the director of the NMR facility at OSU. I appreciate the crash course in NMR and the very valuable insight and guidance you have provided.

Finally, I would like to thank my family. You have borne the brunt of my agonies in this process. Thank you, Jared and Bianca, for the many times you have helped with childcare and child taxi services. Jenna, you have no idea how much I have appreciated you patiently listening to me ramble and rant. Your constant encouragement has delighted me and given me hope when my enthusiasm waned. Jane, thank you for all your help at home and in the lab. I have so very much enjoyed sharing this time with you. You take amazing lab notes and do a great job standing up to Joe! My dear husband, Mark, where do I start? You have offered tremendous support throughout. Uncomplainingly, you have kept things running smoothly. You have cooked meals, done laundry, and coached soccer, all while working a full-time job. You have quietly done what's needed and made me laugh when I wanted to scream. None of this would have been possible without you. Thank you, thank you. I love you all very much.

Aber die auf den Herrn hoffen, gewinnen neue Kraft: sie heben die Schwingen empor wie die Adler, sie laufen und ermatten nicht, sie gehen und ermüden nicht.
Jesaja 40, 31

Freut euch allezeit! Betet unablässig! Sagt in allem Dank! Denn dies ist der Wille Gottes in Christus Jesus für euch.
1. Thessalonicher 5, 16-18

CONTRIBUTION OF AUTHORS

Chapter 2**:** PRB, ET, LB, and JSB designed experiments. PRB, ET, RN-B, SI, CSB performed experiments. PRB, ET, LB, and JSB analyzed data and wrote the manuscript.

Chapter 3**:** PRB, TMH, and JSB designed the research. PRB performed the experiments. PRB and JSB analyzed data and wrote the manuscript.

Chapter 4**:** PRB, PNR, and JSB designed experiments. PRB and PNR performed experiments. PRB, PNR, and JSB analyzed the data. PRB and JSB wrote the manuscript.

TABLE OF CONTENTS

		Page
1	Introduction and Dissertation Overview …….....	1
	1.1 Amyotrophic Lateral Sclerosis ……..	2
	1.2 Cellular Senescence ……..	4
	1.3 Glutathione and ALS ……..	8
	1.4 Mitochondrial Targeting of Antioxidants ……..	30
	1.5 Nuclear Magnetic Resonance and Solution Dynamics …….	34
	1.6 Dissertation Contents …….	37
2	Microglial Cell Senescence in Amyotrophic Lateral Sclerosis	39
	2.1 Abstract …….	40
	2.2 Introduction ……..	42
	2.3 Materials and Methods ……..	44
	2.3.1 Animals …….	44
	2.3.2 Primary Microglia Culture ……..	44
	2.3.3 Flow Cytometry of Senescence-Associated-β-Galactosidase Activity……..	45
	2.3.4 Flow Cytometry of Cell Cycle Progression ……..	45
	2.3.5 Immunohistochemical Staining of Rat Spinal Cords …….	46
	2.3.6 Quantitative Analysis of $p16^+$, $GFAP^+/p16^+$ and $Iba1^+/p16^+$ cells in the ventral horn of the spinal cord …….	47
	2.3.7 Western Blot Analysis ……	47
	2.4 Results ……..	49
	2.4.1 $SOD1^{G93A}$ Spinal Cord Microglia Demonstrate Senescence-Associated-β-galactosidase Activity …….	49

TABLE OF CONTENTS (Continued)

Page

2.4.2 High Expression of Senescence Markers in the Spinal Cord 51
2.4.3 $SOD1^{G93A}$ Microglia and Aberrant Glial Cells Express High Levels of the Senescence Marker $p16^{INK4a}$ 52

2.5 Discussion 55

3 Design and Synthesis of Mitochondrially-Targeted Glutathione 60

3.1 Abstract 61

3.2 Introduction 62

3.3 Results and Discussion 67

3.4 Conclusion 75

3.5 Materials and Methods 76

3.5.1 Reagents 76
3.5.2 General Experimental 76
3.5.3 Syntheses 77

4 NMR characterization of mitochondrially-targeted oxidized glutathione .. 80

4.1 Abstract 81

4.2 Introduction 82

4.3 Results and Discussion 86

4.4 Conclusion 92

4.5 Experimental 93

5 Conclusion 94

TABLE OF CONTENTS (Continued)

Page

Bibliography 104

LIST OF FIGURES

Figure		Page
1.1	Glutathione synthesis …….....	9
1.2	Glutathione metabolism ……	11
1.3	SOD1 glutathione modification ……	15
1.4	Uptake of triphenylphosphonium (TPP) cations by mitochondria …..	31
1.5	Structure of glutathione choline ester (MitoGSH) …….	33
1.6	Applied magnetic field effect on spin populations …….	34
1.7	Bruker pulse program hsqct1etgpsi3D ……	36
2.1	Senescence-associated beta-galactosidase activity in $SOD1^{G93A}$ microglia ……	50
2.2	Senescence markers are highly expressed in $SOD1^{G93A}$ ALS rats during the symptomatic phase of disease ……..	52
2.3	A sub-population of aberrant glial cells and microglia express high levels of the senescence marker p16 …….	53
3.1	Synthesis of mitochondrially-targeted glutathione in its oxidized form (TPP-GSSG) ……..	65
3.2	Synthesis of mitochondrially-targeted glutathione in its reduced form (TPP-GSH) ……..	66
3.3	Meerwein's Reagent – triethyloxonium tetrafluoroborate …….	68
3.4	Mass spectrometry analysis of glutathione disulfide tetraethyl ester (Et_4GSSG) ……	70
3.5	Mass spectrometry analysis of Triphenylphosphonium glutathione disulfide tetraethyl ester dibromide ($Et_4GSSGTPP_2Br_2$) ……..	72
3.6	Mass spectrometry analysis of Triphenylphosphonium glutathione	

LIST OF FIGURES (Continued)

Figure		Page
	diethyl ester bromide (Et_2GSSGTPPBr) …….	73
4.1	Uptake of triphenylphosphonium (TPP) cations by mitochondria …..	83
4.2	Glutathione derivatives ……..	86
4.3	Dependence of carbon relaxation rate on delay time for glutamate residue of GSSG, Et_4GSSG, and Et_4GSSGTPP_2Mes …….	88
4.4	Dependence of carbon relaxation rate on delay time for cysteine and glycine residues of GSSG, Et_4GSSG, and Et_4GSSGTPP_2Mes ……..	89
5.1	Relationship between glutathione, oxidative stress and cellular senescence …….	103

LIST OF TABLES

Table Page

4.1 Carbon spin-lattice relaxation times, T_1 (s), for GSSG, Et_4GSSG, and $Et_4GSSGTPP_2Mes$ in PBS, pH 7.4, 10 % D_2O …….. 90

Oxidative Stress in Amyotrophic Lateral Sclerosis: The Role of Cellular Senescence and Glutathione

Chapter 1

Introduction and Thesis Overview

1.1 Amyotrophic Lateral Sclerosis

Amyotrophic lateral sclerosis (ALS) was first described by that name in the scientific literature in the late nineteenth century by Jean-Martin Charcot [2]. ALS, also known as Lou Gehrig's disease in the United States, is an age-related, relentlessly progressive neurodegenerative disease leading to the death of motor neurons of the brain and spinal cord. Onset typically occurs between the ages of 50 and 70, although most cases appear when the patient is over 60. ALS has been designated an orphan disease, with an incidence rate of approximately 1.89 per 100,000/year, and prevalence recorded at 5.2 per 100,000/year [3].

The majority of cases are sporadic in nature with unknown etiology (sALS). Less than 10% of cases have a familial inheritance as the basis of disease (fALS). In 1993, the first genetic mutation associated with ALS disease pathogenesis was discovered - the G93A mutation to the gene coding for superoxide dismutase-1 (SOD1) [4]. Since then, more than 150 mutations to this gene have been identified, accounting for approximately 20% of all fALS cases (2-5% of all cases). Several other proteins with missense mutations have also been found, including the TAR DNA-binding protein 43 (TDP-43), Fused in Sarcoma (FUS), optineurin, and dynactin [5-8].

Outside of genetic inheritance, many mechanisms have been identified as having a role in the disease process. Spinal cord mitochondria exhibit morphological abnormalities early in the ALS disease process [9], and mitochondrial dysfunction alters calcium buffering, fusion/fission processes, and

energy metabolism, leading to motor neuron death [10-15]. Endoplasmic reticulum (ER) stress also exhibits a pronounced role early in pathogenesis, enhancing motor neuron vulnerability [16, 17]. Neuromuscular junction decay leads to muscular denervation, typically preceding symptom onset and neuronal loss [9, 18]. Abundant evidence also testifies to the involvement of glial cell toxicity in ALS [19-23].

Oxidative stress is a fundamental component of ALS disease pathology and is a common underlying theme present with most other mechanisms. In comparison with healthy controls, elevated oxidative stress has been observed in ALS patients as increased protein tyrosine nitration [24], higher levels of oxidized DNA, as measured by 8-hydroxy-2´-deoxyguanosine [25], and increased 4-hydroxynonenal, as a marker of lipid peroxidation [26]. Transgenic rodent and cell culture models have also indicated a direct link between oxidative stress and motor neuron death [27-29], as well as demonstrated oxidative damage to neurons mediated through astrocytes and microglia [19, 23, 30, 31].

Reactive oxygen species (ROS), such as superoxide ($O_2^{\bullet -}$), hydrogen peroxide (H_2O_2), and nitric oxide ($^{\bullet}NO$), are constantly generated within the cell, as signaling molecules or byproducts of metabolism. Superoxide and nitric oxide combine quickly in a diffusion-limited reaction, creating peroxynitrite ($ONOO^-$) [32]. In pathological states, generation of reactive oxygen species increases. Thus, if rates of creation of $^{\bullet}NO$ and $O_2^{\bullet -}$ each increase a hundredfold, the rate of formation of peroxynitrite increases ten thousandfold.

1.2 Cellular senescence

Levels of oxidative stress increase with age, and the accompanying changes alter basal function of many cellular mechanisms. In 1961 Hayflick and Moorhead first described cellular senescence as a cessation of the replicative life cycle of a normal cell after multiple population doublings. It was postulated that these changes leading to growth arrest were indicative of changes due to aging of the organism [33]. Additionally, cellular senescence might serve as a cancer-suppressing mechanism *in vivo*. Since then, many advances have been made in understanding fundamental features of the function of senescence, which is often observed in contrary roles, restricting cell growth in some cells and fostering proliferation in others. For example, we now know that senescence suppresses cancer development, but unrestricted accumulation of senescent cells can contribute in other circumstances to tumorigenesis [34]. Factors involved in the induction of senescence include telomere dysfunction, DNA damage, oncogene activation, and oxidative stress [35].

Recently, researchers have discovered evidence of enhanced accumulation of senescent cells in tissues of aging primates and rodents [36, 37]. Cellular senescence also appears to have an increasing role in many age-related pathologies in addition to cancer [38]. Pancreatic β-cell senescence contributes to type II diabetes - researchers observed that beta cells in mice fed a high-fat diet demonstrate increasingly higher levels of senescence markers [39]. Senescent osteoblasts, through creation of a proinflammatory bone microenvironment,

promote the development of osteoporosis [40]. Muscle stem cell senescence has been shown to be a contributing factor in sarcopenia, and inactivation of p16 [41] or inhibition of the p38 pathway [42, 43] restored muscle regenerative potential.

Within the field of cellular senescence, relatively little is understood about the contribution of senescent cells to neurodegenerative diseases. Glial cell senescence has been proposed as having a role in Parkinson's disease, but that has yet to be fully studied [44]. One recent study evaluated astrocyte senescence in Alzheimer's disease (AD) [45]. They discovered that beta-amyloid peptides induced senescence in human astrocytes, as determined by senescence-associated beta-galactosidase (SA-βgal) and $p16^{INK4a}$ expression. Additionally, they found increased populations of senescent astrocytes in the brains of autopsied older patients and those having AD. Senescence markers were accompanied by astrocytic production of a robust senescence-associated secretory phenotype (SASP). The SASP is a complex, cell- and context-dependent mixture of inflammatory cytokines and chemokines, extracellular matrix-altering proteins, and growth factors. These secreted proteins can be beneficial, i.e., stimulating tissue repair and relaying damage signals [46]. But the SASP also may cause damage when chronically present or persistent by disrupting tissue structure and stimulating growth of undesired cell populations [47]. A core set of conserved SASP proteins exists, but the characteristic SASP of glial cells remains to be determined.

Neuroinflammation underlies many age-related neurodegenerative disorders, including ALS. Inflammation is maintained by prolonged production of proinflammatory factors at an elevated level. The cause of increased inflammation with age is still not totally clear. Recent evidence incriminates cellular senescence as a contributor to chronic inflammation, primarily through production of the SASP. Many SASP proteins (e.g., IL-6, IL-8, granulocyte macrophage colony stimulating factor (GM-CSF), and multiple monocyte chemotactic proteins) stimulate inflammation [48]. Neuroinflammation in ALS involves activated microglia and astrocytes that are instrumental in the death of motor neurons, yet glial cell senescence remains essentially unexplored this disease. Increased knowledge of glial cell senescence in ALS will assist in providing understanding of the impact of these cells in the disease process and provide a potential solution to the mystery of unidentified secreted toxic proteins, as well as reveal a prospective therapeutic target.

Age, along with the accompanying changes that accrue, is a fundamental concern when studying many degenerative diseases. Advancing age leads to the accumulation of senescent cells [49]. Age is a risk factor for ALS and it is known that over time glial cells experience a negative transformation from neuroprotective to neurodestructive behavior in ALS. Our lab has cultivated and depicted the toxic glial cell type known as aberrant glial cells. These aberrant cells are microglia isolated from adult symptomatic $SOD1^{G93A}$ rats. After ten days *in vitro*, these microglia begin to transition to a cell expressing an astrocyte-like phenotype and

begin rapidly proliferating. This rapid disease progression is paralleled *in vivo*. Unlike G93A mice, which become symptomatic around 90-100 days and slowly deteriorate over the course of weeks, the $SOD1^{G93A}$ rats become symptomatic at approximately 120-125 days and then die in less than a week. Although aberrant glial cells cannot be cultured from age-matched $SOD1^{WT}$ or non-transgenic rats, we serendipitously discovered that cells with a similar phenotype grow and transform when harvested from *old* (age > 1 year) wild-type or non-transgenic animals. This pointed to the aging process itself as playing a role in driving this phenotype development. In particular, it suggested that glial cell senescence and the accompanying senescence-associated phentoype fuel this transformation.

1.3 Glutathione and ALS

1.3.1 Introduction

Glutathione (GSH), the most abundant intracellular non-protein thiol and cellular antioxidant, is found in most mammalian cell types. In 1888, Joseph de Rey-Pailhade discovered a compound in yeast that reacted with elemental sulfur and generated hydrogen sulfide, and he called this new compound “philothion” [50]. Sir Frederick G. Hopkins, was a British biochemist, who shared a Nobel Prize with Christiaan Eijkman for the discovery of vitamins. In 1921, he described a compound, which he considered a dipeptide containing glutamate and cysteine. Based on its reactive properties, he concluded that this was the same compound discovered by de Rey-Pailhade. He selected the name glutathione because of its glutamate residue and the historic connection to philothion [50]. GSH plays a critical role in many aspects of the healthy function of the cell, including detoxification of xenobiotics, maintenance of intracellular oxidation-reduction balance, and cysteine storage/transport.

Glutathione is produced in a two-step synthesis mediated by ATP and catalyzed by γ-glutamylcysteine ligase (GCL), followed by the incorporation of glycine by GSH synthase (Figure 1.1) [51-53]. The GCL heterodimer consists of a 73-kDa catalytic subunit (GCLC) and a 28-kDa regulatory subunit (GCLM). Cytosolic concentrations of glutathione are generally present in millimolar amounts, but this varies from organ to organ, with liver typically maintaining the highest levels, at 5-10 mM. Within the central nervous system (CNS), glutathione

levels tend to be lower. In the cerebrospinal fluid (CSF), for example, GSH exists in μM concentrations [54]. In the brain itself, concentrations differ somewhat depending on region, with levels usually around 2-3mM [55]. Glial cells contain greater amounts of glutathione than do neurons, with astrocytes and oligodendrocytes having approximately equal levels, but both lower than microglia [56, 57]. In addition to the cytosol, three organelles maintain their own pool of glutathione: the nucleus, endoplasmic reticulum, and mitochondria [58-62].

The redox potential for glutathione oxidation/reduction couple (GSH/GSSG), E_h, is defined as: $E_h = E_o + (RT/NF)\ln([GSSG]/[GSH]^2)$. The square of the GSH concentration suggests that the absolute concentration of GSH must be taken into account when examining the redox state, not just relying on an estimation of the GSH/GSSG ratio [63]. The glutathione redox couple exists in a non-equilibrium steady condition, i.e, it is not at equilibrium with other redox couples and the glutathione redox potentials vary among intracellular compartments, such as mitochondria or the nucleus [64, 65].

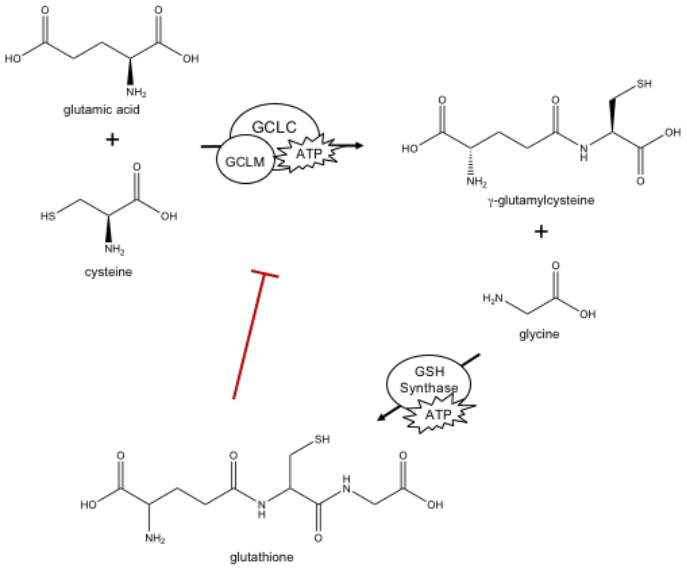

Figure 1.1. Glutathione Synthesis. The tripeptide glutathione is formed in the two-step, ATP-catalyzed process. Glutamate-cysteine ligase (GCL), composed of a catalytic (GCLC) and regulatory (GCLM) subunit, incorporates the condensation of glutamic acid and cysteine in a γ-glutamyl linkage. In the last step, glutathione synthase joins glycine to γ-glutamylcysteine, forming glutathione. Increasing levels of glutathione inhibit GCL activity.

Glutathione levels and the functioning of glutathione-dependent enzymes decline with age humans, other primates, and rodents [66-68], as well as in many pathologies, including Parkinson's disease, multiple sclerosis, chronic kidney disease, Huntington's disease, Alzheimer's disease, cystic fibrosis, diabetes, schizophrenia, and ALS [69-83], critically diminishing the cell's ability to respond to oxidative insults. This complex system utilizes glutathione as a stand-alone defense in response to redox imbalance. It also employs GSH as a co-factor or substrate in enzymatic oxidative stress countermeasures (Figure 1.2). This review summarizes current understanding of the complex role of the glutathione antioxidant system in ALS.

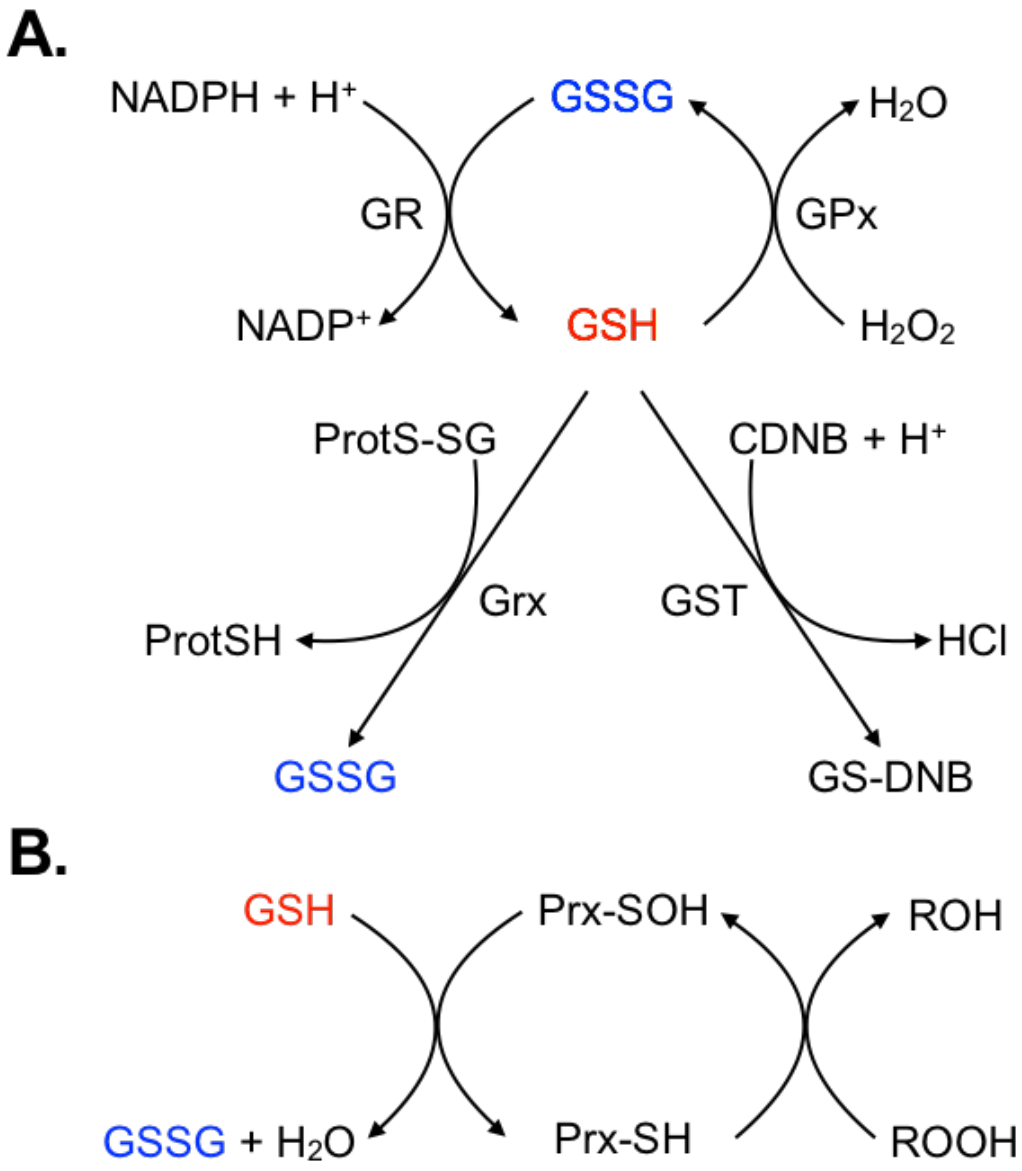

Figure 1.2 Glutathione metabolism. Glutathione serves as a substrate or co-factor for several antioxidant enzymes. A. Glutathione interaction mechanisms with glutathione reductase (GR), glutathione peroxidase (GPx), glutaredoxin (Grx), and glutathione S-transferase. B. Glutathione interaction with peroxiredoxin.

1.3.2 Glutathione Levels in ALS

In ALS patient erythrocytes, glutathione levels were significantly less than healthy controls, with a growing decline as disease duration progressed from 6-24

months [76]. Likewise, serum GSH levels of ALS patients from samples drawn at two separate times, 6 months apart, revealed a severe reduction compared to controls at both times [79]. Magnetic resonance spectroscopy imaging of the motor cortex in ALS patients and age-matched healthy controls examined for the first time *in vivo* GSH levels and disclosed a 31% lower level of glutathione in ALS patients [78].

Decreased delivery of synthesis substrates and enzymes necessary to produce glutathione can result in a decline in glutathione levels. When examining GSH synthesis and enzymatic K_m values and substrate concentrations in the central nervous system, cysteine is considered to be the rate-limiting reagent [55]. In an NSC-34 cell culture model, cells expressing $SOD1^{G93A}$ demonstrated a 56% reduction in cysteine levels versus untransfected cells. Glycine and glutamate levels were elevated, glutamate significantly [84].

The transcription factor, nuclear factor erythroid 2-related factor (Nrf2) is encoded by the *NFE2L2* gene and regulates cellular response to oxidative stress through interactions with the antioxidant response element (ARE) binding site. Nrf2 protein levels decrease with age, weakening the ability of the cell to respond to stressors and attenuating the expression of ARE-associated genes [85]. One of the approximately 200 Nrf2-ARE-controlled genes is GCL.

Diminished activity of either GCL subunit erodes glutathione stores, leading subsequently to neuronal death [86]. Two enzymes are involved in GSH synthesis (see Fig. 1.1), with GCL being the rate-controlling step in the process. GCL

expression is regulated at several levels in response to the redox environment of the cell, including feedback inhibition by glutathione itself and increased activation of nuclear factor erythroid 2-related factor (Nrf2) [87, 88].

In ALS, decreased activity of GCL is observed. In a conditional fALS model, long-term exposure to high levels of mutant SOD1 engendered a reduction in activity of the regulatory subunit of GCL and a 30% drop in GSH levels [89]. In primary motor neuron cultures derived from high-expressing $SOD1^{G93A}$ transgenic mice, mRNA expression levels for both GCL subunits were significantly reduced compared to non-transgenic controls [27]. To examine the effects of further diminution of glutathione levels on disease progression in the $SOD1^{G93A}$ mouse model, a double transgenic model was created, incorporating a knockout of the regulatory subunit of GCL (a KO of the GCLC is lethal). This model demonstrated a remarkable acceleration of the disease process and significant decline in antioxidant defense: 70-80% drop in GSH levels in the CNS. Remarkably, spinal cord mitochondrial GSH levels also declined by 80%. This resulted in a 55% reduction in the lifespan of these animals compared with controls [77].

Decreased activity of synthesis enzymes and reduction in synthesis substrates results in altered glutathione levels in ALS, impacting motor neuron health. Several animal and cell culture models testify to the concomitant decrease in GSH levels with increasing symptom progression. Accumulation of TAR DNA-binding protein 43 (TDP-43) is a pathological hallmark of TDP-43 proteinopathies, including frontotemporal lobar degeneration with ubiquitinated inclusions (FTLD-

TDP) and ALS [90]. Under pathological conditions, TDP-43 distributes to the cytoplasm and aggregates composed of phosphorylated C-terminal fragments develop.

Ethacrynic acid depletes cellular glutathione levels through direct conjugation to GSH mediated by glutathione S-transferase [91]. In NSC34 cells and mouse primary cortical neurons, depletion of glutathione initialized by treatment with ethacrynic acid led to C-terminal phosphorylation of TDP-43, insolubilization, and TDP-43 distribution to the cytosol [92]. GSH depletion induced by ethacrynic acid treatment also promotes motor neuron apoptosis [93].

Decreased glutathione in neurons isolated from $SOD1^{G93A}$ mice renders these neurons vulnerable to p75 neurotrophin receptor-mediated apoptosis, but increasing GSH forestalls death [27]. Astrocytes isolated from $SOD1^{G93A}$ rats are toxic to motor neurons, but increasing GSH levels by activation of Nrf2 counters this harmful effect and fosters neuronal survival [94]. Similarly, treatment of astrocytes from ALS rats with nitro-fatty acids prevented neuron death again by boosting overall GSH levels through activation of Nrf2 [95]. Animal models reflect a similar trend. In spinal cords from mice overexpressing $SOD1^{G93A}$, GSH levels were increasingly reduced as disease progressed, while GSSG levels rose significantly, generating a precarious redox imbalance [93].

1.3.3 Glutathionylation

Glutathione can also interact as a reversible form of post-translational modification of protein cysteine residues, particularly when the local redox environment is altered during conditions of oxidative stress [96]. This occurs spontaneously, but also can be catalyzed by glutaredoxin or glutathione S-transferase, with the reverse reaction catalyzed by glutaredoxin or thioredoxin. A study by Wilcox, *et al.*, in 2009 showed that glutathionylation of SOD1 occurs at C111 in human erythrocytes from healthy subjects, destabilizing the dimer interface, and they postulated that glutathionylation might contribute to protein aggregation (Figure 1.3) [97]. They found that glutathionylated SOD1 has a greater tendency to form monomers, thereby increasing the likelihood of developing SOD1 aggregates [97].

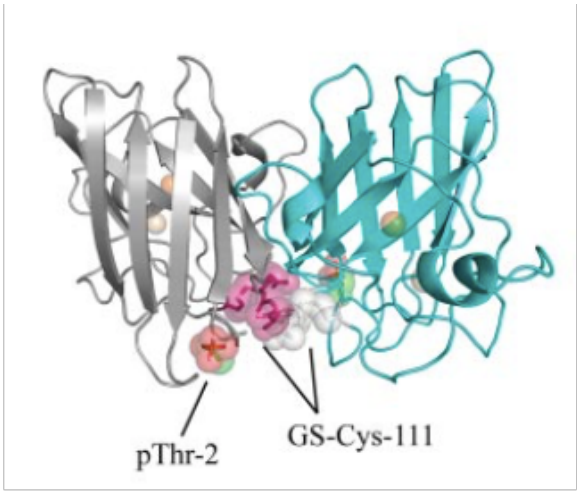

Figure 1.3. SOD1 glutathione modification. Cys111 glutathionylation modeled at the homodimer interface [97].

Previous studies in erythrocytes from fALS patients had also shown glutathione adducts to SOD1, but not the site of glutathionylation, although C111 was a suggested as a possible residue [98, 99]. Investigations of yeast- and bacteria-purified SOD1, both wild-type and several mutants have revealed evidence of glutathionylation at C111, and that this modification leads to dimer destabilization and contributes to pathological SOD1 aggregation [100-103]. Our

mass spectrometry analysis of $SOD1^{G93A}$ mouse tissue, including that from spinal cord, brain, kidney, and liver indicated little or no glutathione modifications to SOD1 [104]. However, it is readily detected in tissue treated with diamide [104]. In astrocytes from $SOD1^{G93A}$ mice, post-translational glutathione modification of the stromal interaction molecule 1 (STIM1), a calcium sensor localized to the endoplasmic reticulum, was observed [105]. This STIM1 glutathionylation was hypothesized to be responsible for ER calcium overload in SOD^{G93A} astrocytes [105].

1.3.4 Enzymatic reactions requiring glutathione

Glutathione reductase (GR)

Many of the antioxidant roles of glutathione result in the oxidation to the disulfide form of the peptide. The flavoenzyme, glutathione reductase, catalyzes the reduction of GSSG, utilizing NADPH as co-factor:

$$GSSG + NADPH + H^+ \rightarrow NADP^+ + 2GSH$$

The GR crystal structure has been well studied [106, 107]. Its catalytic cycle proceeds through several steps: NADPH binding, FAD reduction, Cys58 - Cys63 disulfide reduction, GSSG binding and formation of mixed disulfide with Cys58 and release of one GSH, and Cys63 attack on Cys58 releasing second GSH [106]. GR plays a vital role in the maintenance reduced glutathione levels in the cell, and at least two isoforms exist in humans, one directed to the cytoplasm and one to mitochondria [108, 109].

In the context of ALS, glutathione reductase has primarily been examined as marker of disease, and there is not a clear consensus on how GR activity levels are affected during the disease. One study revealed no difference compared with healthy controls [110], one showed significantly reduced GR activity levels [76], and one demonstrated elevated activities [111]. All studies analyzed GR activity levels in erythrocytes. Two groups used sALS patients, and the group showing higher GR activity which used a combination of fALS and sALS. Each group used slightly different methods for measuring GR activity which may also have contributed to the lack of agreement on GR levels in ALS patients versus controls.

Glutathione S-transferase (GST)

GSTs represent a complex and diverse group of enzymes, consisting of seven distinct classes of soluble isoforms in mammals: alpha, zeta, theta, mu, pi, sigma, and omega [112]. They catalyze the conjugation of GSH to electrophilic substrates, frequently for removal of xenobiotics from the cell, but also participate in other activities such as post-translational modifications to proteins and elimination of cellular oxidants [113]. A simplified reaction mechanism is shown below, using a typical GST model substrate (described in [114]), 1-Chloro-2,4-dinitrobenzene (CDNB):

$$CDNB + GSH + H^{+} \rightarrow GS\text{-}DNB + HCl$$

GST binds GSH, which is then deprotonated, followed by CDNB binding and thiolate attack and conjugation, chlorine elimination, and finally production of GS-DNB [112].

A handful of studies have looked at the role of GSTs in ALS. DNA from blood samples from Caucasian fALS patients from Sweden, Great Britain, and Australia were examined for polymorphisms in the genes for GST-omega 1 and 2 (GSTO1 and GSTO2) to determine if there was any association between these and age of disease onset or survival [115]. They found no association between sequence variation and survival in any of the three groups, none for the British and Australian group for age of onset, and only a weak association in the Swedish group between single nucleotide polymorphisms (SNPs) for either gene and age of onset. They concluded, however, that this association could only be suggestive at this point without further study and larger sample sizes [115].

Others evaluated GST-pi (GSTP) activity and expression. GSTP RNA extracted from formalin-fixed spinal cord and sensory and motor brain cortex tissue of ALS patients was compared to that age-matched controls without evidence of neurodegenerative disease and was found to be significantly lower and was supported by decreased protein levels observed in Western blotting [116]. Cerebrospinal fluid (CSF), blood serum, and peripheral blood mononuclear cells (PMBCs) of ALS patients, in contrast to healthy controls, exhibited a significantly lower GSTP activity and decreased mRNA and protein expression levels only in the PMBCs, but not CSF or blood [117]. A follow-up study to these examined *GSTP1* polymorphisms in ALS and found that the A114V but not I105V polymorphism was indicative of increased risk for motor neuron disease [118].

GSH peroxidase (GPx)

Glutathione peroxidases are ubiquitous in the cell, with the GPx1 isozyme being the most common and found in almost all tissues. GPx reduces hydrogen peroxide and lipid peroxides to water and lipid alcohols:

$$2GSH + H_2O_2 \rightarrow GSSG + 2H_2O$$
$$2GSH + ROOH \rightarrow GSSG + ROH + H_2O$$

These enzymes typically have either a cysteine or selenocysteine at the active site. The mechanism proceeds with oxidation of the selenocysteine residue by hydrogen peroxide, followed by two GSH-mediated reductive steps to regenerate the selenocysteine residue [112]. In addition to the dependence on glutathione, GPx levels are known to decline with age [119, 120]. Because age is a risk factor for ALS, GPx has become an irresistible focus of inquiry in the elucidation of ALS disease mechanisms.

Many studies have reported no difference in GPx activity in either spinal cord tissue homogenates or blood samples from ALS patients (without treatment) versus controls [76, 121-123]. Erythrocyte samples from patients harboring the D90A mutation to SOD1 also demonstrated no difference in GPx activity [124]. However, samples from brain tissue exhibited significantly reduced GPx activity in ALS patients compared to controls [125]. In an examination of erythrocyte antioxidant enzyme function in sALS and fALS patients, GPx activity was decreased only in fALS patients bearing the Leu144Phe mutation to SOD1 [111]. Decreased astrocytic support to motor neurons was also observed in the $SOD1^{G93A}$ mouse model in decreased GPx transcript expression [126]. A recent

study observed that serum GPx activity was significantly reduced in sALS patients compared to controls and remained so during disease progression, with a further decline seen in patients with a more rapid disease progression rate [110]. An analysis of differentially expressed proteins in serum from healthy controls, patients with Alzheimer's disease, Parkinson's disease, muscular dystrophy, ALS, and $SOD1^{H46R}$ symptomatic rats revealed GPx3 protein levels to be significantly lower in sera from ALS patients and the $SOD1^{H46R}$ rats [127].

GPx4 is an inhibitor of a specific type of iron-dependent cell death known as ferroptosis [128], which has been linked to ALS and other forms of neurodegeneration [129, 130]. Ferroptosis is a type of iron-dependent, non-apoptotic cell death characterized by the accumulation of lipid-based reactive oxidative species [131]. Attempts to alter GPx activity and expression have had mixed results. Overexpression of GPx4 in motor neuron-like NSC-34 cells transfected with $SOD1^{G93A}$ reduced mutant SOD1-mediated cell death [132]. On the other hand, $SOD1^{G93A}$ mice crossed with mice overexpressing GPx four-fold in the brain or mice with targeted reduction of brain GPx activity demonstrated no difference in disease onset, progression, or survival compared with the transgenic $SOD1^{G93A}$ mouse model [133]. But, this effect may be due to the GPx isozyme selected. In a recent investigation, creation of a *GPx4* neuronal inducible knockout mouse demonstrated, upon Tamoxifen treatment, development of rapid paralysis and spinal cord motor neuron degeneration [134].

Glutatredoxin, Thioredoxin, and Peroxiredoxin (Grx, Trx, Prx)

Members of the thioredoxin superfamily, the small (around 100 amino acid residues), abundant, and manifold glutatredoxins and thioredoxins are responsible for the reduction of intracellular disulfides, including reversal of glutathionylation [135]. This is shown for Grx below:

$$\text{ProteinS-SG} + \text{GSH} \rightarrow \text{ProteinSH} + \text{GSSG}$$

Glutathione supplies electrons to Grx, which then catalyzes disulfide reduction, either through a monothiol or dithiol pathway for glutathionylated proteins or protein disulfides, respectively [112, 136]. GSSG is then recovered by NADPH and glutathione reductase. The Trx mechanism does not rely on GSH for reducing power, but rather on NADPH-dependent interaction with Trx reductase [137]. It is discussed here, not only due to its similarities with Grx, but also because thioredoxins play a vital role in maintenance of appropriate cellular sulfhydryl and disulfide levels, and thus are intimately connected with the glutathione antioxidant system.

Peroxiredoxins are critical to the cellular antioxidant defense system. They can influence circadian rhythm, and while the circadian clock regulates the cellular redox state, the reverse may also be true [138]. Reversible hyperoxidation of Prx3 participates in a signaling pathway mediating circadian fluctuations in cortisone levels [139]. Peroxiredoxins can activate an inflammatory response by behaving as pathogen-associated molecular patterns (PAMPs) and damage-associated molecular patterns (DAMPs) (reviewed in [140]). Importantly for this review,

peroxiredoxins exhibit peroxidase activity leading to the reduction and detoxification of hydroperoxides and peroxynitrite [141], catalyzing the following reaction:

$$ROOH + 2e^- \rightarrow ROH + H_2O$$

A peroxide binds the cysteine-bearing active site and is attacked by the cysteine, forming a sulfenic acid and water or alcohol [142, 143]. Regeneration of the thiol may occur through Trx, GSH, or ascorbate, depending on the Prx enzyme class [112, 142].

Although these enzymes are critical to cellular success in maintaining a healthy redox environment, not much is known about the roles of these enzymes in the ALS disease process. Lentiviral delivery Prx3 to NSC-34 cells expressing $SOD1^{G93A}$ increased cell survival 27% and decreased oxidative stress levels 42% as measured by the dichlorofluorescein assay [144]. Unfortunately, *in vivo* delivery with an adeno-associated virus type 6 to $SOD1^{G93A}$ mice provided no delay in disease onset, amelioration of disease progression, or increase in survival [144]. One study examined mRNA expression levels in postmortem spinal cord tissue from ALS patients and age-matched controls, and found that Trx expression was elevated 600% over controls, which the authors considered a response to increased oxidative stress [145]. An *in vitro* investigation in NSC-34 cells demonstrated that overexpression of Grx2 reduced mutant SOD1 aggregation formation in mitochondria and prevented mitochondrial fragmentation and cell death induced by mutant SOD1 [146]. A recent set of experiments using

recombinant SOD1, either WT or with the G93A or A4V mutations, showed that the oxidized mutant forms of SOD1 were very susceptible to reduction by the Trx and Grx systems, while the WT protein was not [147]. Additionally, they noted that in schwannoma cells expressing GFP-tagged versions of each of the three proteins, inhibition of the Trx and Grx systems resulted in a significant increase in aggregation of mutant SOD1 in cells expressing A4V and G93A proteins [147]. This recent research provides some more tantalizing evidence of the potential role of thioredoxins and glutatredoxins in ALS, but a great deal remains to be learned about these enzymes, as well as peroxiredoxin, and their impact on the disease process.

1.3.5 Glutathione and copper homeostasis

Copper is an essential transition metal and is an important cofactor for catalysis in many enzymes. In ALS, many copper-containing proteins are involved in the disease process. Genetic mutations to Cu,Zn-superoxide dismutase 1 (SOD1) frequently are associated with ALS, and mice bearing mutations to SOD1 frequently encounter perturbations in copper homeostasis [148-150]. As disease progressed, spinal cord levels of copper-trafficking proteins, Atox1, CCS (the copper chaperone for SOD1), and Cox17 (copper chaperone for cytochrome *c* oxidase) all increased in correspondence with increased copper in the cell [149]. Expression levels of the copper efflux pump, ATP7A, are decreased in ALS models [151], enhancing copper accumulation in the cell. Overexpression of CCS in mice

with mutant SOD1 leads to severe mitochondrial pathology and dramatic acceleration of the disease, decreasing survival by 85% [152]. Treatment of these mice with the copper complex, Diacetyl-bis(4-methylthiosemicarbazonato) copper (II) [CuATSM], increases survival an average of 18 months [28]. The increase in survival is unprecedented. In 25 years, no one had been able to extend survival of these mice by even a month.

Glutathione plays an important role in copper homeostasis. Chaperone-mediated delivery of copper to SOD1 is performed by the copper chaperone for SOD1 (CCS). In the absence of CCS, copper is delivered by glutathione [153]. Glutathione depletion results in downregulation of the copper transporter, CTR1 [154]. Glutathione regulates the ability of Atox1 to bind copper through redox modification of Atox1 thiols [155, 156]. It has been proposed that glutathione binds copper from the Ctr1 transporter and delivers it to cellular copper chaperones, such as ATP7A and CCS [157]. Despite glutathione's prominent role in copper homeostasis, this relationship continues to offer opportunities for exploration, particularly with regard to glutathione metabolism and copper handling in ALS.

1.3.6 Glutathione-related therapies in ALS

Many attempts have been made in animal models and human clinical trials to impact the ALS disease process by raising levels of glutathione. Intramuscular delivery of 600mg GSH/day for 12 weeks in a random, crossover trial demonstrated no significant effect in disease progression [158]. Over 30 years

ago, Alton Meister described the development of glutathione esters, which were designed to enhance cellular GSH levels as the esterification facilitates compound uptake by the cell [159]. In a rat model of motor neuron degeneration caused by chronic α-amino-3-hydroxy-5-methyl-4-isoxazole propionate (AMPA) infusion, glutathione ethyl ester failed to prevent motor deficits or protect spinal motor neurons [160]. Likewise, a random, double-blind trial of *N*-acetylcysteine (NAC), a cysteine prodrug, at 50mg/kg/day subcutaneously for 12 months in ALS patients saw no significant increase in survival or mitigation of disease progression compared with healthy controls [161]. SH-SY5Y cells transfected with $SOD1^{G93A}$ cell saw an improvement in mitochondrial function, as measured by the 3-(4,5-dimethylthiazol-2-yl)-2,5-diphenyltetrazolimium (MTT) assay, after 24-hour exposure to 1mM NAC [162]. High-expressing $SOD1^{G93A}$ mice treated with 1% NAC in drinking water (approximately 2mg/kg/day) starting at 4-5 weeks, experienced a nine-day extension of life and slight preservation of rotarod performance [163]. Cystine, a cysteine precursor, has also been investigated. High-expressing $SOD1^{G93A}$ mice were fed a cystine-rich whey supplement (3.3% solution in drinking water) starting at day 60. The supplement maintained erythrocyte and spinal cord tissue GSH levels, comparable to that seen in non-transgenic controls, and delayed disease onset, but did not extend survival [164].

In addition to trying to boost GSH levels through direct administration of glutathione or precursors, attempts have also addressed activation of the Nrf2/ARE pathway. Two triterpenoids, 2-cyano-3,12-dioxooleana-1,9-dien-28-oic

acid (CDDO) ethylamide and CDDO trifluoroethylamide (CDDO-TFEA) were tested in both NSC-34 cells expressing $SOD1^{G93A}$ and $SOD1^{G93A}$ mice. The researchers found that Nrf2 was activated in both cell culture and in the spinal cord, and an upregulation in antioxidant gene expression was observed, including levels of glutathione reductase and GST [165]. When treatment began at 30 days, survival was extended 20 days for CDDO-EA and 17.6 days for CDDO-TFEA, while treatment started at symptom onset (approximately 85 days) increased survival only slightly less, 17 and 16 days, respectively, for CDDO-EA and CDDO-TFEA [165]. Another investigation employed an acylaminoimidazole derivative, 2- [mesityl(methyl)amino]-N-[4-(pyridin-2-yl)-1H-imidazol-2-yl] acetamide trihydrochloride (WN1316) to address oxidative stress in ALS [166]. In SH-SY5Y cells, WN1316 activated Nrf2 and increased GSH levels. WN1316, administered at symptom onset in $SOD1^{H46R}$ mice, slowed disease progression, suppressed oxidative damage and glial cell inflammation, reduced spinal cord motor neuron loss, and extended survival 7-10 days in a dose-dependent manner (1μg/kg, 10μg/kg, 100μg/kg) [166]. This same group, in a drug screen for oxidative stress-induced apoptosis inhibitors, also discovered bromocriptine methylate (BRC), a dopamine D2 receptor agonist, which demonstrated a similar level of protection as seen with WN1316, albeit at higher dosage levels (1mg/kg, 10mg/kg, 100mg/kg) and with a 5-day extension in survival [167]. A recent clinical trial using riluzole and BRC or riluzole and placebo in Japanese ALS patients found only marginal efficacy of BRC treatment versus the placebo [168].

Another candidate for treatment of ALS is the combination of lithium carbonate and valproic acid (Li+VA) [169]. The ALS functional rating scale, revised version (ALSFRS-R) was determined at the start, measured at 1 month, and then every 4 months until death or other adverse event. Encouragingly, ALSFRS-R scores were maintained for the 21 months of the trial. The progression rate measured at baseline was 0.499, but after 17 months of treatment was 0.325. When matched by age, gender, and disease progression, the survival of those taking Li+VA was significantly higher than controls [169]. After six months of treatment, the Li+VA group also demonstrated increased levels of antioxidant defense, including higher levels of GSH, and glutathione peroxidase and SOD1 activity, although the authors could not conclude definitively if this recovery of the antioxidant protection was responsible for success achieved [169].

1.3.7 Therapeutic directions with glutathione

Therapies that raise glutathione levels have met with mixed success in treating ALS. One aspect that needs to be addressed is how specific pools of glutathione are impacted during ALS. NSC-34 cells transfected with $SOD1^{G93A}$ have cytosolic levels of GSH equivalent to untransfected cells, but mitochondrial GSH is markedly decreased [170]. Spinal cords of $SOD1^{G93A}$ mice also have reduced mitochondrial GSH, and even though a treatment, such as a cystine-rich

supplement, may increase cytosolic GSH levels, they may still fail to rescue mitochondrial glutathione levels and thus not succeed in extending survival [164].

1.3.8 Conclusion

Myriad mechanisms are involved in ALS and the presence of oxidative stress is a common factor. In this review, we have explored the crucial role of glutathione and associated enzymes that are so vital in effectively combating oxidative threats. Levels of cytosolic and mitochondrial glutathione in motor neurons and glial cells are diminished in ALS. Several enzymes, including glutathione reductase, glutathione peroxidase, and glutathione S-transferase exhibit reduced activity levels. Current therapies designed to replete glutathione levels have had little success, in part because they fail to increase the mitochondrial pool of glutathione. Mitochondrial glutathione has a half-life of several days, which is on the same order as the turnover of mitochondria themselves [62]. Cytosolic glutathione turnover, on the other hand, is fifteen times faster, on the order of minutes [62]. Although it was thought that glutathione is transported into the mitochondria via the mitochondrial dicarboxlate and 2-oxoglutarate transporters, recent data indicate that this may not be the case [171]. Better understanding of how glutathione, and compartmentalization of glutathione, particularly in mitochondria, is moderated in ALS and the impact of this on oxidative

stress defense, could promote the development of new therapies for inhibiting disease progression and protecting motor neurons.

1.4 Mitochondrial Targeting of Antioxidants

Mitochondria, double membrane-bound organelles, are crucial to proper function of most eukaryotic cells. The number of mitochondria in each cell can vary considerably depending on location and function of the cell. Red blood cells, for example, have no mitochondria, whereas hepatocytes may have thousands. Mitochondria are involved in cell signaling, calcium homeostasis, and cellular death and differentiation. Their most important role, however, is to generate energy for the cell in the form of adenosine triphosphate (ATP) through a process known as oxidative phosphorylation. Free radicals are frequently generated as a byproduct of respiration and mitochondrial oxidative damage often accrues at a faster rate than the rest of the cell. Oxidative damage-related mitochondrial dysfunction underlies many diseases of aging, including ALS [9-15].

To address oxidative damage in the mitochondria, compounds need to be able to accumulate there. A mitochondrial-targeting moiety such as triphenylphosphonium (TPP), a lipophilic cation, has been used in recent years to propel compounds into the mitochondrial matrix driven by the membrane potential (Figure 1.4) [172-175].

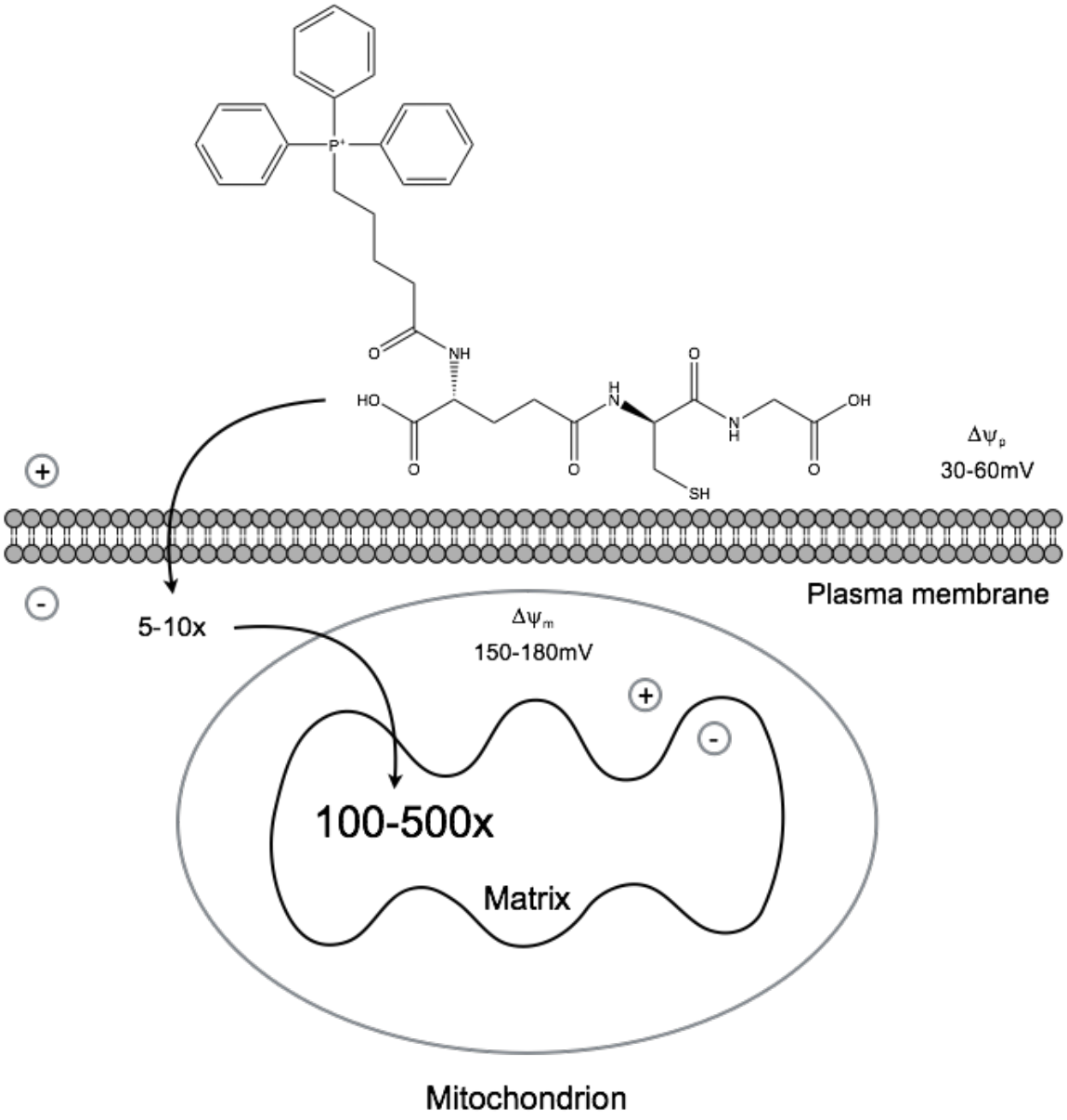

Figure 1.4. Uptake of triphenylphosphonium (TPP) cations by mitochondria [172]. Figure adapted from [172]. Antioxidants, such as glutathione, may be coupled with TPP, a lipophilic cation, to enhance delivery to mitochondria. In response to the membrane potential, the TPP compound accumulates 5-10-fold in the cytosol and 100-500-fold inside the mitochondrial matrix. These compounds pass through lipid bilayers without a need for active transport.

To date, several antioxidants have been covalently linked with TPP and successfully delivered to mitochondria, including Coenzyme Q (MitoQ) [174], lipoic acid [176], and vitamins C [177] and E [178]. With the exception of the ascorbate

derivative, these antioxidants have been largely hydrophobic, facilitating delivery across membranes. Hydrophilic antioxidants present a challenge when attempting to target to the mitochondria. Ascorbate, for example, is polar, hydrophilic, and negatively charged under physiological conditions. Although there is still some controversy, ascorbate transport to the mitochondria is thought to require delivery through glucose transporter 10 (GLUT10) of dehydroascorbate followed by reduction to ascorbate, or sodium-coupled ascorbic acid transporter-2 [179, 180]. However, coupling with TPP and increasing the hydrophobicity of the linker region provided a way to overcome the challenges presented by the antioxidant and permitted accumulation of this ascorbate derivative in the mitochondrial matrix [177].

Glutathione is another hydrophilic, charged antioxidant that plays a critical role in cellular defense. As discussed in Section 1.3, glutathione levels decline with age and its loss plays a role in many pathologies. Mitochondrial glutathione levels drop even more dramatically in these situations, leaving the mitochondria increasingly vulnerable to oxidative stress. One attempt has been made to target glutathione to mitochondria by appending a choline ester moiety [181] (Figure 1.5). Some preliminary data showed that this compound delayed H_2O_2-induced mitochondrial depolarization in rat ventricular myocytes and may offer some defense against oxidative insult [181]. No further studies have appeared.

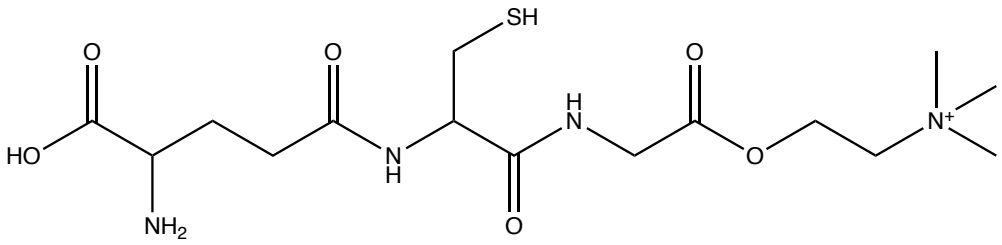

Figure 1.5. Structure of glutathione choline ester (MitoGSH).

Designing and synthesizing a mitochondrially-targeted glutathione derivative to combat oxidative stress experienced in ALS and other degenerative diseases has formed a significant part of my research. We have developed unique glutathione derivatives, targeted to mitochondria using the TPP lipophilic cation.

1.5 Nuclear Magnetic Resonance and Solution Dynamics

Nuclear magnetic resonance (NMR) is a powerful analytical tool that allows examination of small molecules and proteins at the atomic level. The underlying principle of NMR concerns a property of an atomic nuclei known as spin (*I*). Nuclei with spin ½, including ^{1}H, ^{13}C, and ^{31}P, are the most useful for NMR.

A nucleus with spin *I* will have 2*I* + 1 available orientations in an applied magnetic field. A nucleus with spin ½ will therefore have 2 possible orientations and energy levels associated with these positions. Spins aligned with the magnetic field will populate the +½ energy state, while spins opposed to the field populate the -½ state (Figure 1.6).

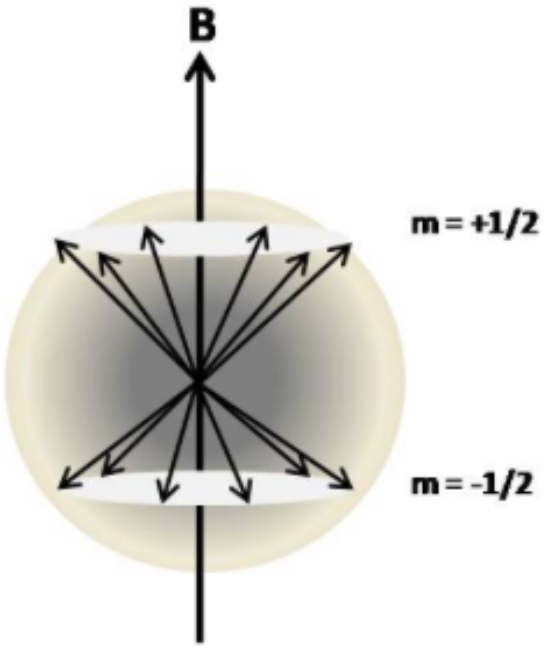

Figure 1.6. Applied magnetic field effect on spin populations. When a magnetic field, B, is applied, the energy levels split. Spins aligned with the magnetic field occupy the +½ energy level, and spins opposed the -½ level [1].

Particles do not necessarily remain at a given level. A proton, for example, can transition energy levels by absorbing energy matching the difference separating the two levels. The energy, E, is equivalent to $h\nu$, where h is Planck's constant (6.62×10^{-34} J•s), and ν is the resonance frequency.

The direction of the applied magnetic field, B, lies in the z-direction of three-dimensional space at equilibrium. At equilibrium, magnetization of the ^{13}C spins are aligned with the magnetic field. After a pulse of energy is applied, the magnetization vector of the nuclear spin system is displaced from its equilibrium position along the z-axis into the xy-plane. Without further energy input, the spins will relax and precess around the z-axis until finally reaching its equilibrium position. The time required to achieve the original equilibrium state is known as longitudinal, or spin-lattice relaxation time (T_1). Increasing size and complexity tend to reduce T_1.

In Chapter 4, NMR is used to examine how the modifications to oxidized glutathione alter its dynamic properties in solution under simulated physiological conditions (PBS, pH 7.4). To accomplish this, ^{13}C relaxation of protonated carbons was measured with ^{1}H-^{13}C HSQC in a pseudo-3D experiment, implementing the Bruker pulse sequence, hsqct1etgpsi3D (Figure 1.7).

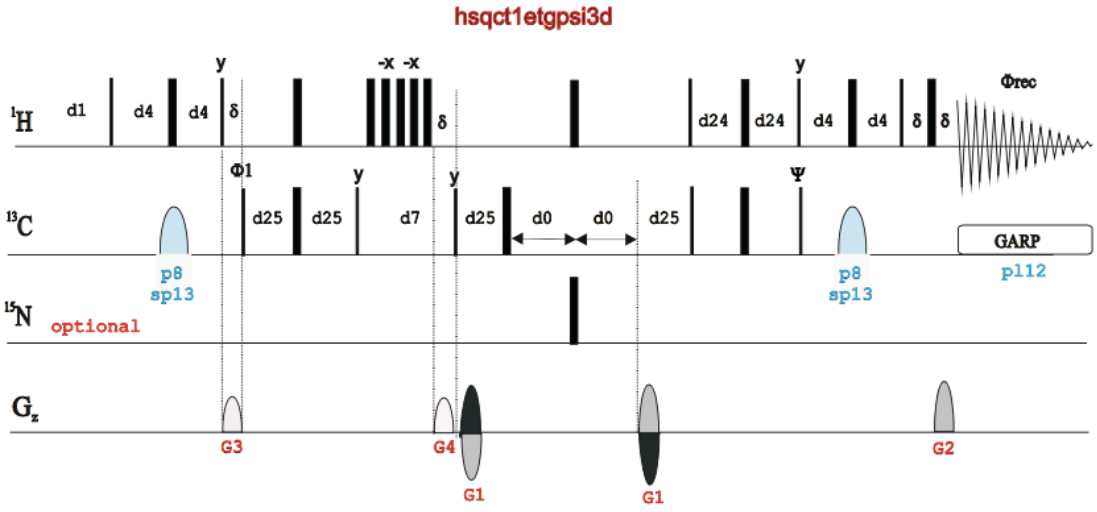

Figure 1.7. Bruker pulse program hsqct1etgpsi3D [182]. This is a standard program for acquiring a series of HSQC spectra with increasing delay times for each acquisition. In the diagram, d-values are various delay times, p- and sp-values are power levels for specific channels. In our experiment the ^{15}N channel is not used. G_z is the gradient strength, which reflects the amount of current in the gradient coil that generates the magnetic field. GARP is a decoupling scheme.

Once data are acquired, the intensity of each carbon peak is measured for each plane and plotted versus time. The resulting plot represents a decaying exponential with the following equation: $f(t) = I_o * e^{-t/T1}$, from which T_1 may be determined. Smaller T_1 values for a specific carbon reflect a smaller degree of motion.

1.6 Dissertation Contents

The following four chapters examine aspects of oxidative stress in ALS and a potential means of mitigating the damage caused thereby. Chapters 2-4 are research chapters. Chapter 5 summarizes the research in which I have participated over the last five years.

Chapter 2: Microglial cell senescence in amyotrophic lateral sclerosis. Pamela R. Beilby, Emiliano Trias, Romina Barreto-Núñez, Sofia Ibarburu, Pablo Díaz-Amarilla, C. Samuel Bradford, Luis Barbeito, Joseph S. Beckman

This chapter elucidates the role of senescence of microglia in ALS. We demonstrated that microglia isolated from the spinal cords of adult $SOD1^{G93A}$ transgenic mice undergo cellular senescence over the course of the disease. As the disease progresses this phenotype becomes more pronounced. This represents the first time that senescent microglia have been identified in ALS transgenic animals.

Chapter 3: Design and synthesis of mitochondrially-targeted glutathione. Pamela R. Beilby, Tory M. Hagen, Joseph S. Beckman

The loss of cytosolic glutathione occurs with age and in many pathological conditions, and the mitochondrial pool of glutathione suffers an even greater loss. Therapies that attempt replenish cellular stores of glutathione often fail to increase the mitochondrial pool. Glutathione is a hydrophilic molecule, with several reactive functional groups. Our design addresses these challenges by esterification of the carboxlates of oxidized glutathione, followed by a peptide coupling reaction which appends a mitochondrially-targeting moiety, triphenylphosphonium, a lipophilic cation, to the amino groups of the glutamate residues.

Chapter 4: NMR characterization of mitochondrially-targeted oxidized glutathione. Pamela R. Beilby, Patrick N. Reardon, and Joseph S. Beckman

To begin characterization of this new therapeutic, nuclear magnetic resonance (NMR) was used to study the dynamics of the derivatives in solution. Using ^{1}H-^{13}C-HSQC NMR, we determined T_1 spin-lattice relaxation times. Glutathione is a relatively flexible molecule in solution. This study demonstrated that the esterification of glutathione carboxylic acids and amino group coupling with TPP significantly reduce the motion of mitochondrially-targeted glutathione.

Chapter 5: Conclusions

This chapter summarizes my research career in the Beckman lab, provides context for the directions I have taken, and offers conclusions that may be drawn from these efforts. It also provides a framework for future work examining oxidative stress in ALS and potential therapeutic targets and solutions.

Chapter 2

Microglial cell senescence in amyotrophic lateral sclerosis

Pamela R. Beilby, Emiliano Trias, Romina Barreto-Núñez, Sofia Ibarburu, Pablo Díaz-Amarilla, C. Samuel Bradford, Luis Barbeito, Joseph S. Beckman

2.1 Abstract

Age is the primary risk factor for amyotrophic lateral sclerosis (ALS). A hallmark of aging is the accumulation of senescent cells that enlarge and cannot proliferate, but secrete trophic factors and cytokines that promote inflammation and alter the surrounding cellular microenvironment. We previously reported that a population of rapidly proliferating microglial cells can be isolated from the spinal cord of adult transgenic rats expressing the ALS-linked G93A mutation to superoxide dismutase-1 ($SOD1^{G93A}$). These cells exhibit an aberrant phenotype and selectively kill motor neurons *in vitro.* We hypothesized that at least some features of aberrant glial cell behavior in ALS could be associated with senescence. Using primary cultures of microglia isolated from symptomatic adult $SOD1^{G93A}$ rats, we identified a cell population that expressed senescence-associated-beta-galactosidase (SA-β-gal) activity, a well-established marker of senescence. SA-β-gal-positive cells co-existed with a rapidly proliferating population of smaller cells that were negative for SA-β-gal. In the spinal cord of symptomatic $SOD1^{G93A}$ rats, we observed increased expression of two other markers of senescence, $p16^{INK4a}$ and matrix metalloproteinase 1, that in part co-localized with aberrant glial cells that typically surrounded motor neurons. Together, these results demonstrate an association between a population of senescent microglia cells with the increased proliferation and phenotypic changes in surrounding glial cells. Glial cell senescence could drive microgliosis and

promote the emergence of aberrant glia phenotypes, contributing to the rapid progression of motor neuron demise in ALS.

2.2 Introduction

Amyotrophic lateral sclerosis (ALS) is a devastating, fatal disease resulting from the relentless progressive death of motor neurons. While the causes of ALS are unknown, approximately 10% of all cases have a familial inheritance. The first gene linked to ALS harbored a mutation to the antioxidant enzyme copper-zinc superoxide dismutase-1 (SOD1). A causal connection was established when mutant SOD expression was shown in mice and rats to induce a progressive motor neuron disease [183, 184]. Motor neuron degeneration is associated with increased oxidative stress, mitochondrial dysfunction, and disruption of protein homeostasis. These stresses are well known to induce cellular senescence, where irreversibly damaged senescent cells can profoundly alter tissue behavior to promote inflammation. Senescent cells accrue with age in many different tissues [35], but the role of senescence remains obscure in neurodegenerative disease.

Although senescent cells are unable to proliferate, they remain metabolically active and alter the surrounding tissue microenvironment. Cellular senescence is characterized by permanent cell-cycle arrest without cell death. Prominent biomarkers of cellular senescence include senescence-associated beta-galactosidase (SA-β-gal) activity and expression of the tumor suppressor/cell cycle regulator protein, $p16^{INK4a}$. SA-β-gal activity reflects specific activity at pH 6 that is strongly associated with senescent cells [185]. Cells also enlarge and frequently develop a senescence-associated secretory phenotype (SASP), releasing trophic factors, pro-inflammatory signaling molecules,

proteases, and other factors such as extracellular matrix components [46]. Non-neuronal cells contribute to motor neuron death and many studies have demonstrated the prominent role of glial cells in the pathology of ALS [22, 23, 186-189]. Previous reports showed that a subpopulation of aberrant microglia could be isolated from the degenerating spinal cords of adult symptomatic transgenic $SOD1^{G93A}$ rats that could rapidly proliferate and secrete neurotoxic factors [20, 190]. Recent research suggests that accumulation of senescent non-neuronal cells in the central nervous system corresponds with neurodegeneration [191-195]. Senescent astrocytes and microglia have been identified in Alzheimer's disease [45, 196] and hypothesized to exist in Parkinson's disease [44]. ALS astrocytes have recently been shown to exhibit markers of senescence, and that the increased accumulation of senescent cells with heightened SA-β-gal activity corresponds to disease progression and reduced support for motor neurons [197]. Because age is the primary risk factor for ALS, we hypothesized that a subpopulation of senescent cells might contribute to the aberrant behavior observed in these glial cells. In this study, we examined glial cells from the spinal cord of adult symptomatic $SOD1^{G93A}$ rats for expression of three senescence biomarkers: SA-β-gal activity, $p16^{INK4a}$, and matrix metalloproteinase 1 (MMP1).

2.3 Materials and Methods

2.3.1 Animals

All procedures using laboratory animals were performed in accordance with the international guidelines for the use of live animals and were approved by either the Oregon State University Institutional Animal Care Use Committee or for experiments performed in Uruguay in strict accordance with the requirements of the IIBCE Bioethics Committee under the ethical regulations of the Uruguayan Law N° 18.611 governing animal experimentation. Uruguayan law follows the Guide for the Care and Use of Laboratory Animals of the National Institutes of Health (USA). Male hemizygous NTac:SD-TgN(SOD1^{G93A})L26H rats (Taconic), originally developed by Howland *et al*. [198], were bred locally by crossing with wild-type Sprague-Dawley female rats. Male SOD1^{G93A} progenies were used for further breeding to maintain the line. Rats were housed in a centralized animal facility with a 12-h light-dark cycle with *ad libitum* access to food and water. Symptomatic disease onset was determined by periodic clinical examination for abnormal gait, typically expressed as subtle limping or dragging of one hind limb. Rats were killed well before they reached the end stage of the disease.

2.3.2 Primary microglia culture

Microglia cells were isolated from adult symptomatic SOD1^{G93A} rats as previously described [199] with slight modifications. Rats were terminally anesthetized and the spinal cords were dissected with the meninges carefully

removed. The cords were mechanically chopped then enzymatically dissociated in 0.25% trypsin for 10 minutes at 37°C. Fetal Bovine Serum (FBS) 10%(vol/vol) in Dulbecco's Modified Eagle Medium (DMEM) was then added to halt trypsin digestion. Repetitive pipetting thoroughly disaggregated the tissue, which was then strained through an 80-μm mesh and spun down. The pellet was resuspended in culture medium [DMEM + FBS 10%(vol/vol), HEPES buffer (3.6 g/mL), penicillin (100 IU/mL), and streptomycin (100 μg/mL)] and plated in 25-cm^2 tissue culture flasks. Culture medium was replaced every 72 hours.

2.3.3 Flow cytometry analysis of senescence-associated-β-galactosidase (SA-β-gal) activity

After 14 days *in vitro*, microglia were quantitatively analyzed for SA-β-gal activity as described [200]. Briefly, cells were treated with Bafilomycin A1 to inhibit lysosomal acidification, followed by incubation with C_{12}FDG (Molecular Probes/Life Technologies), a fluorogenic substrate for β-galactosidase for 2 hours at 37°C with 5% CO_2. Microglia were then rinsed with PBS, harvested by trypsinization, centrifuged, and resuspended in ice-cold PAB. Cells were immediately run on a Beckman-Coulter FC500 flow cytometer. Data were analyzed using Winlist (Verity Software).

2.3.4 Flow cytometry analysis of cell cycle progression

Cells were trypsinized, washed, and centrifuged. The cell pellet was then resuspended in ice-cold 70% ethanol and incubated at -20°C for 30 minutes for

fixation. Subsequently, cells were washed, centrifuged, then resuspended in 0.1% Triton X-100 in Dulbecco's Phosphate-Buffered Saline (DPBS). RNase A (10 μg/mL) and propidium iodide (20 μg/mL) were added and cells were incubated for 60 minutes at room temperature. They were then filtered through a 37-μm mesh and run on Beckman-Coulter FC500 flow cytometer and analyzed using Multi-Cycle (Phoenix Software).

2.3.5 Immunohistochemical staining of rat spinal cords

Animals were deeply anesthetized and perfused transcardially with 0.9% saline and 4% paraformaldehyde in 0.1 M PBS (pH 7.2–7.4) at a constant flow of 1 mL/min. Fixed spinal cord was removed, post-fixed by immersion for 24 h, and then cut into transverse serial 30–40 μm sections with a vibrating microtome. Serial sections were collected in PBS for immunohistochemistry. Free-floating sections were permeabilized for 30 min at room temperature with 0.3% Triton X-100 in PBS, passed through washing buffered solutions, blocked with 5% BSA:PBS for 1 hour at room temperature, and incubated overnight at 4 °C in a solution of 0.3% Triton X-100 and PBS containing the primary antibodies, mouse anti-p16 (1:200, Abcam), rabbit anti-glial fibrillary acidic protein (GFAP) (1:500, Sigma), rabbit anti-Iba1 (1:300, Abcam). After washing, sections were incubated in 1:1,000-diluted secondary antibodies conjugated to Alexa Fluor 488 and/or Alexa Fluor 633 (1:1000, Invitrogen). Antibodies were detected by confocal microscopy using a confocal LEICA TCS-SP5-DMI6000.

2.3.6 Quantitative Analysis of $p16^+$, $GFAP^+/p16^+$ and $Iba1^+/p16^+$ cells in the ventral horn of the spinal cord

The number of cells co-labeled with the senescence marker p16 and the astrocytic marker GFAP or co-labeled with p16 and the microglial marker Iba1, were assessed by counting the double-positive cells in the gray matter of the lumbar cord of non-transgenic, asymptomatic or symptomatic $SOD1^{G93A}$ rats. Quantification was performed only in the ventral horn, comparing the cell numbers in Rexed laminae VII versus those in Rexed laminae IX. These regions respectively display a low versus high density of large motor neurons. The analysis was performed using 10 histological sections per animal (with three different rats for each condition) using the cell counter tool of the Image J software. Values were expressed as the percentage of p16-expressing cells or double-positive cells relative to non-transgenic animals. Statistical studies were performed using statistical tools of Origin 8.0. Descriptive statistics were used for each group, and one-way ANOVA, followed by Scheffé *post hoc* comparison if necessary, was used among groups. All experiments were performed in duplicate or triplicate and were replicated at least three times. All results are presented as mean ± SD, with $p < 0.05$ considered significant.

2.3.7 Western blot analysis

For extraction of protein, spinal cords were completely dissected and embedded in lysis buffer [50 mM HEPES (pH 7.5), 50 mM NaCl, 1% Triton X-100, and complete protease inhibitor mixture] (Sigma) and then sonicated six times for

3 s. Protein concentration was measured with a bicinchoninic acid (BCA) kit (Sigma). Protein extracts were placed in loading buffer containing 15% SDS, 0.3 M Tris (pH 6.8), 25% glycerol, 1.5 M β-mercaptoethanol, and 0.01% bromophenol blue. Protein samples (40 μg) were resolved on 12% SDS-polyacrylamide gel and transferred to PVDF membrane (Amersham). Membranes were blocked for 1 h in Tris-buffered saline (TBS), 0.1% Tween-20, and 5% non-fat dry milk, followed by overnight incubation with the corresponding primary antibody, rabbit anti-MMP1 (1:1000, Novus), mouse anti-p16 (1:1000, Cell Signaling), mouse anti-p53 (1:1000, Abcam) and mouse anti-β-actin (1:4000, Sigma), diluted in the same buffer. After washing with 0.1% Tween in TBS, the membrane was incubated with peroxidase-conjugated secondary antibodies (goat anti-mouse-HRP and goat anti-rabbit-HRP 1:5000, Thermo) for 1 h and washed and developed using the ECL chemiluminescent detection system (Thermo). MMP1, p53, p16 and β-actin bands were used to quantify the data. The intensities of all protein bands were normalized with β-actin using ImageJ software.

2.4 Results

2.4.1 SOD1^{G93A} spinal cord microglia demonstrate senescence-associated β-galactosidase (SA-β-gal) activity

Microglial cells *in vitro* show two distinct subpopulations two weeks after isolation from the spinal cord of symptomatic SOD1^{G93A} rats, based on size as seen in the scatter diagram of the cells (Figs 2.1A, C, F). When examining the entire cell population, approximately 50% of the cells demonstrated activation of a senescence program as measured by β-galactosidase activity (Fig 2.1B). Only 8% of the subpopulation of smaller microglial cells (Fig 2.1D) expressed β-gal staining compared to 92% of the subpopulation of larger cells (Fig 2.1G). SA-β-galactosidase activity determination was consistent with the FACS analysis of the cell cycle progression. The smaller microglia subpopulation demonstrated normal cell cycle behavior (Fig 2.1E), corresponding to the large number of non-senescent cells. The larger cells, with a higher percentage of senescent cells, revealed significant S-phase arrest (Fig 2.1H), indicative of inhibition of cell growth and proliferation. *In vitro* senescent microglial cells demonstrate an enlarged, flattened morphology and exhibit positive chromogenic SA-β-gal staining (Fig 2.1I, J, red arrows).

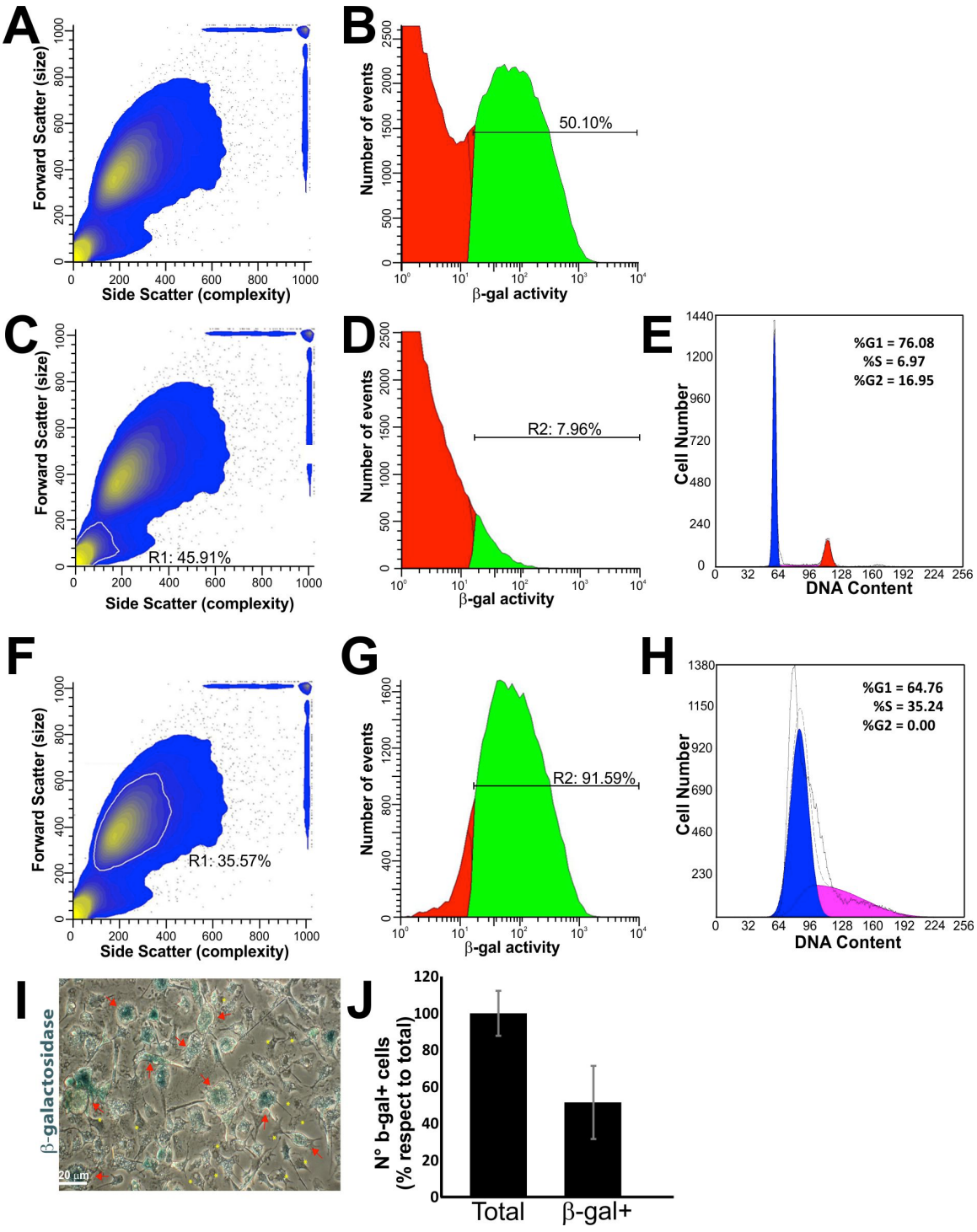

Figure 2.1. Senescence-associated beta-galactosidase activity in SOD1^{G93A} microglia. Transitioning microglia population two weeks after culturing from spinal cord of G93A adult symptomatic rats display dramatic SA-β-galactosidase activity. **(A)** The scatter diagram, a population density heat map, indicates the gate for the sample and includes the entire population of cells. **(B)** Approximately 50% of the cells demonstrate SA-β-gal activity. **(C)** The scatter diagram

for the smaller population (inside white outline, R1 indicates percentage of total population encompassed by this subset). **(D)** The gate for the smaller cell population (R2) indicates almost 8% of these cells are senescent. **(E)** Cell cycle analysis for smaller cell population. **(F)** Scatter diagram for larger cell population (inside white outline, R1 as in **C**). **(G)** In the larger cell population (R2), over 90% of the cells demonstrate SA-β-gal activity. The R2 value in diagrams **D** and **G** is gated on the R1 scatter and shows the percentage of the subset demonstrating senescence as measured by SA-β-galactosidase activity. **(H)** Cell cycle analysis for the larger cell population showing significant S-phase arrest. **(I)** Representative chromogenic SA-β-gal stain of microglia in culture. Note that bigger cells show SA-β-gal activity (red arrows) when compared with smaller cells (yellow stars) **(J)** Quantitative analysis of SA-β-gal staining (percentage relative to total).

2.4.2 High expression of senescence markers in the spinal cord of SOD1^{G93A} rats

Having found that microglia from SOD1^{G93A} rats experience senescence as determined by SA-β-gal activity *in vitro*, we examined spinal cord tissue of asymptomatic and symptomatic SOD1^{G93A} rats for evidence of a senescent phenotype. Immunohistochemistry revealed greater p16 expression in the ventral horn of the spinal cord of asymptomatic and symptomatic rats compared to non-transgenic animals (Figs 2.2A-B). Matrix metalloproteinase 1 (MMP1), a secreted protease that modifies the surrounding extracellular [201], is also frequently up regulated as part of the senescent associated secretory phenotype (SASP) [46]. Western blot analysis demonstrated elevated MMP1 levels in SOD1^{G93A} rats when compared with non-transgenic littermates (Fig 2.2C).

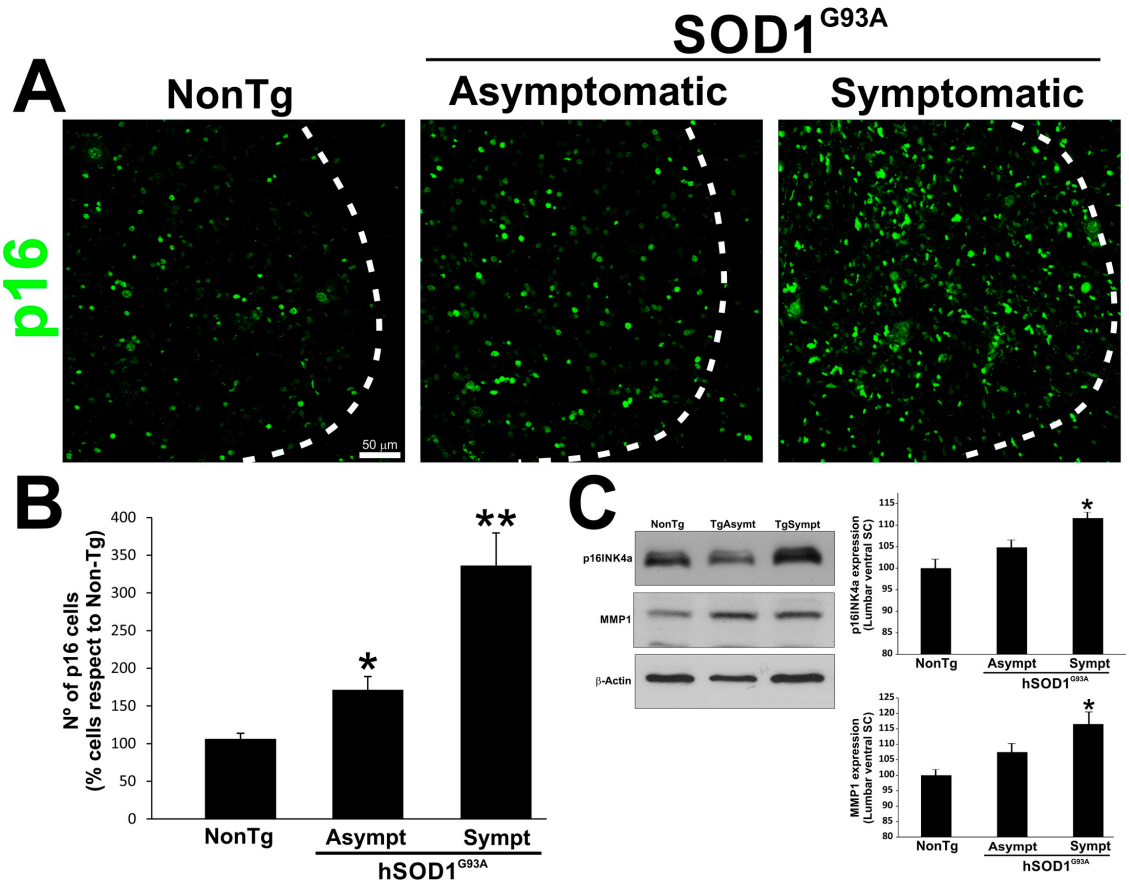

Figure 2.2. **Senescence markers are highly expressed in SOD1^{G93A} ALS rats during the symptomatic phase of disease.** Representative figures showing the expression of p16 and MMP1 by immunohistochemistry and western blot analysis, respectively, in the degenerating spinal cord of SOD1^{G93A} animals and non-transgenic controls. **(A)** Note the increased levels of p16^{+} cells (green) in the ventral horn of the spinal cord in a symptomatic rat compared with asymptomatic or non-transgenic controls (white dotted lines indicate separation of white from grey matter). **(B)** Quantitative analysis of the p16^{+} cells in the degenerating spinal cord. Note the progressive increase of p16 expression that accompanies the progression of the disease. Data are expressed as mean ± SEM *p<0.05. **(C)** Western blot that shows the increased expression of p16 and MMP1 in the spinal cord during the symptomatic phase of ALS, with respect to non-transgenic and SOD1 asymptomatic rats. The graph in the right panel shows the quantitative analysis of the western blot. Data are expressed as mean ± SEM *p<0.05.

2.4.3 SOD1^{G93A} microglia and aberrant glial cells express high levels of the senescence marker p16^{INK4a}

A subpopulation of GFAP^{+} aberrant glial cells also express higher levels of p16 in asymptomatic and symptomatic ALS rats. Aberrant glial cells could not be

identified in non-transgenic rats, and only a few astrocytes are positive for p16 (Fig 2.3A). Next we analyzed the expression of p16 in Iba1^{+} microglia surrounding motor neurons in the SOD1^{G93A} rat spinal cord. During the symptomatic phase, p16 expression was significantly augmented in a subpopulation of microglia compared to non-transgenic or SOD1^{G93A} asymptomatic rats (Fig 2.3B).

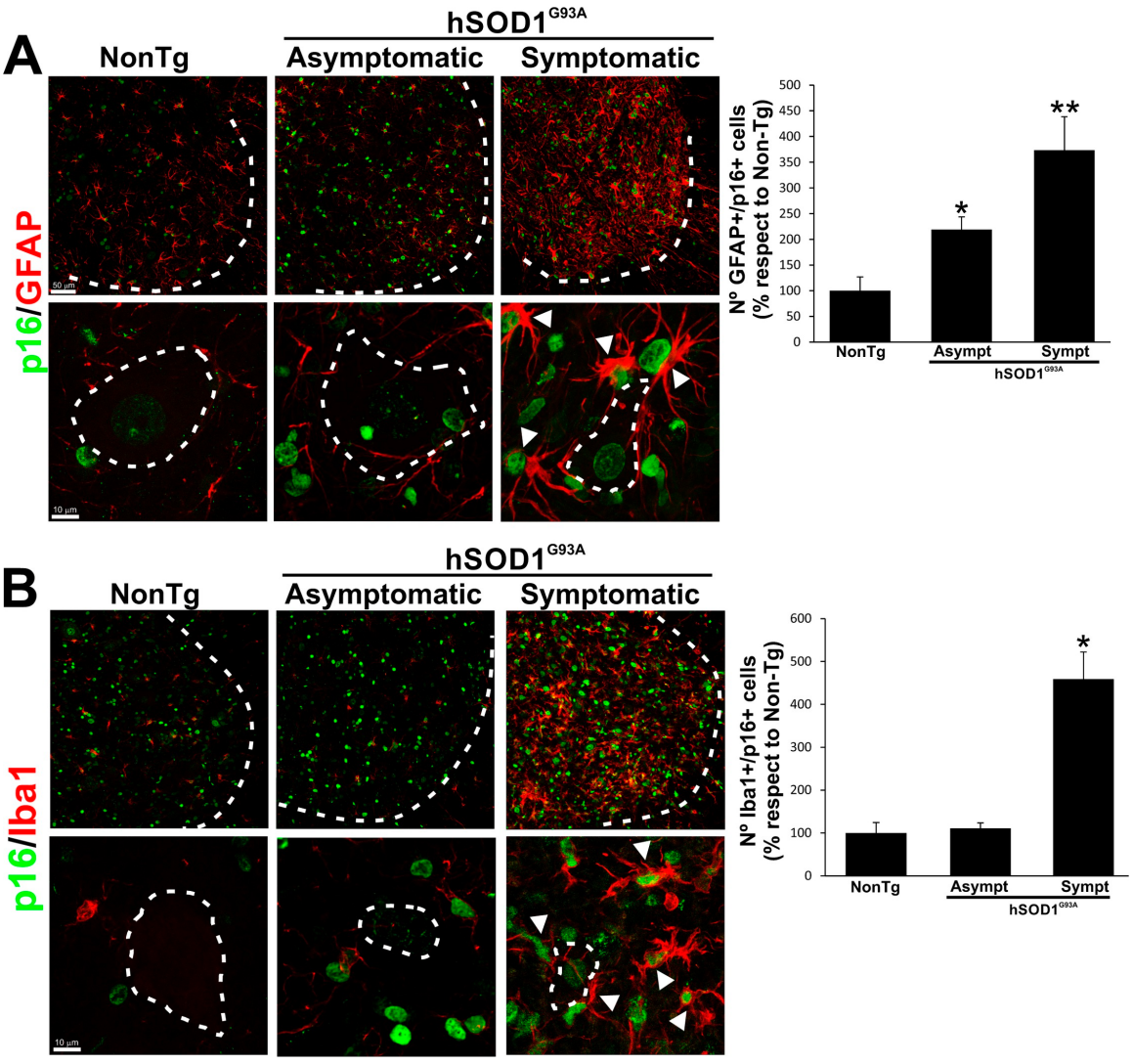

Figure 2.3. A sub-population of aberrant glial cells and microglia express high levels of the senescence marker p16. Representative confocal images showing the expression of p16 (green), GFAP (red, A) and Iba1 (red, B) in non-transgenic, SOD1^{G93A} asymptomatic and symptomatic rats. White dotted lines in upper panels of A and B indicate separation of white and grey matter. White dotted lines in lower panels of A and B outline motor neurons. **(A)** Photomicrographs showing

p16/GFAP stained lumbar spinal cord sections measured in non-transgenic, asymptomatic and symptomatic $SOD1^{G93A}$ rats. Low magnification panels (upper panels) show the increase in the number of $p16^{+}/GFAP^{+}$ cells in the symptomatic rats, as compared to low markers co-expression in asymptomatic or non-transgenic rats. Note the expression of p16 marker in a sub-population of aberrant glial cells that surround motor neurons in the degenerating spinal cord of $SOD1^{G93A}$ symptomatic animals. In the quantitative analysis (lower panel) note the significant increase of the co-expression of GFAP with the senescence marker p16 as the disease progresses (white arrows). Data are expressed as mean ± SEM *p<0.05. **(B)** The confocal representative image shows the expression of microglia marker Iba1 and the senescence marker p16 in the non-transgenic, asymptomatic and symptomatic $SOD1^{G93A}$ spinal cord. A significant increase of $p16^{+}/Iba1^{+}$ cells during the symptomatic stage of the disease is observed compared to NonTg animals or $SOD1^{G93A}$ asymptomatic stage. Note the increased number of swollen microglia cells that express p16 and that surround motor neurons in the degenerating symptomatic spinal cord. The quantitative analysis (lower panel) of the expression of p16/Iba1 shows a marked increase of the co-expression of p16 in Iba1 cells during the end stage of the disease (white arrows). Data are expressed as mean ± SEM *p<0.05.

2.5 Discussion

Glial cell senescence may be an important contributor to disease pathology in neurodegeneration [45, 196, 197]. Although microglia play a prominent role in ALS pathology and can directly contribute to the demise of motor neurons. [20, 22, 187], the role of senescence in microglia-associated neuroinflammation remains largely unknown.

The research presented in this report provides a stronger link between microglial and aberrant glial cell senescence and ALS. Senescence was strongly associated with microglia and astrocytes in rats symptomatic for motor neuron disease. However, there was also a population of microglia capable of multiplying in the symptomatic spinal cord. Remarkably, these cells could be isolated and continued to proliferate when cultured [199]. We have demonstrated previously that these microglia undergo a phenotype transition during the course of disease progression and ultimately exhibit an anomalous glial cell phenotype [20, 199]. Transitioning microglia isolated from the degenerating spinal cords of adult symptomatic $SOD1^{G93A}$ rats proliferate in culture and are extremely toxic to motor neurons [199]. This alteration to a different glial cell phenotype is consistent with the gradual disappearance of a microglial signature and spinal cord presence with disease progression [202]. The driving force behind this transition is unknown, although the accumulation of senescent microglia may dramatically influence this process. In this current study, we found that only half of the isolated population of microglial cells from rat spinal cord proliferated. These cells tended to be the

smaller cells and <10% expressed senescence markers. In contrast, most of the larger microglia were positive for senescence-associated β-galactosidase (SA-β-gal) activity and did not proliferate.

SA-β-gal activity at pH 6, commonly used to distinguish senescent cells [185], is perceptible due to the increased lysosomal content present in senescent cells [203] and to the activation of autophagy that occurs upon senescence induction [204]. Our result of significantly increased SA-β-gal activity in symptomatic $SOD1^{G93A}$ rats is consistent with increased induction of autophagy at disease onset in SOD1 transgenic mice [205]. Cell cycle arrest provides further *in vitro* confirmation of potential senescence.

Levels of matrix metalloproteinases increase with age in many tissues and organs and are associated with the senescence-associated secretory phenotype (SASP) [48]. MMP1 levels have been shown to be higher in glial cells in Alzheimer's disease pathology [45]. Here we demonstrate an increased expression level of MMP1 in the spinal cord, even when animals are asymptomatic, suggesting the development of a SASP as influential in the ALS disease process. Recent studies also suggest that metalloproteinases become increasingly dysregulated during disease progression in ALS, although this has not yet been considered in relationship to the SASP [206, 207].

We found that rats carrying the $SOD1^{G93A}$ human transgene expressed higher levels of $p16^{INK4a}$ compared to non-transgenic animals. As animals became symptomatic, this difference became much more prominent and coincided with

disease progression. Clearance of $p16^{+}$ cells has been demonstrated to inhibit the progression of age-related disorders [41]. Accumulation of these senescent cells, on the other hand, enhances the decline of healthy function [41].

Cellular senescence through the p16 pathway is accompanied by up regulation of many microRNAs, including miR-146b [208]. Dysregulation of microRNAs underlies the development and progression of many neuroinflammatory diseases such as ALS [209]. In fact, miR-146b has been shown to be significantly upregulated in ALS [202, 210], and is driven by activation of the P2X7 receptor [210]. This purinergic receptor has been long understood to play a prominent role in microglial pathology in ALS [211], as well as in the death of motor neurons, where nitration of Hsp90 leads to activation of the P2X7 receptor and subsequently the FADD-mediated Fas pathway [212, 213]. miR-146b has also been observed to increase in senescent fibroblasts with vigorous IL-6 production [214]. Increased IL-6 and IL-8 levels are also observed in senescent glial cells in ALS [197].

Critical for p16 expression and senescence-related growth arrest is activation of the p38 mitogen-activated protein kinase (p38MAPK), likely due to its downstream influence on the nuclear factor-kappa B (NF-κB) activity [215]. As with other MAPK family members, phosphorylation and activation of p38 occurs in response to cellular stress [216]. Additionally, activation of the p38 pathway is required for induction of the SASP and blocking this pathway using SB203580, a known p38 inhibitor, suppresses generation of the SASP in cultured primary

human dermal fibroblasts [217]. In ALS, the loss of motor neurons in the ventral spinal cord occurs in conjunction with an increase in p38 activation in both neurons and microglia [218]. *In vitro* microglial activation with accompanying production of nitric oxide and neuronal apoptosis were prevented with SB203580 treatment. Our work in this study suggests a link between microglial senescence and motor neuron death mediated by the p38/NF-κB pathway.

NF-κB is a key controller of inflammation and is upregulated in the spinal cords of ALS patients [219], and also in the glial cells surrounding motor neurons in $SOD1^{G93A}$ mice [23, 220]. However, it is only NF-κB activity in microglia that has been associated with disease progression and motor neuron death [23]. NF-κB is also implicated in the induction of miR-146b and is required for generation of the SASP [215, 221].

Neuroinflammation underlies many age-related neurodegenerative diseases, including ALS. Inflammation is maintained by prolonged production of proinflammatory factors. Recent evidence incriminates cellular senescence as a contributor to chronic inflammation, primarily through production of the SASP, as many SASP proteins, such as IL-6, IL-8, and multiple monocyte chemotactic proteins, stimulate inflammation [48]. Although not yet defined within the context of cellular senescence, SASP proteins such as CCL2, MCP-1 and IL-1β are expressed by microglia during the ALS disease process [202, 222, 223].

Chronic inflammation is accompanied by oxidative stress, which delivers a slow, but progressively lethal blow with age and in disease progression. This stress

has been shown to hasten the onset of senescence [224]. Oxidative stress has also been shown to be instrumental in neurodegeneration, including ALS, particularly in anomalous glial cell phenotypes [10, 225, 226]. While we have demonstrated senescence in $SOD1^{G93A}$-derived microglia, the precise relationship between senescent glial cells and motor neuron degeneration remains to be elucidated. However, based on the evidence presented in this paper, we suggest that senescent microglia in the spinal cord contribute prominently to ALS pathology.

Chapter 3

Design and synthesis of mitochondrially-targeted glutathione

Pamela R. Beilby, Tory M. Hagen, Joseph S. Beckman

3.1 Abstract

Glutathione is the primary non-enzymatic antioxidant in mitochondria. The mitochondrial pool of glutathione diminishes significantly with age and in many disease states, including cardiovascular disease, neurodegeneration, and diabetes. Traditional efforts to elevate cellular glutathione levels typically raise cytosolic levels, but mitochondrial pools are regulated independently. Therefore, customary methods to elevate cytosolic glutathione fail to impact the mitochondrial pool of glutathione. To address this limitation, we have developed a novel synthesis of glutathione derivatives for enhanced delivery directly to mitochondria. The preferred synthesis begins with esterification of the carboxylic acids, followed by conjugation to a triphenylphosphonium mitochondrially-targeting moiety. A final step accomplishes a counterion exchange, significantly improving water solubility.

3.2 Introduction

Glutathione is the most abundant non-protein thiol and cellular antioxidant found in mammalian cells. This nearly ubiquitous tripeptide plays a prominent role in redox cycling, protein folding, regulation of cellular proliferation, and metabolism of heavy metals. Glutathione is synthesized in the cytosol in a two-step, ATP-mediated process [51-53]. Glutamate-cysteine ligase catalyzes the first step, the conjugation of glutamate and cysteine to form γ-glutamylcysteine, and is the rate-limiting step. The generation of glutathione follows through the linkage of glycine to γ-glutamylcysteine, which is catalyzed by glutathione synthase. Cytosolic glutathione exists in millimolar concentrations, mostly in the reduced state. The cell also maintains three specific compartmentalized pools of glutathione in the nucleus, endoplasmic reticulum, and the mitochondria [58-62]. This compartmentalization is essential for addressing organelle-specific redox requirements.

Oxidative damage to mitochondria is a hallmark of many pathological conditions, including cancer, diabetes, and neurodegenerative disorders such as amyotrophic lateral sclerosis, Alzheimer's disease and Parkinson's disease [227-232]. Mitochondria are a source of oxidative stress through generation of reactive oxidative species, such as superoxide from the respiratory chain, and are themselves exposed and susceptible to oxidative overload. A complex antioxidant defense system exists to combat the continuous oxidative onslaught within mitochondria. The premier non-enzymatic defense is glutathione.

Mitochondrial glutathione plays a critical, fundamental role in mitigating oxidative stress generated during normal aerobic metabolism, as well as responding to additional reactive oxidative species (ROS) created under toxic insult or other pathological conditions. The mitochondria do not produce glutathione, but instead must import glutathione from the cytosol. Turnover of the mitochondrial pool of glutathione is slower than the cytosolic pool and constitutes 10-15% of the total glutathione content of the cell [62]. Levels of mitochondrial glutathione decrease with age much more dramatically than cytosolic levels [66-68].

Several strategies have been implemented to increase glutathione levels in the cell, including treatment with glutathione and its precursors, such as N-acetylcysteine and other GSH derivatives like glutathione ethyl esters [160, 164, 233]. Many succeed in raising cytosolic levels but all fail to increase mitochondrial glutathione levels. We sought to overcome this difficulty by designing a glutathione derivative specifically targeted to mitochondria. In this study, we describe the design and synthesis of novel glutathione derivatives targeted to mitochondria.

Triphenylphosphonium (TPP) is a lipophilic cation capable of delivering an antioxidant to the mitochondrial matrix and allowing accumulation, driven by the membrane potential. Most TPP derivatives developed as mitochondrially-targeted antioxidants have modified hydrophobic molecules, such as Coenzyme Q, [174], lipoic acid [176] or vitamin E [178]. However, glutathione is a slightly larger, hydrophilic molecule and thus presents some formidable obstacles to overcome to

be delivered efficiently to mitochondria. For example, glutathione has two negatively charged carboxylic acid functional groups and a positively charged amino group. These charged moieties will prevent crossing plasma and mitochondrial membranes if left unmodified. Additionally, glutathione has a very reactive sulfhydryl moiety. The challenge we address here is how to specifically couple the TPP moiety to glutathione while also efficiently modifying the charged moieties with groups that can be efficiently cleaved *in vivo*.

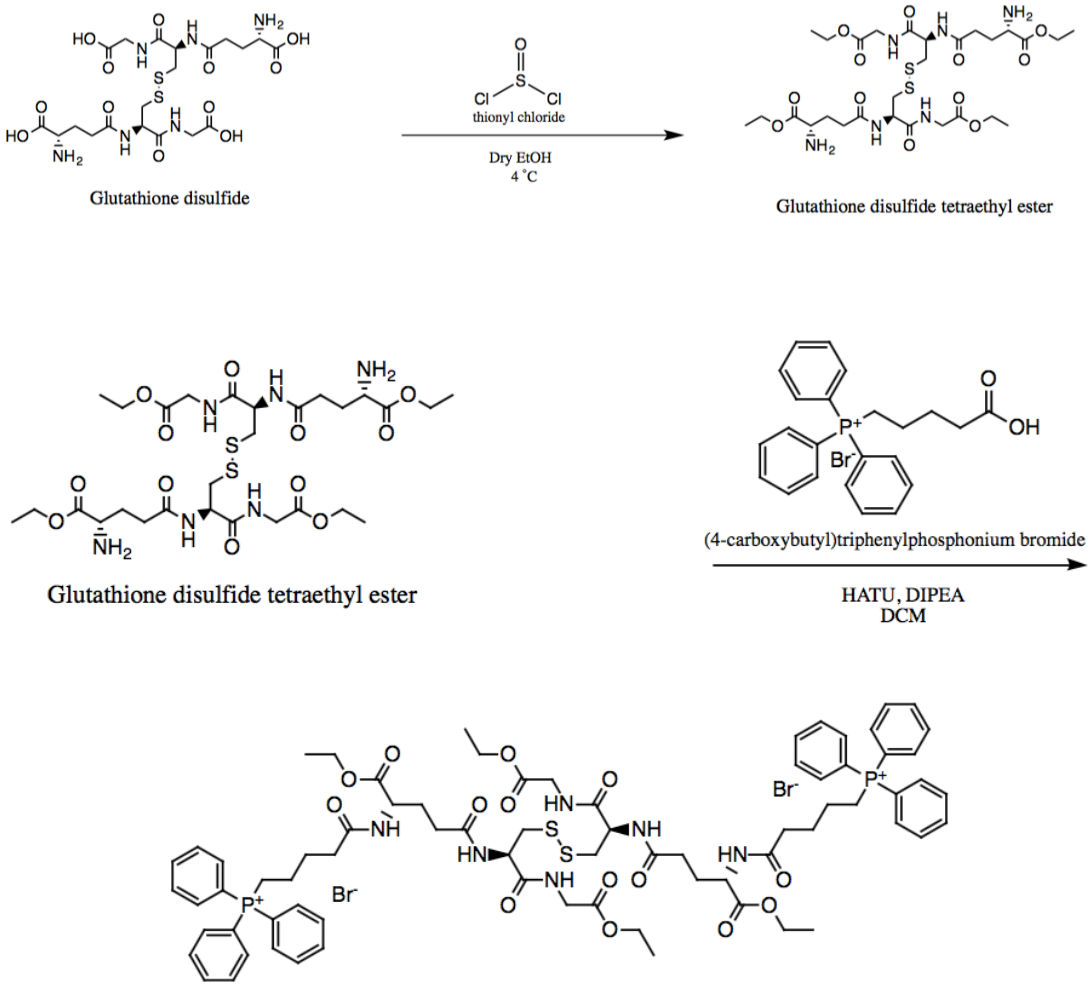

Figure 3.1. Synthesis of mitochondrially-targeted glutathione in its oxidized form (TPP-GSSG).

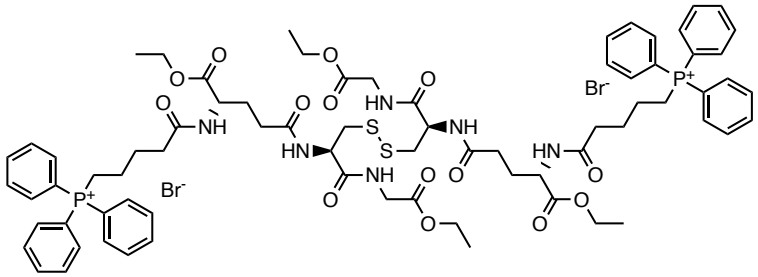

Triphenylyphosphonium glutathione disulfide tetraethyl ester dibromide

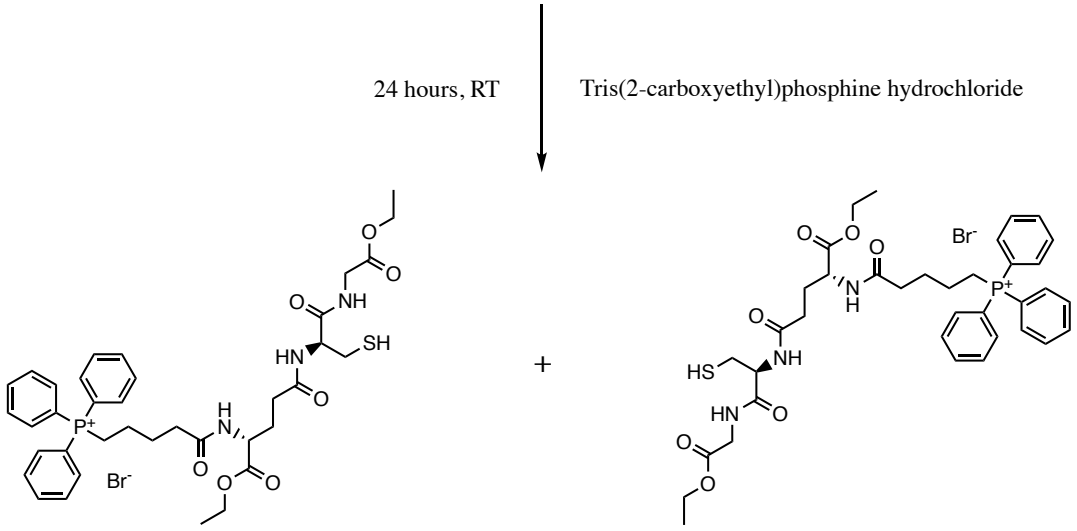

Triphenylyphosphonium glutathione diethyl ester bromide

Figure 3.2. Synthesis of mitochondrially-targeted glutathione in its reduced form (TPP-GSH). This requires one step following completion of synthesis step shown in Figure 3.1.

3.3 Results and Discussion

The overall strategy for producing a TPP-modified glutathione is shown in Figure 3.1. The thiol group was protected by using the oxidized form of glutathione, GSSG. The carboxyl groups were esterified with ethanol. Through a standard peptide coupling reaction, the amino groups were conjugated to carboxybutyl-TPP. The final step involved replacing the bromine counterion from TPP with a mesylate group to improve water solubility (this was done over a column and is not shown in Figure 3.1). The reduced compound results from treatment with Tris(2-carboxyethyl)phosphine hydrochloride (Figure 3.2).

Esterification of glutathione is well known to be an effective way to block the carboxylic acids and enhance transport across cell membranes. This concept was first explored in the 1980s by Alton Meister and colleagues [159, 234]. They produced the diethyl ester of glutathione by the acid-catalyzed reaction of glutathione dissolved in ethanol. The reaction was initiated by adding sulfuric acid that was then left to react for several days at 4 °C. The yields were diminished because the acidic conditions also hydrolyzed the peptide backbone of glutathione. This required a complicated workup to remove degradation products that reduced the yield to only 20-30%. However, Levy, *et al.*, established that the glutathione diethyl ester was swiftly taken up by mammalian cells and could be de-esterified within minutes in the cytosol [234].

Due to the low yield and multiple undesired side reactions, we investigated alternative approaches. Several articles reported that rapid esterification of carboxylic acids in aqueous solution, with good yield (> 75%), could be achieved through the use of the oxygen-directed alkylating agent known as Meerwein's Reagent (Figure 3.3) [235-237]. It did, indeed, work in alkylating glutathione. However, we realized after several attempts resulted in alkylation of the sulfhydryl and amino groups, despite carefully controlling pH, that we would first need to block these groups before proceeding.

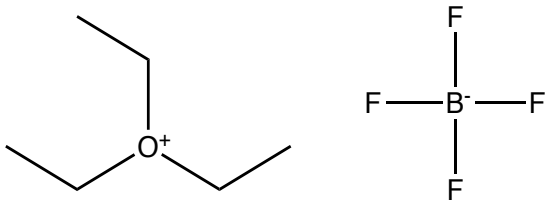

Figure 3.3. Meerwein's Reagent - triethyloxonium tetrafluoroborate.

The sulfhydryl was successfully protected by simply using the oxidized, disulfide form of glutathione. Amino group protection was achieved through reaction with tert-butyloxycarbonyl (t-Boc). However, once the amines were protected, the Meerwein's reagent was no longer as efficient in completely alkylating the third and fourth carboxylates of GSSG.

During our investigations with Meerwein's reagent, Vogel, Jackson, and Masterson published a straightforward method using thionyl chloride ($Cl_2S=O$) to efficiently produce methyl or ethyl esters of oxidized glutathione [238]. (Note that thionyl chloride is tightly controlled under the Chemical Weapons Convention and is also quite hazardous as it reacts violently with water to generate hydrochloric acid and sulfur dioxide). Based on the Vogel, *et al.*, method, 5 mL thionyl chloride

was added dropwise over several minutes to 500 mg GSSG in 100 mL absolute ethanol at 0 °C in a round-bottomed flask. The reaction was allowed to proceed for an additional nine days at 4 °C. While the original paper noted that this reaction in ethanol should go to completion in six days, we found the additional time was necessary for complete reaction because we had used twice the amount of glutathione and other reagents. The reaction was quite efficient and yielded greater than 95% esterification of the four carboxylates of GSSG without modifying the unprotected amino groups (Figure 3.4). Impurities included some ethanol and GSSG with incomplete esterification.

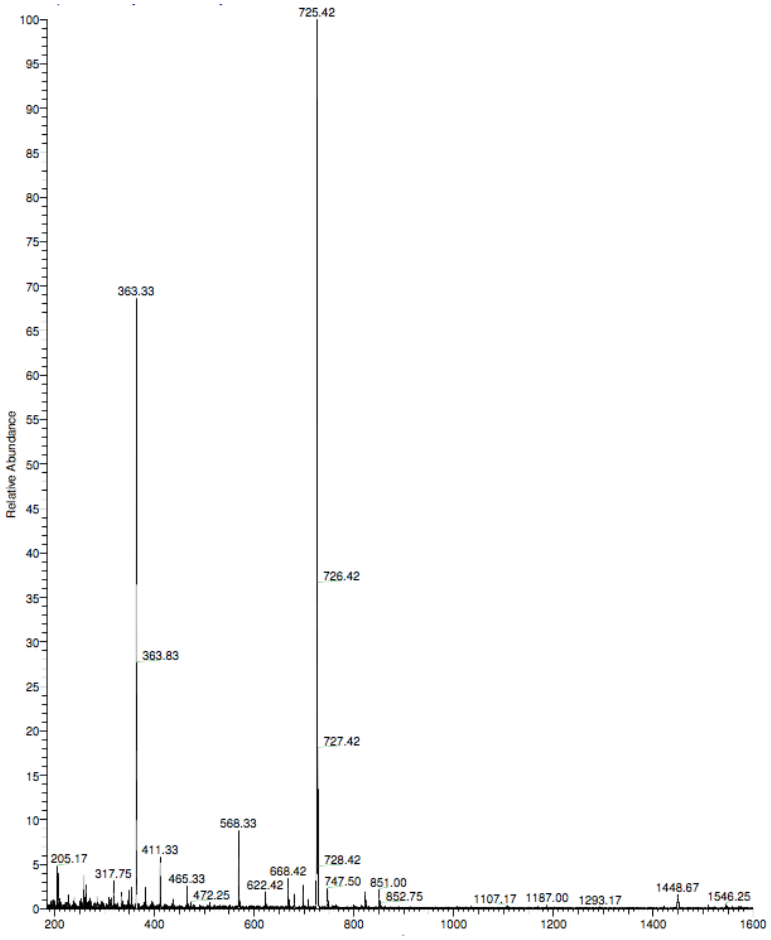

Figure 3.4. Mass spectrometry analysis of glutathione disulfide tetraethyl ester (Et_4GSSG). Compounds were analyzed under positive ESI-MS conditions. Et_4GSSG showed an $[M+H]^+$ ion at m/z 725 and $[M+2H]^{2+}$ at m/z 363.

The next step was to add the TPP moiety to target this glutathione derivative to mitochondria. We selected a relatively inexpensive, commercially available form, 4-(Carboxybutyl)triphenylphosphonium bromide, to conjugate with the free amino groups, through a standard peptide coupling reaction [239]. O-(7-Aza-1H-benzotriazol-1-yl)-N,N,N',N'-tetramethyluronium hexafluorophosphate (HATU) was selected to catalyze this reaction due to its efficient performance.

This coupling reaction works quite well, catalyzing almost complete conversion to our desired product, Triphenylphosphonium glutathione disulfide tetraethyl ester dibromide ($Et_4GSSGTPP_2Br_2$ in 90 minutes (Figure 3.5). The yields (60-65%) do not reflect the efficiency of the coupling procedure. In part, this is due the several washes (three with sodium bicarbonate and one with sodium bromide) and trituration steps of the workup protocol. Also, we start out with less than the molar amounts of carboxybutyl-TPP necessary for the reaction to preclude side coupling reactions with any of the unreacted reagent.

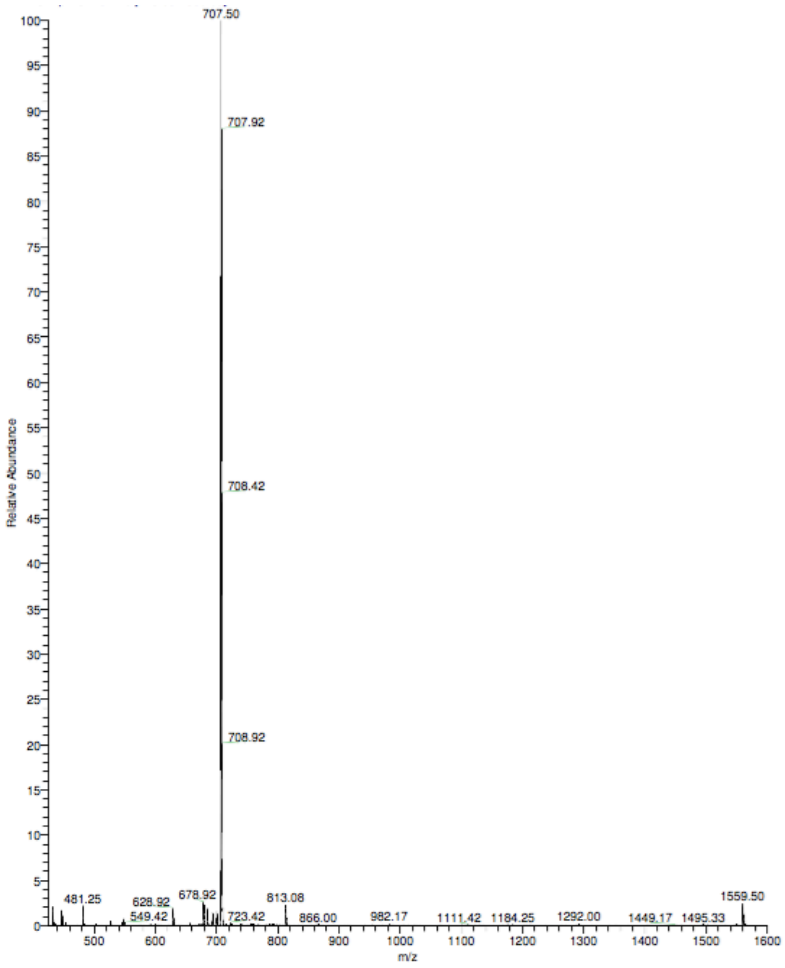

Figure 3.5. Mass spectrometry analysis of Triphenylphosphonium glutathione disulfide tetraethyl ester dibromide ($Et_4GSSGTPP_2Br_2$) . Compounds were analyzed under positive ESI-MS conditions. TPP-GSSG-Br showed an $[M+2H]^{2+}$ ion at m/z 707.

To create a reduced form of the compound, we stirred the crude product, after the first washing step, with 3 equivalents of Tris(2-carboxyethyl)phosphine hydrochloride (TCEP-HCl) for 24 hours. This resulted in complete reduction of $Et_4GSSGTPP_2Br_2$ (Figure 3.6).

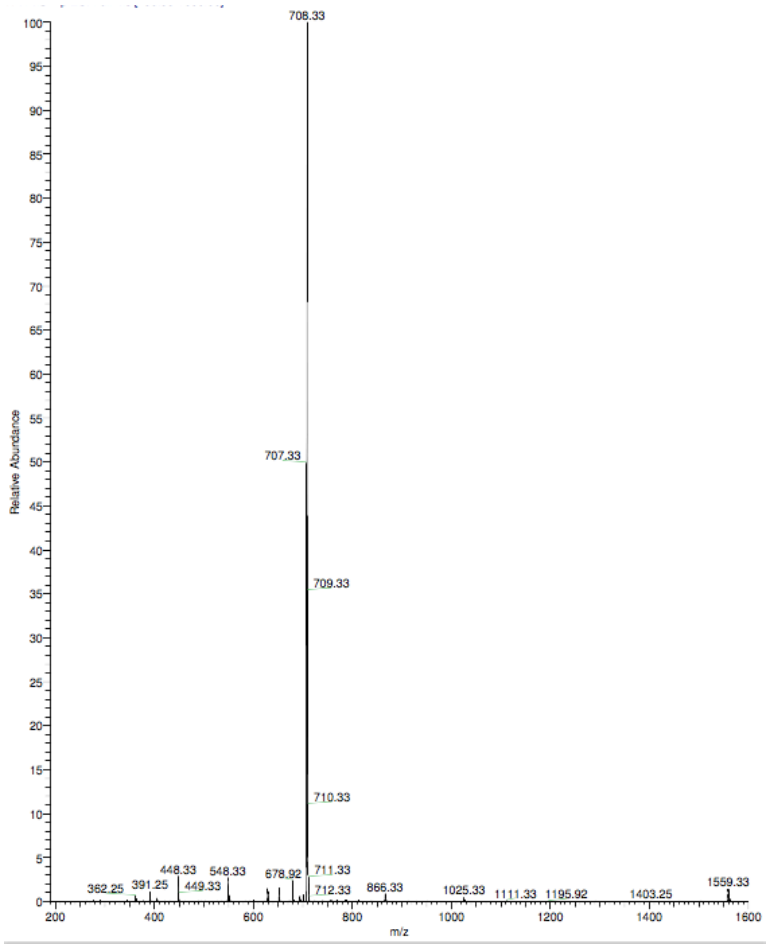

Figure 3.6. Mass spectrometry analysis of Triphenylphosphonium glutathione diethyl ester bromide (Et_2GSSGTPPBr) . Compounds were analyzed under positive ESI-MS conditions. TPP-GSSG-Br showed an $[M+2H]^{2+}$ ion at m/z 708.

The bromine salts of TPP-glutathione derivatives were essentially insoluble in water. To make a water-soluble version that might perform better under physiological conditions, we chose to displace bromine with mesylate ($CH_3SO_3^-$). Mesylate formulations are widely employed to make pharmaceutical preparations more soluble. These are generally considered to be safe when produced with appropriate considerations of experimental procedure [239]. We first attempted to accomplish a counterion exchange as described in other syntheses of TPP-

containing compounds, by mixing the compound with sodium mesylate [240]. We tried collecting both aqueous and non-aqueous layers with little success. Anything recovered from the organic layer remained insoluble in water. Any TPP-glutathione converted to the mesylate salt and found in the aqueous layer proved to be difficult to separate from the sodium mesylate salt itself.

We succeeded using an anion exchange column to exchange the counterion [241]. A column was constructed using about 2.5-3 g of Amberlyst® A-26 (OH form) ion exchange resin. The column was then treated with a 1% solution of methanesulfonic acid until the eluate was of the same pH as the original acid solution. The conversion of TPP-GSSG-Br worked well for small amounts with an approximately 70% yield. Care must be taken with TPP-GSSG-Mes to keep it dry as it is hygroscopic.

3.4 Conclusion

The design of an efficient synthesis of mitochondrially-targeted glutathione derivatives proved to be delightfully challenging. However, once the development was completed, the final synthesis pathway is relatively straightforward, and resulted in good yields with few side products. The procedure, though, is slow due to the long incubation necessary to complete esterification. The synthesis is flexible, allowing the ethyl groups to be replaced with methyl groups. Furthermore, the length of the linker to TPP can be altered to affect the hydrophobicity of the modified glutathione. Further work with these variants of TPP-glutathione in cell culture and mice will help identify the optimal modification to protect against toxic and oxidative insults affecting the mitochondria pool of glutathione.

3.5 Materials and Methods

3.5.1 Reagents

Glutathione disulfide (G4376) was purchased from Sigma-Aldrich (St. Louis), and O-(7-Aza-1H-benzotriazol-1-yl)-N,N,N',N'-tetramethyluronium hexafluorophosphate from Alfa Aesar.

Thionyl chloride (T2040), triethylamine (T0424), *N, N*-diisopropylethylamine (D1599), 4-(carboxybutyl) triphenylphosphonium bromide (C1061), and Tris(2-carboxyethyl)phosphine hydrochloride (T1656) were purchased from TCI America (Portland, OR).

Anhydrous methanol (MX0472-6) and ethyl acetate (EX0241-6) were purchased from EMD Millipore, absolute ethanol (111000200CSPP) from Pharmco-Aaper, and dichloromethane (BDH23373.100E) from VWR.

Amberlyst® A-26 (OH) ion exchange resin was acquired from Sigma Aldrich.

3.5.2 General Experimental

Proton NMR spectra were acquired on a Bruker Ascend 800 MHz NMR spectrometer. Multiplicities in the ^{1}H NMR spectra are described as follows: s = singlet, d = doublet, t = triplet, q = quartet, m = multiplet. Carbon NMR spectra were recorded on a Bruker Ascend 800 MHz spectrometer. Phosphorus NMR spectra were recorded on a Bruker Ascend 500MHz spectrometer. Chemical shifts are reported in parts per million (ppm) (δ) and are referenced to sodium 2,2-dimethyl-2-silapentane-5-sulfonate. Sample concentration was 10mM in phosphate-

buffered saline (PBS), pH 7.4 with 10% D_2O. TPP-GSSG-Br and TPP-GSH-Br are insoluble in water and were run in CD_3OD, referenced to tetramethylsilane (TMS).

Mass spectrometry. ESI-MS was performed on a ThermoFisher LTQ ESI-ion trap mass spectrometer in positive ion mode using LC-MS grade acetonitrile and water (1:1) with 0.1% formic acid.

3.5.3 Syntheses

Glutathione disulfide tetraethyl ester (Et_4GSSG). To a solution of glutathione disulfide (500 mg, 0.816 mmol) in dry ethanol (100mL) at 0 °C, thionyl chloride (5.0 mL, 68.8 mmol) was added very slowly by syringe. The solution was swirled and allowed to react for 9 days at 4 °C. The reaction mixture was concentrated under reduced pressure, and used without further purification (571 mg, 96% yield). ESI-MS of $[M + H]^+$ calculated $[C_{28}H_{48}N_6O_{12}S_2]^+$, 725.28, found 725.58. ^1H NMR (800MHz, PBS, pH 7.4 with 10% D_2O) δ 4.3 (m), 4.20 (q), 4.12 (q), 4.01 (m), 3.25 (dd), 3.00 (dd), 2.59 (m), 2.24 (m), 1.31 (overlapping t), 1.25 (t). ^{13}C NMR δ 176.7, 175.1, 173.6, 172.4, 66.0, 65.0, 62.8, 55.0, 54.8, 44.0, 41.0, 33.2, 28.0, 17.0, 15.7.

Triphenylphosphonium glutathione disulfide tetraethyl ester dibromide ($Et_4GSSGTPP_2Br_2$). To a solution of glutathione disulfide tetraethyl ester (592 mg, 0.818 mmol) in dichloromethane (80 mL) was added 4-(carboxybutyl) triphenylphosphonium bromide (709 mg, 1.6 mmol), O-(7-Aza-1H-benzotriazol-1-yl)-N,N,N',N'-tetramethyluronium hexafluorophosphate 777 mg, 2.04 mmol), and

N,*N*-Diisopropylethylamine (500 μL, 2.9 mmol). The reaction mixture was stirred at room temperature for 90 minutes. The organic layer was washed three times with saturated *aq*. $NaHCO_3$ (80mL), NaBr (80mL), dried over Na_2SO_4, and concentrated under reduced pressure to yield an oily crude. This was dissolved in a minimum of DCM and triturated with EtOAc. The solvents were removed under reduced pressure to yield the final compound (802 mg, 62.5% yield). ESI-MS of $[M + H]^{2+}$ calculated $[C_{74}H_{92}Br_2N_6O_{14}P_2S_2]^{2+}$ 1574.4, found 1574.6.

Triphenylphosphonium glutathione diethyl ester (Et_2GSSGTPPBr). To the crude reaction mixture from the synthesis of triphenylphosphonium tetraethyl ester was added Tris(2-carboxyethyl)phosphine hydrochloride (3 molar equivalents), after the first washing step. The solution was stirred for 24 hours at room temperature. The organic layer was washed two more times was washed with saturated *aq*. $NaHCO_3$ (80mL), one time with NaBr (80mL), dried over Na_2SO_4, and concentrated under reduced pressure to yield a white solid (57% yield). ESI-MS of $[M + H]^+$ calculated $[C_{37}H_{47}BrN_3O_7PS]^+$ 788.21, found 788.33.

Triphenylphosphonium glutathione disulfide tetraethyl ester mesylate (Et_4GSSGTPP_2Mes). To exchange the counteranion and render the compound water-soluble, we performed a halide exchange as described [241]. In brief, a small column was packed with 2.5g Amberlyst A-26 (OH form) anion exchange resin. The column was washed with 1% methanesulfonic acid until the eluate had the

same pH as the original 1% solution. The column was then washed with methanol until the eluate had a constant pH. A solution of TPP-GSSG-Br (145 mg, 0.1 mmol) in 3 mL methanol was slowly applied to the column. The column was then washed with 100 mL methanol. Each 20 mL fraction was checked by mass spectrometry and the collected eluates were concentrated under reduced pressure to yield TPP-GSSG-Mes (100 mg, 68% yield). ESI-MS of $[M + H]^{2+}$ calculated $[C_{76}H_{98}N_6O_{20}P_2S_4]^{2+}$ 1606.52, found 1606.6.^{1}H NMR (800MHz, PBS, pH 7.4, 10%D_2O) δ 7.85 (t), 7.70 (d), 4.23 (m), 4.17 (q), 4.05 (q), 3.98 (d), 3.30 (m), 3.23 (dd), 2.91 (dd), 2.81 (s), 2.32 (t), 2.26 (m), 2.07 (m), 1.90 (m), 1.81 (t), 1.68 (m), 1.23 (t), 1.14 (t). ^{13}C NMR (201 MHz, PBS, pH 7.4, 10%D_2O) δ 175.8, 174.8, 173.1, 172.6, 171.2, 135.1, 133.6, 130.2, 118.2, 117.8, 62.5, 52.4, 41.6, 38.6, 38.0, 34.3, 31.5, 26.2, 21.3, 13.4 ^{31}P NMR (500MHz, PBS, pH 7.4, 10% D_2O) δ 23.06.

Chapter 4

NMR characterization of mitochondrially-targeted oxidized glutathione

Pamela R. Beilby, Patrick N. Reardon, Joseph S. Beckman

4.1 Abstract

We previously described the design and synthesis of a mitochondrially-targeted derivative of oxidized glutathione (Triphenylphosphonium glutathione disulfide tetraethyl ester mesylate). The alterations to glutathione include esterification of the carboxylic acid functional groups and append a large triphenylphosphonium moiety to the amino groups, which more than double the size of the original tripeptide. In this paper, we characterize the changes in dynamics of oxidized glutathione derivatives and examine how the ethyl groups and mitochondrial-targeting moiety alter the dynamic behavior of glutathione in solution. The cysteine residue remained the most restricted region throughout, with little dynamic change as modifications occurred. The glutamate C_α carbon experiences largest alteration in its motion, from being the most freely moving region of glutathione to the most restricted after cysteine.

4.2 Introduction

Glutathione (GSH) is the primary cellular antioxidant and plays a critical role in the maintenance of the intracellular redox balance, as well as defending the cell against toxic insults. This ubiquitous tripeptide is formed in a two-step process mediated by ATP and catalyzed by γ-glutamylcysteine ligase (GCL), followed by the incorporation of glycine by GSH synthase [51-53]. Under physiological conditions, it exists primarily in the reduced form at millimolar concentrations depending on cell type and location, and at 10 to 100 times greater amounts than oxidized glutathione (GSSG).

Glutathione levels decline with age and in many pathological conditions, including Parkinson's disease, multiple sclerosis, Huntington's disease, Alzheimer's disease, and ALS [69, 70, 72, 73, 76-78], but mitochondrial glutathione levels are depleted even more dramatically [66-68]. This specific redox pool does not correspondingly increase as cytosolic levels of glutathione are raised. One previous attempt has been made to target glutathione to mitochondria through a covalent addition of a choline ester to the glycine carboxylic acid [181]. No studies have appeared, however, to demonstrate efficacy of this modification in increasing mitochondrial glutathione levels.

The mitochondrial-targeting functional group, triphenylphosphonium (TPP), has been conjugated to several antioxidants including vitamin E, lipoic acid, and Coenzyme Q (MitoQ) [174, 176, 178] to successfully direct these compounds to

mitochondria. TPP compounds accumulate several hundredfold in mitochondria, driven by the membrane potential (Figure 4.1) [172].

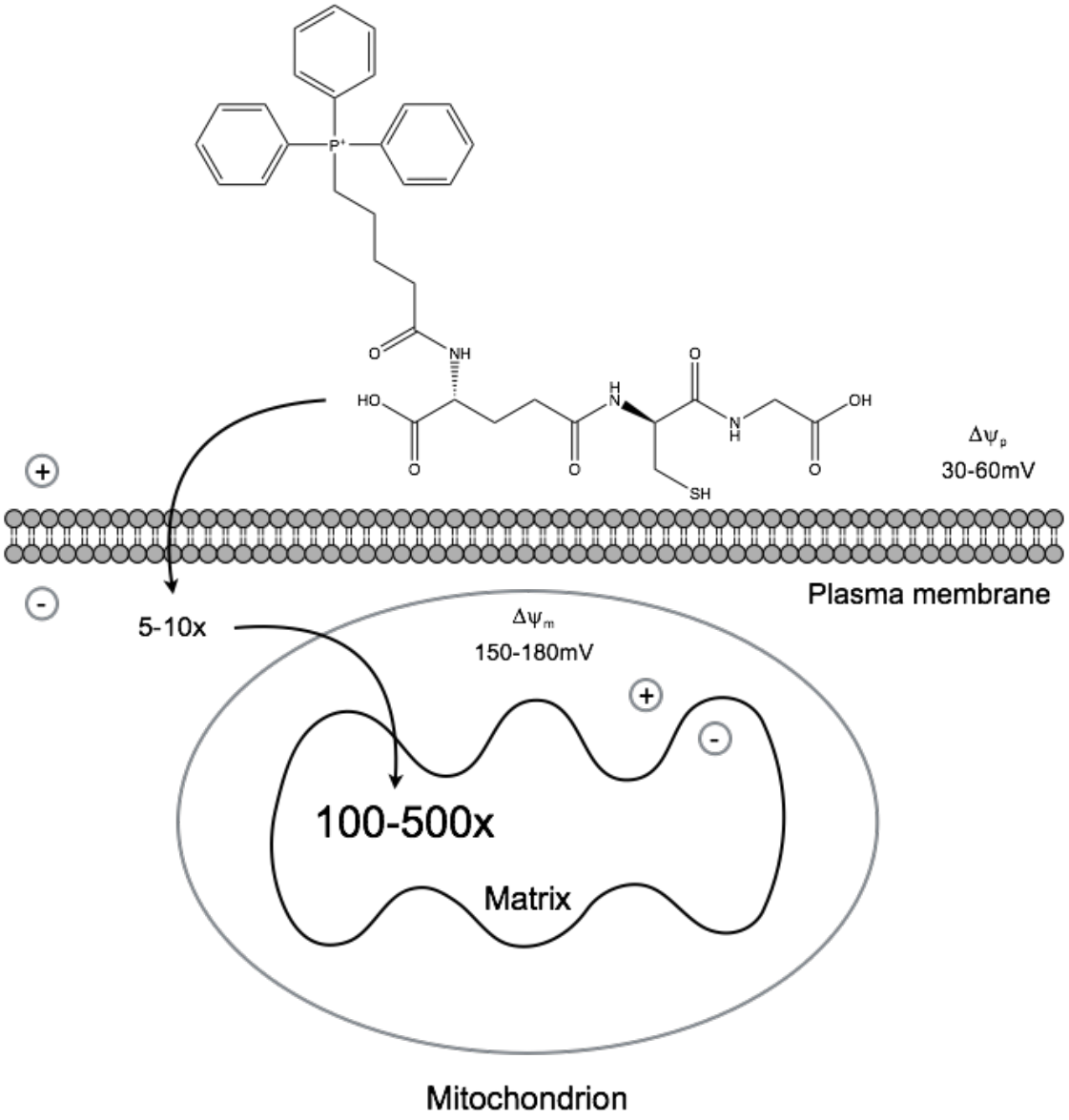

Figure. 4.1. Uptake of triphenylphosphonium (TPP) cations by mitochondria [172]). Figure adapted from [172]. Antioxidants, such as glutathione, may be coupled with TPP, a lipophilic cation, to enhance delivery to mitochondria. In response to the membrane potential, the TPP compound accumulates 5-10-fold in the cytosol and 100-500-fold inside the mitochondrial matrix. These compounds pass through lipid bilayers without a need for active transport.

We have utilized this strategy in developing our glutathione derivative and conjugated this moiety to the amino groups of glutathione disulfide (Figure 4.2) [242]. The use of glutathione disulfide effectively protects the reactive sulfhydryl. Additionally, esterification of the carboxylic acids masks the negative charge of these groups at physiological pH and enhances cell penetration.

NMR has been used in many conformational and dynamics studies of glutathione, but only one study so far examined oxidized glutathione [243]. GSSG can be created by reactions of GSH with electrophiles, as well as through catalysis of hydrogen peroxide reduction by glutathione peroxidase (GPx). The disulfide influences copper homeostasis, particularly during neuronal development [244]. It also participates in non-enzymatic interconversion disulfide exchange with thiolynated proteins [245], and the Cu(II)-GSSG is an inhibitor of the opiate receptor site [246].

The reduced form of glutathione is a conformationally flexible molecule in solution, glutathione disulfide somewhat less so. The previous study of GSSG found the cysteine region to be most restricted in motion. Glycine C_α was less hindered than the two inner glutamate carbons, but the glutamate C_α was the least restrained [243].

However, our new compound increases the molecular weight significantly to more than double that of GSSG alone, and alters all the reactive functional groups as well. In this study, ^{13}C relaxation of protonated carbons was measured with ^{1}H-^{13}C HSQC in a pseudo-3D experiment, for GSSG, glutathione disulfide

tetraethyl ester, and TPP-GSSG to determine changes in dynamic behavior. We report that these modifications to glutathione result in an overall enhanced restriction of motion for the molecule, with the most significant change observed in the Glu C_α carbon.

4.3 Results and Discussion

Three compounds were evaluated in this study: GSSG, Et_4GSSG, and $Et_4GSSGTPP_2Mes$ (Figure 4.2).

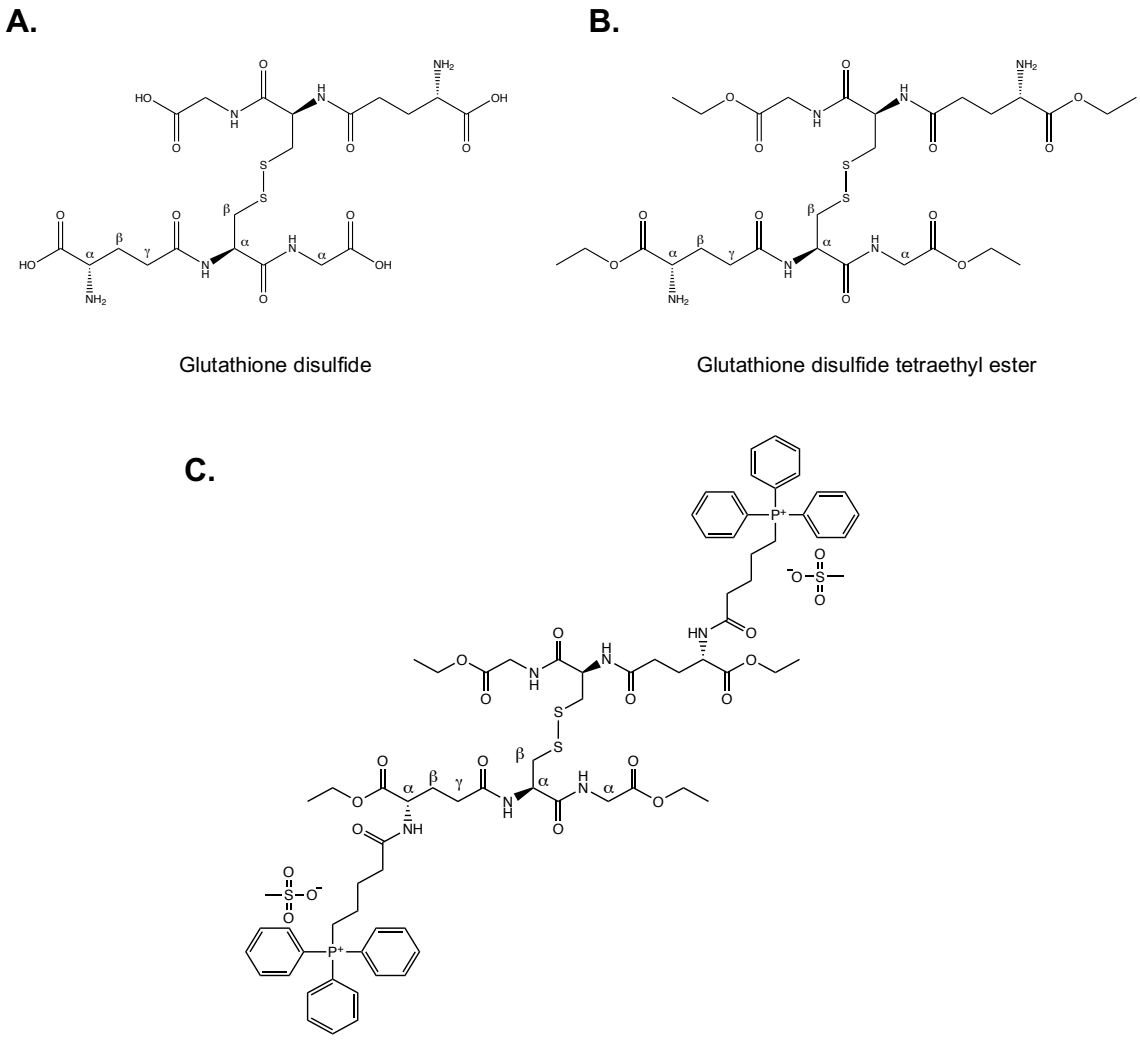

Figure 4.2. Glutathione derivatives. The three increasingly complex glutathione compounds are shown above. **A.** Glutathione disulfide (GSSG) is composed from three amino acids (from left to right along the bottom half of the molecule): glutatmate, cysteine, and glycine. All references in this study are made with respect to the α, β, and/or γ carbons of these residues. **B.** GSSG is modified by the esterification of the carboxylic acids. **C.** Triphenylphosphonium glutathione disulfide tetraethyl ester mesylate contains a mitochondrial-targeting TPP moiety on the amino groups.

The dynamic properties were analyzed by examination of the carbon spin-lattice relaxation times through a series of ^{1}H-^{13}C HSQC spectra. In Figure 3, six carbons forming the basic structure are labeled for their position in the amino acid residue. Carbonyl carbons are not included in these measurements because they do not share a bond with hydrogens, and thus will not appear in HSQC spectra. Also, because the experiments were performed in phosphate-buffered saline (PBS) at pH 7.4 to approximate biological conditions, the Cys C_α is unobservable, because the chemical shift of its proton is lost in the water peak. Therefore, five carbons that can be measured: Glu C_α, C_β, and C_γ; Cys C_β; and Gly C_α.

In each experiment for a single compound, eight measurements (HSQC spectral planes) were made for each of the five carbons. Each HSQC measurement had a different delay time, resulting in a correspondingly changed spin-lattice relaxation time, T_1. The intensities for the carbon peaks fit the function $f(t) = I_o * e^{-t/T1}$. The graphs for each of the five carbons were plotted as the natural log of the intensities (normalized to I_0) versus delay time (Figure 4.3 and 4.4).

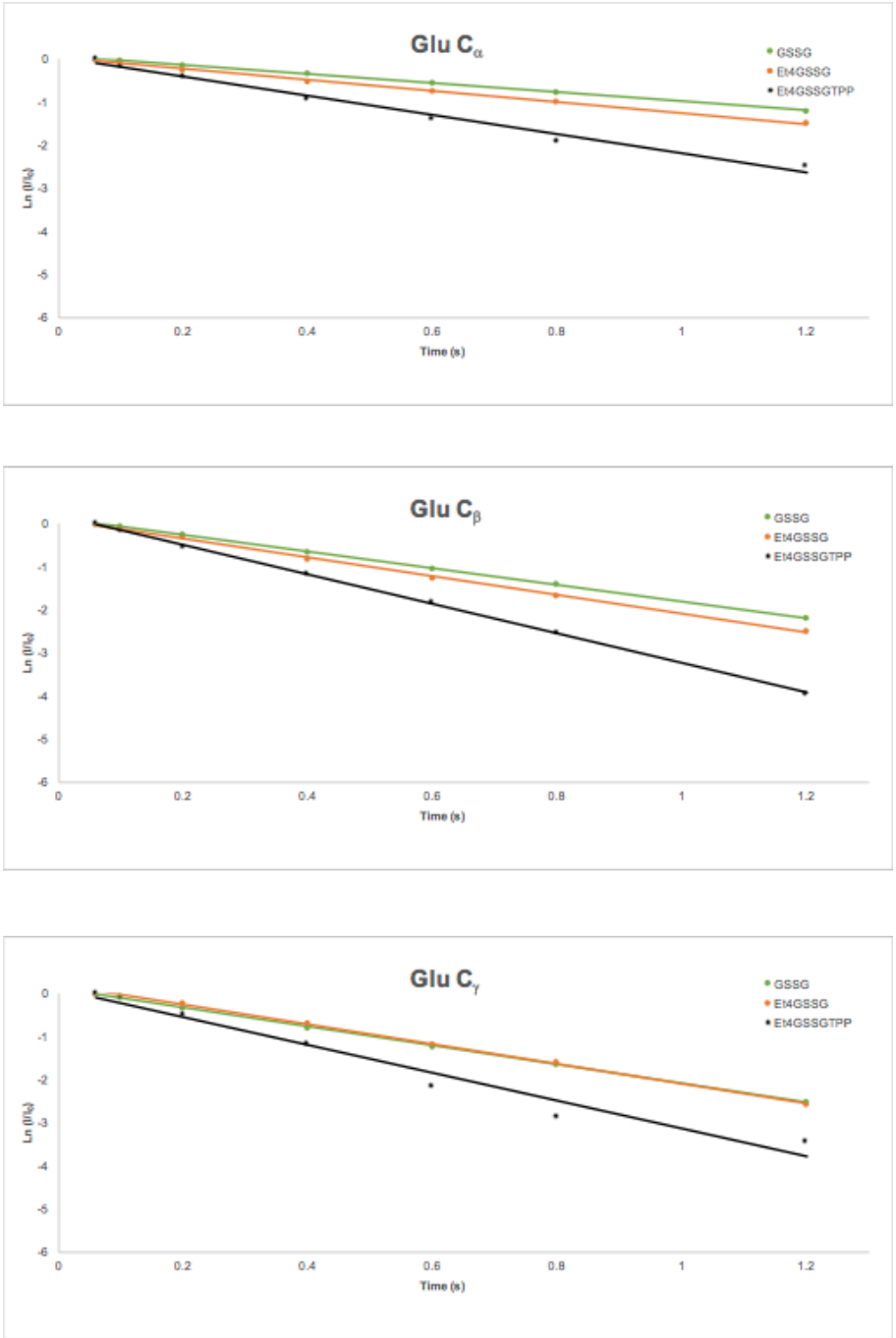

Figure 4.3. Dependence of carbon relaxation rate on delay time for glutamate residue of GSSG, Et_4GSSG, and $Et_4GSSGTPP_2Mes$. Dependence of carbon peak intensity on increasing pulse sequence delay time for pseudo-3D ^{1}H-^{13}C HSQC spin-lattice relaxation time. The fit function of the original data is $f(t) = I_o * e^{-t/T1}$. Data shown as the natural log of this function (normalized to I_0) plotted versus delay time. The negative inverse of the slope is equal to the spin relaxation time, T_1. The α, β, and/or γ carbons are as shown in Figure 4.2. All samples in PBS, pH 7.4, 10% D_2O.

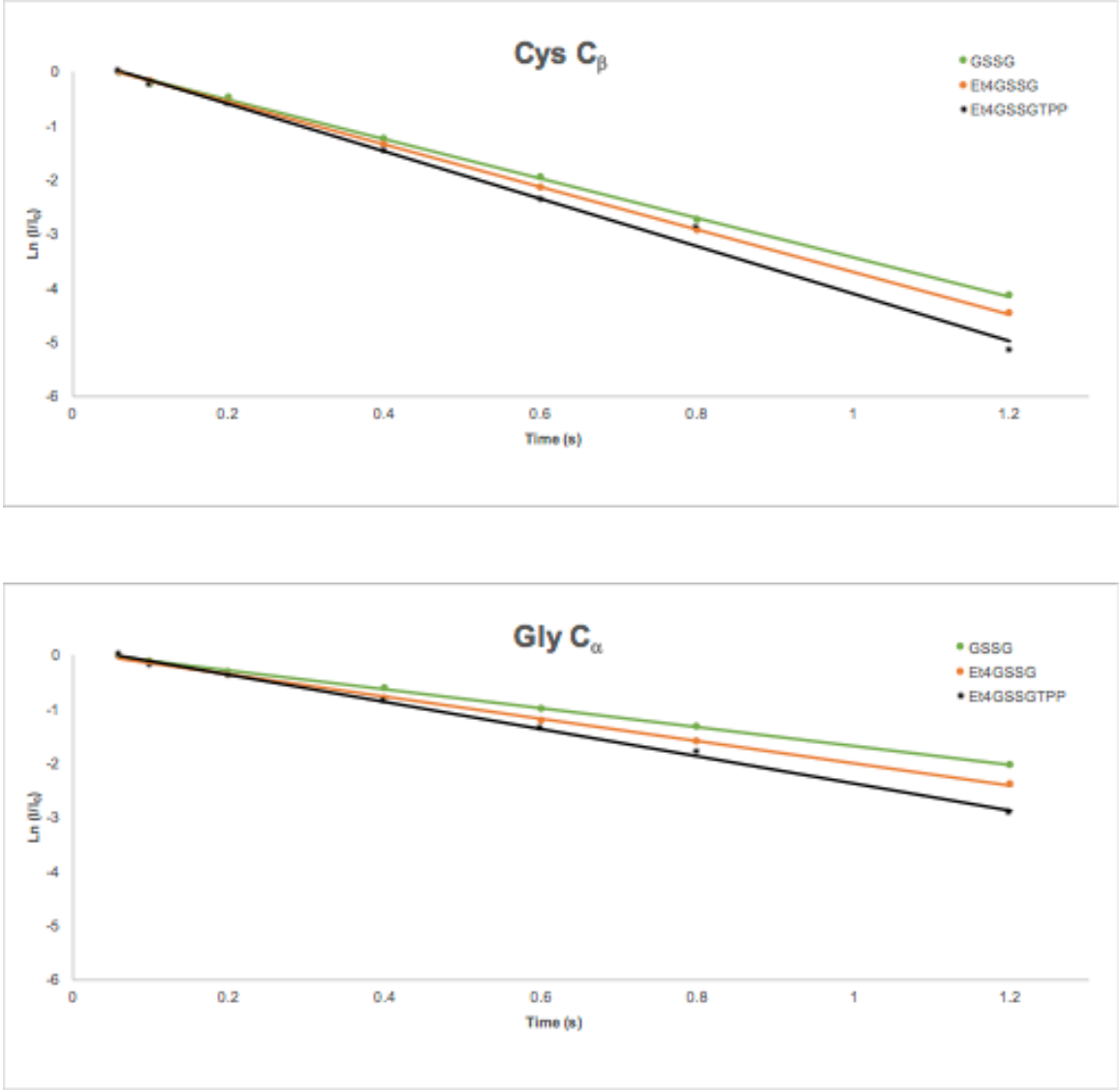

Figure 4.4. Dependence of carbon relaxation rate on delay time for cysteine and glycine residues of GSSG, Et_4GSSG, and Et_4GSSGTPP$_2$Mes. Dependence of carbon peak intensity on increasing pulse sequence delay time for pseudo-3D ^{1}H-^{13}C HSQC spin-lattice relaxation time. The fit function of the original data is $f(t) = I_o * e^{-t/T1}$. Data shown as the natural log of this function (normalized to I_0) plotted versus delay time. The negative inverse of the slope is equal to the spin relaxation time, T_1. The α, β, and/or γ carbons are as shown in Figure 4.2. All samples in PBS, pH 7.4, 10% D_2O.

From these graphs spin-lattice relaxation times for the five carbons from each carbon may now be determined and are summarized in Table 4.1.

Table 4.1. Carbon spin-lattice relaxation times, T_1 (s), for GSSG, Et_4GSSG, and $Et_4GSSGTPP_2Mes$ in PBS, pH 7.4, 10 % D_2O.

Carbon	Chemical Shift (C/H)	GSSG T_1 (s)	Chemical Shift (C/H)	Et_4GSSG T_1 (s)	Chemical Shift (C/H)	$Et_4GSSGTPP_2Mes$ T_1 (s)
Glu C_α	54.5/3.73	0.949	51.9/4.04	0.781	52/4.18	0.448
Glu C_β	26.1/2.08	0.519	26.3/2.15	0.456	26.2/1.73	0.29
Glu C_γ	31.4/2.45	0.452	31.3/2.5	0.432	31.4/2.23	0.309
Cys C_β	39/3.2/2.9	0.276	39/3.17/2.92	0.255	39/3.14/2.83	0.228
Gly C_α	41.7/3.85	0.568	41.7/3.94	0.484	41.7/3.85	0.400

As previously reported with GSSG, the cysteine carbon experiences the greatest restriction in motion. The α-carbon of glutamate has the most freedom, followed by glycine, while the other carbons experience roughly equivalent flexibility.

As oxidized glutathione was modified, the glutamate carbons exhibited reduced flexibility, with the C_α carbon in particular becoming significantly more rigid with the addition of the bulky TPP moiety. Glycine, too, experienced restricted motion with the modifications, but less dramatically than the glutamate carbons. Cysteine underwent little change with modification, as this region was already

characterized by restricted movement. Overall, this novel mitochondrially-targeted glutathione experiences dramatic loss of flexibility in the glutamate residue compared to unaltered oxidized glutathione.

4.4 Conclusion

This study offers a first look at how alterations to oxidized glutathione affect its dynamic behavior. A next step would examine also proton relaxation for corresponding changes in motion. A T_1 ^{13}C relaxation experiment determined with inversion recovery could also provide confirmation of the results presented here. This would also allow visualization of the Cys C_α. The studies could also be extended to acidic and alkaline conditions to understand impact of pH.

Changes in the dynamic behavior of glutathione are observed, which potentially could impact biological processes. The flavoenzyme, glutathione reductase, catalyzes the reduction of GSSG, utilizing NADPH as a cofactor. The primary recognition site is the glutamate group on glutathione [247]. In addition to the TPP moiety alteration to the glutamate amino group, the increased restriction of motion may prevent access to the binding site, ultimately preventing reduction of GSSG. Glutathione plays a role in copper transport and sequestration in the cell. The alterations to glutathione, and the accompanying changes in dynamic behavior, may modify interactions with copper and affect binding constants.

4.5 Experimental

Glutathione disulfide (G4376) was purchased from Sigma-Aldrich. Glutathione disulfide tetraethyl ester and TPP-GSSG were synthesized as described [242] . The compounds were prepared in phosphate-buffered saline (PBS), pH7.4, with 10%D_2O, at a final concentration of 10mM.

NMR spectra were recorded at 25°C on a Bruker Ascend 800MHz spectrometer, operating at 800 MHz for ^{1}H and 201 MHz for ^{13}C. Carbon spin-lattice relaxation times (T_1) were determined using ^{1}H-^{13}C HSQC in a pseudo-3D experiment.

Spectra were processed using TopSpin3.5pl6 (Bruker). The peak intensities were plotted against time in Excel and the resulting exponential curve is described by the following equation: $f(t) = I_o * e^{-t/T1}$, from which T_1 may then be calculated.

Chapter 5

Conclusion

Research in the Beckman lab has revolved around understanding oxidative stress-mediated mechanisms in the ALS disease process. These investigations have focused on essential biological processes and support systems that can go rogue with age and disease progression. What once was necessary to survive, metamorphoses into something that harms and exacerbates the pathological progression.

Astrocytes make up a large portion of the glial cell population. They perform functions critical in maintaining neuronal homeostasis, and provide many trophic factors for neurons, as well as for endothelial cells comprising the blood-brain barrier. They play a role in neurotransmitter signaling, regulating synaptic cleft transmissions. But what happens when astrocytes no longer function adequately?

Astrocytosis characterizes the regions around motor neurons in ALS patients [248]. Oxidative stress plays a role in the transformation of astrocytes to a toxic phenotype. Astrocytes from wildtype rat pups undergo a transition to an inflammatory phenotype when treated with peroxynitrite and become lethal to motor neurons [226]. Prior work from our lab has shown that expression of SOD^{G93A} in astrocytes leads to the death of co-cultured wildtype motor neurons [94]. Although adult motor neurons do not typically express the $p75^{NTR}$ receptor, it is induced in the motor neurons of ALS patients [249]. We discovered that reactive astrocytes surrounding $p75^{NTR}$- expressing motor neurons in the spinal cord of $SOD1^{G93A}$ mice expressed nerve growth factor (NGF) which activates the receptor and leads to neuron death [21].

A long-term goal is to understand how glial cells transform and develop a deleterious phenotype harmful to motor neurons. Glial cells derived from adult animals typically are incapable of further growth. We found, however, that glial cells isolated from the spinal cords of symptomatic adult $SOD1^{G93A}$ rats do indeed rapidly proliferate [30]. These cells expressed some astrocytic markers, such as S100β and glial fibrillary acidic protein (GFAP), but not others like glutamate transporter 1. The aberrant glial cells also secreted soluble factors that were highly toxic to co-cultured non-transgenic motor neurons [30]. Further study of the aberrant glial cells revealed that, not only do they express astrocytic markers, but also markers characteristic of microglia, such as Iba1 and CD11b [20]. When cells were first plated, they exhibited the microglial markers, but after two weeks in cell culture undergo a transition to a more astrocyte-like phenotype. This dual phenotype was also observed in the rat spinal cord of symptomatic animals [20]. The underlying cause of this transition was unclear.

Although glial cells isolated from adult animals generally fail to thrive, our lab found that glial cells isolated from the spinal cord of $SOD1^{WT}$ rats older than one year can also proliferate and appear to express a phenotype similar to the aberrant glial cells described above cells (unpublished data). Age is a risk factor for ALS and these cells can be cultured only from older $SOD1^{WT}$ rats. This led us to postulate the possible involvement of cellular senescence in the anomalous behavior observed in these glial cells.

Cellular senescence is a generally irreversible process whereby cells stop replicating, but continue to function and produce a variety of proinflammatory factors including cytokines, chemokines, and proteases. This inflammatory cocktail is known as the senescence-associated secretory phenotype (SASP). Through the SASP, senescent cells can alter the surrounding tissue microenvironment and trigger pathogenic mechanisms. Recently, cellular senescence has been recognized as an intrinsic component of age-related pathologies, including atherosclerosis, Alzheimer's disease, and cancer. Senescent cells accumulate with age in various tissues and, although ALS risk rises with age, the role of senescent cell accumulation in nervous tissue has not been explored in this context.

My objective was to understand how the accumulation of senescent glial cells impacts ALS disease progression and alters the tissue microenvironment, thereby creating an environment in which toxic glial cells may flourish. The fundamental hypothesis for this project was that a subset of $SOD1^{G93A}$ glial cells activates a formidable senescence program compared to glial cells isolated from $SOD1^{WT}$ or non-transgenic rats and that this drives the transition from a healthy neuroprotective glial cell phenotype to a toxic one within the framework of ALS.

As depicted in Chapter 2, we successfully demonstrated that $SOD1^{G93A}$ spinal cord microglia from symptomatic rats are associated with senescence in the context of ALS. This is the first study to support the age-associated accumulation of a senescent microglial cell population as a driver for spinal cord tissue

microenvironment alterations that lead ultimately to the development of the deleterious glial cell phenotype observed in ALS. However, we have not yet shown that senescence drives the transition. Future studies should include a full examination of the SASP for evidence of factors that may stimulate the development of this aberrant phenotype.

The Beckman lab has also been interested in processes that accelerate the disease process. The most frequently studied mouse model of ALS is the line bearing the G93A mutation to SOD1. $SOD1^{G93A}$ mice become symptomatic around 90 days and then die a few weeks later. The disease process in characterized by mitochondrial dysfunction, gliosis, spinal cord motor neuron loss, and neuromuscular junction decay. Overexpression of the human SOD1, with its requirement for a copper at the active site, creates a demand for copper that the mouse CCS cannot supply. Facilitating copper delivery to SOD1 by increasing CCS would be expected to enhance the activation of SOD1 and ameliorate the disease progression. The exact opposite occurs. Overexpression of CCS in the $SOD1^{G93A}$ mouse line exacerbates the pathology, leading to severe mitochondrial dysfunction and death in about 30 days [152].

In our hands the results are even more dramatic. We have been studying the $SOD1^{G93A}$ x CCS mouse model for several years and the mice rarely live beyond two weeks. A promising compound for treating ALS emerged just a couple years ago - diacetyl-bis(4-methylthiosemicarbazonato) copper (II) [CuATSM]. It had been tested in the $SOD1^{G37R}$ and low-expressing $SOD1^{G93A}$ models, achieving

extension in survival of 26% and 15%, respectively. We began experiments in our accelerated mouse model in 2013 and had remarkable results. When treated from day 5 after birth, mice that should have been dead within three weeks lived over 18 months. In addition to the incredible life extension, astrogliosis and protein nitration were reduced, and cytochrome *c* oxidase activity levels were restored [28]. This experiment involved nearly three years of work requiring treatment of mice twice daily with careful coordination. Our success with CuATSM has provided a strong rationale for therapy development and the early safety studies in humans showing promising trends. Currently, we are designing CuATSM derivatives to enhance the effects provided by CuATSM.

Another route to exacerbate the disease process is through glutathione depletion. Glutathione homeostasis is necessary for motor neuron survival. $SOD1^{G93A}$ transgenic astrocytes are toxic to motor neurons in part through an NGF-$p75^{NTR}$-mediated pathway [21]. We found that these astrocytes produced equivalent amounts of glutathione as non-transgenic astrocytes, but produced almost twice as much nitric oxide [94]. When they were treated with *tert*-butylhydroquinone (tBHQ), a well-characterized activator of Nrf2, for 24 hours prior to motor neuron plating, it resulted in prevention of motor neuron loss. This protection was negated by treatment of the cells with buthionine sulfoximine (BSO), an inhibitor of glutathione synthesis [94]. Additionally, we know that administration of ethacrynic acid or BSO to motor neuron-like cells depletes glutathione and leads to motor neuron apoptosis [93]. As described in chapter 1,

all enzymes involved in glutathione metabolism are affected to some degree in the disease process, and glutathione levels in motor neurons and glial cells are frequently lower than in healthy, age-matched controls.

To directly study how glutathione depletion accelerates the disease process in ALS, a double transgenic animal was created that expressed both the SOD^{G93A} mutation and a knockout of the gene coding for the regulatory subunit of gamma-gultamyl cysteine ligase (GCL). GCL is the enzyme catalyzing the first step in glutathione biosynthesis, and the ensuing formation of γ-glutamylcysteine is rate limiting [250]. GCL is composed of two subunits, a catalytic subunit (GCLC) and a regulatory one (GCLM). Deletion of GCLC is lethal, but knockout mice for GCLM are viable with significantly reduced glutathione levels [251]. $SOD1^{G93A}$ x GCLM (-/-) mice have significantly reduced lifespans compared to the G93A mutation alone and severe mitochondrial pathology [77]. Survival is decreased from 136 days to 59 days, and astrocyte reactivity is also accelerated, appearing at 30 days. Total glutathione levels are decreased 70-80% in the central nervous system, with a reduction in spinal cord mitochondrial glutathione of 80%.

The fundamental importance of glutathione in the ALS disease process has motivated our development of cell-penetrant, mitochondrially-targeted glutathione derivatives. The many attempts to raise glutathione levels as a therapy for ALS have had limited success. This is presumably due to mitochondrial levels of glutathione being unaffected in these treatments.

My goal when starting this project was to synthesize a mitochondrially-targeted glutathione derivative and then validate this compound in cell culture and animal models, including the $SOD1^{G93A}$ x GCLM (-/-) line. A synthesis process has been designed and is described in the patent [252], but understanding how this compound functions in cell culture and *in vivo* requires further optimization. Evaluating mitochondrial uptake of the glutathione derivatives, and success in defending against oxidative insult caused by age, disease, or chemical interventions, will be crucial in informing the evolution of subsequent generations of compounds.

Strategies to enhance delivery of these compounds include modifying the alkyl linker of the TPP moiety, changing the location of the TPP conjugation, adding additional TPP units, and further modification of other charged residues. Adjusting the TPP-alkyl linker length impacts how the compound interacts with plasma and mitochondrial membranes. The location of the TPP moiety could alter how closely the TPP-glutathione can imitate unmodified glutathione in serving as an enzyme substrate or co-factor. We have also begun to develop fluorescent derivatives to more easily allow observation of cellular uptake and localization.

In an ideal world, the research presented here would come full circle, and mitochondrially-targeted glutathione would mitigate accumulation of senescent cells with age and in degenerative diseases of aging, like ALS. Oxidative stress and mitochondrial dysfunction are associated with increased senescence [253]. Disturbances in glutathione homeostasis also contribute to cellular senescence.

As fumarate accumulates, it binds glutathione, forming succinicGSH. Chronic glutathione depletion due to long-term succination of glutathione leads to senescence in cell culture and in fumarate hydratase (FH)-deficient mice [254]. Caveolin-1 inhibition of Nrf2, a regulator of glutathione synthesis, fosters initiation of oxidative stress-induced premature senescence [255]. In colorectal cancer cells, glutathione depletion is accompanied by increased senescence [256]. It is to be hoped that this link between glutathione and senescence will continue to be examined, particularly in the context of aging and neurodegeneration.

A potential scenario describing the interconnection between oxidative stress, glutathione, and cellular senescence is shown below (Figure 5.1). In the context of ALS, this cycle likely occurs in the glial cells, and contributes to their toxicity towards motor neurons. Oxidative stress in glial cells has a reciprocal relationship with both glutathione and senescence. However, although some studies do indicate a direct link between glutathione depletion and senescent cell accumulation, this has not yet been shown in ALS or other neurodegenerative diseases.

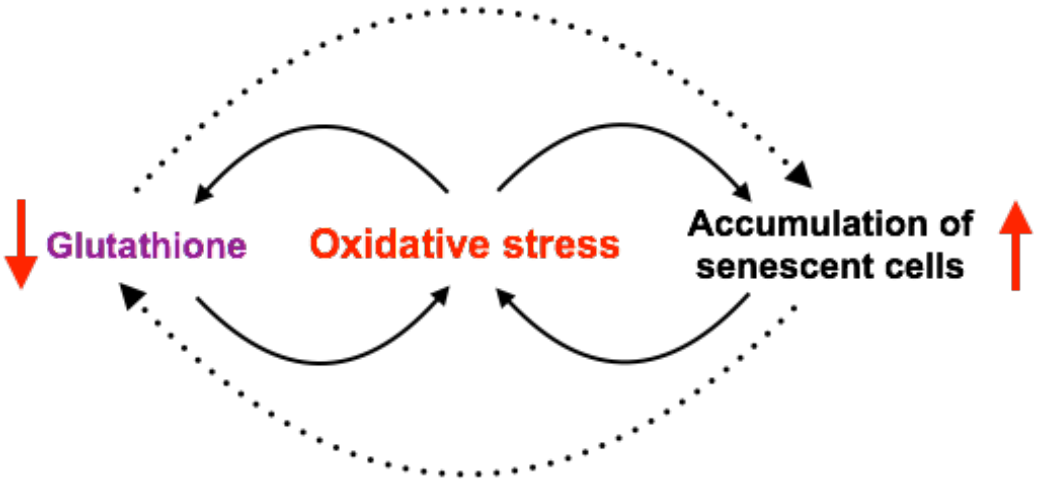

Figure 5.1. Relationship between glutathione, oxidative stress and cellular senescence. As glutathione levels decline, oxidative stress increases as the primary cellular antioxidant is no longer functioning optimally. Chronic oxidative stress drives accumulation of senescent cells over time, which in turn increases oxidative damage in the surrounding tissue microenvironment. Increasing oxidative stress precipitates further glutathione depletion, restarting the damaging cycle. The dotted lines depict a tentative link that requires further elucidation.

As we continue to enhance the mitochondrially-targeted glutathione and deliver glutathione derivatives to the cell, I anticipate augmented deterrence to oxidative stress and cellular senescence, and development of a new therapeutic agent for neurodegeneration and other rogue inflammatory conditions.

Bibliography

[1] Kaseman, D. NMR:Theory. *Chemistry LibreTexts*. Web: UCDavis; 2015.
[2] Rowland, L. P. How Amyotrophic Lateral Sclerosis Got Its Name. *Arch Neurol* **58:**512-515; 2001.
[3] Wijesekera, L. C.; Leigh, P. N. Amyotrophic lateral sclerosis. *Orphanet J Rare Dis* **4**; 2009.
[4] Rosen, D. R.; Siddique, T.; Patterson, D.; Figlewicz, D. A.; Sapp, P.; Hentati, A.; Donaldson, D.; Goto, J.; O'Regan, J. P.; Deng, H. X.; Rahmani, Z.; Krizus, A.; McKenna-Yasek, D.; Cayabyab, A.; Gaston, S. M.; Berger, R.; Tanzi, R. E.; Halperin, J. J.; Herzfeldt, B.; Van den Bergh, R.; Hung, W. Y.; Bird, T.; Deng, G.; Mulder, D. W.; Smyth, C.; Laing, N. G.; Soriano, E.; Pericak-Vance, M. A.; Haines, J.; Rouleau, G. A.; Gusella, J. S.; Horvitz, H. R.; Brown, R. H., Jr. Mutations in Cu:Zn superoxide dismutase gene are associated with familial amyotrophic lateral sclerosis. *Nature* **362:**59-62; 1993.
[5] Sreedharan, J.; Blair, I. P.; Tripathi, V. B.; Hu, X.; Vance, C.; Rogelj, B.; Ackerley, S.; Durnall, J. C.; Williams, K. L.; Buratti, E.; Baralle, F.; de Belleroche, J.; Mitchell, J. D.; Leigh, P. N.; Al-Chalabi, A.; Miller, C. C.; Nicholson, G.; Shaw, C. E. TDP-43 mutations in familial and sporadic amyotrophic lateral sclerosis. *Science* **319:**1668-1672; 2008.
[6] Vance, C.; Rogelj, B.; Hortobágyi, T.; De Vos, K. J.; Nishimura, A. L.; Sreedharan, J.; Hu, X.; Smith, B.; Ruddy, D.; Wright, P.; Ganesalingam, J.; Williams, K. L.; Tripathi, V. B.; Al-Saraj, S.; Al-Chalabi, A.; Leigh, P. N.; Blair, I. P.; Nicholson, G.; de Belleroche, J.; Gallo, J. M.; Miller, C. C.; Shaw, C. E. Mutations in FUS, an RNA processing protein, cause familial amyotrophic lateral sclerosis type 6. *Science* **323:**1208-1211; 2009.
[7] Maruyama, H.; Morino, H.; Ito, H.; Izumi, Y.; Kato, H.; Watanabe, Y.; Kinoshita, Y.; Kamada, M.; Nodera, H.; Suzuki, H.; Komure, O.; Matsuura, S.; Kobatake, K.; Morimoto, N.; Abe, K.; Suzuki, N.; Aoki, M.; Kawata, A.; Hirai, T.; Kato, T.; Ogasawara, K.; Hirano, A.; Takumi, T.; Kusaka, H.; Hagiwara, K.; Kaji, R.; Kawakami, H. Mutations of optineurin in amyotrophic lateral sclerosis. *Nature* **465:**223-226; 2010.
[8] Puls, I.; Jonnakuty, C.; LaMonte, B. H.; Holzbaur, E. L.; Tokito, M.; Mann, E.; Floeter, M. K.; Bidus, K.; Drayna, D.; Oh, S. J.; Brown, R. H., Jr.; Ludlow, C. L.; Fischbeck, K. H. Mutant dynactin in motor neuron disease. *Nat Genet* **33:**455-456; 2003.
[9] Vinsant, S.; Mansfield, C.; Jimenez-Moreno, R.; Del Gaizo Moore, V.; Yoshikawa, M.; Hampton, T. G.; Prevette, D.; Caress, J.; Oppenheim, R. W.; Milligan, C. Characterization of early pathogenesis in the SOD1(G93A) mouse model of ALS: part II, results and discussion. *Brain Behav* **3:**431-457; 2013.
[10] Cassina, P.; Cassina, A.; Pehar, M.; Castellanos, R.; Gandelman, M.; de Leon, A.; Robinson, K. M.; Mason, R. P.; Beckman, J. S.; Barbeito, L.; Radi, R. Mitochondrial dysfunction in SOD1G93A-bearing astrocytes promotes motor

neuron degeneration: prevention by mitochondrial-targeted antioxidants. *J Neurosci* **28:**4115-4122; 2008.
[11] Tradewell, M. L.; Cooper, L. A.; Minotti, S.; Durham, H. D. Calcium dysregulation, mitochondrial pathology and protein aggregation in a culture model of amyotrophic lateral sclerosis: mechanistic relationship and differential sensitivity to intervention. *Neurobiol Dis* **42:**265-275; 2011.
[12] Nguyen, K. T.; Garcia-Chacon, L. E.; Barrett, J. N.; Barrett, E. F.; David, G. The Psi(m) depolarization that accompanies mitochondrial Ca2+ uptake is greater in mutant SOD1 than in wild-type mouse motor terminals. *Proc Natl Acad Sci U S A* **106:**2007-2011; 2009.
[13] Luo, G.; Yi, J.; Ma, C.; Xiao, Y.; Yi, F.; Yu, T.; Zhou, J. Defective mitochondrial dynamics is an early event in skeletal muscle of an amyotrophic lateral sclerosis mouse model. *PLoS One* **8:**e82112; 2013.
[14] Vande Velda, C.; Miller, T. M.; Cashman, N. R.; Cleveland, D. W. Selective association of misfolded ALS-linked mutant SOD1 with the cytoplasmic face of mitochondria. *Proc Natl Acad Sci USA* **105:**4022-4027; 2008.
[15] Sotelo-Silveira, J. R.; Lepanto, P.; Elizondo, V.; Horjales, S.; Palacios, F.; Martinez-Palma, L.; Marin, M.; Beckman, J. S.; Barbeito, L. Axonal mitochondrial clusters containing mutant SOD1 in transgenic models of ALS. *Antioxid Redox Signal* **11:**1535-1545; 2009.
[16] Filezac de L'Etang, A.; Maharjan, N.; Cordeiro Brana, M.; Ruegsegger, C.; Rehmann, R.; Goswami, A.; Roos, A.; Troost, D.; Schneider, B. L.; Weis, J.; Saxena, S. Marinesco-Sjogren syndrome protein SIL1 regulates motor neuron subtype-selective ER stress in ALS. *Nat Neurosci* **18:**227-238; 2015.
[17] Saxena, S.; Cabuy, E.; Caroni, P. A role for motoneuron subtype-selective ER stress in disease manifestations of FALS mice. *Nat Neurosci* **12:**627-636; 2009.
[18] Clark, J. A.; Southam, K. A.; Blizzard, C. A.; King, A. E.; Dickson, T. C. Axonal degeneration, distal collateral branching and neuromuscular junction architecture alterations occur prior to symptom onset in the SOD1(G93A) mouse model of amyotrophic lateral sclerosis. *J Chem Neuroanat* **76:**35-47; 2016.
[19] Haidet-Phillips, A. M.; Hester, M. E.; Miranda, C. J.; Meyer, K.; Braun, L.; Frakes, A.; Song, S.; Likhite, S.; Murtha, M. J.; Foust, K. D.; Rao, M.; Eagle, A.; Kammescheidt, A.; Christensen, A.; Mendell, J. R.; Burghes, A. H.; Kaspar, B. K. Astrocytes from familial and sporadic ALS patients are toxic to motor neurons. *Nat Biotechnol* **29:**824-828; 2011.
[20] Trias, E.; Diaz-Amarilla, P.; Olivera-Bravo, S.; Isasi, E.; Drechsel, D. A.; Lopez, N.; Bradford, C. S.; Ireton, K. E.; Beckman, J. S.; Barbeito, L. Phenotypic transition of microglia into astrocyte-like cells associated with disease onset in a model of inherited ALS. *Front Cell Neurosci* **7:**274; 2013.
[21] Pehar, M.; Cassina, P.; Vargas, M. R.; Castellanos, R.; Viera, L.; Beckman, J. S.; Estevez, A. G.; Barbeito, L. Astrocytic production of nerve growth factor in motor neuron apoptosis: implications for amyotrophic lateral sclerosis. *J Neurochem* **89:**464-473; 2004.

[22] Liao, B.; Zhao, W.; Beers, D. R.; Henkel, J. S.; Appel, S. H. Transformation from a neuroprotective to a neurotoxic microglial phenotype in a mouse model of ALS. *Exp Neurol* **237:**147-152; 2012.
[23] Frakes, A. E.; Ferraiuolo, L.; Haidet-Phillips, A. M.; Schmelzer, L.; Braun, L.; Miranda, C. J.; Ladner, K. J.; Bevan, A. K.; Foust, K. D.; Godbout, J. P.; Popovich, P. G.; Guttridge, D. C.; Kaspar, B. K. Microglia induce motor neuron death via the classical NF-kappaB pathway in amyotrophic lateral sclerosis. *Neuron* **81:**1009-1023; 2014.
[24] Beal, M. F.; Ferrante, R. J.; Browne, S. E.; Matthews, R. T.; Kowall, N. W.; Brown, R. H., Jr. Increased 3-nitrotyrosine in both sporadic and familial amyotrophic lateral sclerosis. *Ann Neurol* **42:**644-654; 1997.
[25] Bogdanov, M.; Brown, R. H.; Matson, W.; Smart, R.; Hayden, D.; O'Donnell, H.; Beal, M. F.; Cudkowicz, M. Increased oxidative damage to DNA in ALS patients. *Free Radic Biol Med* **29:**652-658; 2000.
[26] Simpson, E. P.; Henry, Y. K.; Henkel, J. S.; Smith, R. G.; Appel, S. H. Increased lipid peroxidation in sera of ALS patients- a potential biomarker of disease burden. *Neurology* **62:**1758-1765; 2004.
[27] Pehar, M.; Vargas, M. R.; Robinson, K. M.; Cassina, P.; Diaz-Amarilla, P. J.; Hagen, T. M.; Radi, R.; Barbeito, L.; Beckman, J. S. Mitochondrial superoxide production and nuclear factor erythroid 2-related factor 2 activation in p75 neurotrophin receptor-induced motor neuron apoptosis. *J Neurosci* **27:**7777-7785; 2007.
[28] Williams, J. R.; Trias, E.; Beilby, P. R.; Lopez, N. I.; Labut, E. M.; Bradford, C. S.; Roberts, B. R.; McAllum, E. J.; Crouch, P. J.; Rhoads, T. W.; Pereira, C.; Son, M.; Elliott, J. L.; Franco, M. C.; Estevez, A. G.; Barbeito, L.; Beckman, J. S. Copper delivery to the CNS by CuATSM effectively treats motor neuron disease in SOD(G93A) mice co-expressing the Copper-Chaperone-for-SOD. *Neurobiol Dis* **89:**1-9; 2016.
[29] Franco, M. C.; Ye, Y.; Refakis, C. A.; Feldman, J. L.; Stokes, A. L.; Basso, M.; Melero Fernández de Mera, R. M.; Sparrow, N. A.; Calingasan, N. Y.; Kiaei, M.; Rhoads, T. W.; Ma, T. C.; Grumet, M.; Barnes, S.; Beal, M. F.; Beckman, J. S.; Mehl, R. A.; Estévez, A. G. Nitration of Hsp90 induces cell death. *Proc Natl Acad Sci U S A* **110:**E1102-1111; 2013.
[30] Díaz-Amarilla, P.; Olivera-Bravo, S.; Trias, E.; Cragnolini, A.; Martinez-Palma, L.; Cassina, P.; Beckman, J.; Barbeito, L. Phenotypically aberrant astrocytes that promote motoneuron damage in a model of inherited amyotrophic lateral sclerosis. *Proc Natl Acad Sci U S A* **108:**18126-18131; 2011.
[31] Yamanaka, K.; Chun, S. J.; Boillee, S.; Fujimori-Tonou, N.; Yamashita, H.; Gutmann, D. H.; Takahashi, R.; Misawa, H.; Cleveland, D. W. Astrocytes as determinants of disease progression in inherited amyotrophic lateral sclerosis. *Nat Neurosci* **11:**251-253; 2008.
[32] Huie, R. E.; Padmaja, S. The reaction of no with superoxide. *Free Radic Res Commun* **18:**195-199; 1993.

[33] Hayflick, L.; Moorhead, P. S. The serial cultivation of human diploid cell strains. *Exp Cell Res* **25:**585-621; 1961.
[34] Campisi, J.; d'Adda di Fagagna, F. Cellular senescence: when bad things happen to good cells. *Nat Rev Mol Cell Biol* **8:**729-740; 2007.
[35] Rodier, F.; Campisi, J. Four faces of cellular senescence. *J Cell Biol* **192:**547-556; 2011.
[36] Jeyapalan, J. C.; Ferreira, M.; Sedivy, J. M.; Herbig, U. Accumulation of senescent cells in mitotic tissue of aging primates. *Mech Ageing Dev* **128:**36-44; 2007.
[37] Wang, C.; Jurk, D.; Maddick, M.; Nelson, G.; Martin-Ruiz, C.; von Zglinicki, T. DNA damage response and senescence in tissues of aging mice. *Aging Cell* **8:**311-323; 2009.
[38] Muñoz-Espin, D.; Serrano, M. Cellular senescence: from physiology to pathology. *Nat Rev Mol Cell Biol* **15:**482-496; 2014.
[39] Sone, H.; Kagawa, Y. Pancreatic beta cell senescence contributes to the pathogenesis of type 2 diabetes in high-fat diet-induced diabetic mice. *Diabetologia* **48:**58-67; 2005.
[40] Kassem, M.; Marie, P. J. Senescence-associated intrinsic mechanisms of osteoblast dysfunctions. *Aging Cell* **10:**191-197; 2011.
[41] Baker, D. J.; Wijshake, T.; Tchkonia, T.; LeBrasseur, N. K.; Childs, B. G.; van de Sluis, B.; Kirkland, J. L.; van Deursen, J. M. Clearance of p16Ink4a-positive senescent cells delays ageing-associated disorders. *Nature* **479:**232-236; 2011.
[42] Bernet, J. D.; Doles, J. D.; Hall, J. K.; Kelly Tanaka, K.; Carter, T. A.; Olwin, B. B. p38 MAPK signaling underlies a cell-autonomous loss of stem cell self-renewal in skeletal muscle of aged mice. *Nat Med* **20:**265-271; 2014.
[43] Cosgrove, B. D.; Gilbert, P. M.; Porpiglia, E.; Mourkioti, F.; Lee, S. P.; Corbel, S. Y.; Llewellyn, M. E.; Delp, S. L.; Blau, H. M. Rejuvenation of the muscle stem cell population restores strength to injured aged muscles. *Nat Med* **20:**255-264; 2014.
[44] Chinta, S. J.; Lieu, C. A.; Demaria, M.; Laberge, R. M.; Campisi, J.; Andersen, J. K. Environmental stress, ageing and glial cell senescence: a novel mechanistic link to Parkinson's disease? *J Intern Med* **273:**429-436; 2013.
[45] Bhat, R.; Crowe, E. P.; Bitto, A.; Moh, M.; Katsetos, C. D.; Garcia, F. U.; Johnson, F. B.; Trojanowski, J. Q.; Sell, C.; Torres, C. Astrocyte senescence as a component of Alzheimer's disease. *PLoS One* **7:**e45069; 2012.
[46] Coppe, J. P.; Desprez, P. Y.; Krtolica, A.; Campisi, J. The senescence-associated secretory phenotype: the dark side of tumor suppression. *Annu Rev Pathol* **5:**99-118; 2010.
[47] Tchkonia, T.; Zhu, Y.; van Deursen, J.; Campisi, J.; Kirkland, J. L. Cellular senescence and the senescent secretory phenotype: therapeutic opportunities. *J Clin Invest* **123:**966-972; 2013.

[48] Freund, A.; Orjalo, A. V.; Desprez, P. Y.; Campisi, J. Inflammatory networks during cellular senescence: causes and consequences. *Trends Mol Med* **16:**238-246; 2010.
[49] Burton, D. G. Cellular senescence, ageing and disease. *Age (Dordr)* **31:**1-9; 2009.
[50] Meister, A. On the discovery of glutathione. *Trends Biochem Sci* **13:**185-188; 1988.
[51] Snoke, J. E., Bloch, K. Formation and utilization of gamma-glutamylcysteine in glutathione synthesis. *J. Biol. Chem.* **199:**407-414; 1952.
[52] Snoke, J. E., Yanari, S., Bloch, K. Synthesis of Glutathione from Gamma-glutamylcysteine. *J. Biol. Chem* **201:**573-586; 1953.
[53] Snoke, J. E., Bloch, K. Studies on the mechanism of action of glutathione synthetase. *J. Biol. Chem* **213:**825-835; 1955.
[54] Anderson, M. E.; Underwood, M.; Bridges, R. J.; Meister, A. Glutathione metabolism at the blood-cerebrospinal fluid barrier. *FASEB J.* **3:**2527-2531; 1989.
[55] Aoyama, K.; Nakaki, T. Impaired glutathione synthesis in neurodegeneration. *Int J Mol Sci* **14:**21021-21044; 2013.
[56] Dringen, R.; Pawlowski, P. G.; Hirrlinger, J. Peroxide detoxification by brain cells. *J Neurosci Res* **79:**157-165; 2005.
[57] Hirrlinger, J.; Gutterer, J. M.; Kussmaul, L.; Hamprecht, B.; Dringen, R. Microglial cells in culture express a prominent glutathione system for the defense against reactive oxygen species. *Dev Neurosci* **22:**384-392; 2000.
[58] Tirmenstein, M. A. a. R., D.J. The glutathione status of rat kidney nuclei following administration of buthionine sulfoximine. *Biochem. Biophys. Res. Comm.* **155:**956-961; 1988.
[59] Bellomo, G., Vairetti, M., Stivala, L., Mirabelli, F., Richelmi, P., and Orrenius, S. Demonstration of nuclear compartimentalization of glutathione in hepatocytes. *Proc. Natl. Acad. Sci.* **89:**4412-4416; 1992.
[60] Hwang, C., Sinskey, A.J., Lodish, H.F. Oxidized redox state of glutathione in the endoplasmic reticulum. *Sci.* **257:**1496-1502; 1992.
[61] Jocelyn, P. C. a. K., A. The non-protein thiol of rat liver mitochondria. *Biochim. Biophys. Acta* **343:**356-362; 1974.
[62] Meredith, M. J. a. R., D.J. Status of the mitochondrial pool of glutathione in the isolated hepatocyte. *J. Biol. Chem* **257:**3747-3753; 1982.
[63] Schafer, F. Q.; Buettner, G. R. Redox environment of the cell as viewed through the redox state of the glutathione disulfide/glutathione couple. *Free Radic Biol Med* **30:**1191-1112; 2001.
[64] Go, Y. M.; Jones, D. P. Redox compartmentalization in eukaryotic cells. *Biochim Biophys Acta* **1780:**1273-1290; 2008.
[65] Kemp, M.; Go, Y. M.; Jones, D. P. Nonequilibrium thermodynamics of thiol/disulfide redox systems: a perspective on redox systems biology. *Free Radic Biol Med* **44:**921-937; 2008.

[66] Paredes, J.; Jones, D. P.; Wilson, M. E.; Herndon, J. G. Age-related alterations of plasma glutathione and oxidation of redox potentials in chimpanzee (Pan troglodytes) and rhesus monkey (Macaca mulatta). *Age (Dordr)* **36:**719-732; 2014.
[67] Jones, D. P.; Mody, V. C., Jr.; Carlson, J. L.; Lynn, M. J.; Sternberg, P., Jr. Redox analysis of human plasma allows separation of pro- oxidant events of aging from decline in antioxidant defenses. *Free Radic Biol Med* **33:**1290-1300; 2002.
[68] Suh, J. H.; Shenvi, S. V.; Dixon, B. M.; Liu, H.; Jaiswal, A. K.; Liu, R. M.; Hagen, T. M. Decline in transcriptional activity of Nrf2 causes age-related loss of glutathione synthesis, which is reversible with lipoic acid. *Proc Natl Acad Sci U S A* **101:**3381-3386; 2004.
[69] Zeevalk, G. D.; Razmpour, R.; Bernard, L. P. Glutathione and Parkinson's disease: is this the elephant in the room? *Biomed Pharmacother* **62:**236-249; 2008.
[70] Martin, H. L.; Teismann, P. Glutathione--a review on its role and significance in Parkinson's disease. *FASEB J* **23:**3263-3272; 2009.
[71] Ceballos-Picot, I.; Witko-Sarsat, V.; Merad-Boudia, M.; Nguyen, A. T.; Thévenin, M.; Jaudon, M. C.; Zingraff, J.; Verger, C.; Jungers, P.; Descamps-Latscha, B. Glutathione antioxidant system as a marker of oxidative stress in chronic renal failure. *Free Radic Biol Med* **21:**845-853; 1996.
[72] Peña-Sánchez, M.; Riverón-Forment, G.; Zaldívar-Vaillant, T.; Soto-Lavastida, A.; Borrero-Sánchez, J.; Lara-Fernández, G.; Esteban-Hernández, E. M.; Hernández-Díaz, Z.; González-Quevedo, A.; Fernández-Almirall, I.; Pérez-López, C.; Castillo-Casañas, Y.; Martínez-Bonne, O.; Cabrera-Rivero, A.; Valdés-Ramos, L.; Guerra-Badía, R.; Fernández-Carriera, R.; Menéndez-Sainz, M. C.; González-García, S. Association of status redox with demographic, clinical and imaging parameters in patients with Huntington's disease. *Clin Biochem* **48:**1258-1263; 2015.
[73] Pocernich, C. B.; Butterfield, D. A. Elevation of glutathione as a therapeutic strategy in Alzheimer disease. *Biochim. Biophys. Acta* **1822:**625-630; 2012.
[74] Seghrouchni, I.; Drai, J.; Bannier, E.; Rivière, J.; Calmard, P.; Garcia, I.; Orgiazzi, J.; Revol, A. Oxidative stress parameters in type I, type II and insulin treated type 2 diabetes mellitus; insulin treatment efficiency. *Clin Chim Acta* **321:**89-96; 2002.
[75] Do, K. Q.; Trabesinger, A. H.; Kirsten-Krüger, M.; Lauer, C. J.; Dydak, U.; Hell, D.; Holsboer, F.; Boesiger, P.; Cuénod, M. Schizophrenia- glutathione deficit in cerebrospinal fluid and prefrontal cortex in vivo. *Eur J Neurosci* **12:**3721-3728; 2000.
[76] Babu, G. N.; Kumar, A.; Chandra, R.; Puri, S. K.; Singh, R. L.; Kalita, J.; Misra, U. K. Oxidant-antioxidant imbalance in the erythrocytes of sporadic amyotrophic lateral sclerosis patients correlates with the progression of disease. *Neurochem Int* **52:**1284-1289; 2008.

[77] Vargas, M. R.; Johnson, D. A.; Johnson, J. A. Decreased glutathione accelerates neurological deficit and mitochondrial pathology in familial ALS-linked hSOD1(G93A) mice model. *Neurobiol Dis* **43:**543-551; 2011.
[78] Weiduschat, N.; Mao, X.; Hupf, J.; Armstrong, N.; Kang, G.; Lange, D. J.; Mitsumoto, H.; Shungu, D. C. Motor cortex glutathione deficit in ALS measured in vivo with the J-editing technique. *Neurosci Lett* **570:**102-107; 2014.
[79] Ehrhart, J.; Smith, A. J.; Kuzmin-Nichols, N.; Zesiewicz, T. A.; Jahan, I.; Shytle, R. D.; Kim, S. H.; Sanberg, C. D.; Vu, T. H.; Gooch, C. L.; Sanberg, P. R.; Garbuzova-Davis, S. Humoral factors in ALS patients during disease progression. *J Neuroinflammation* **12:**127; 2015.
[80] Tohgi, H.; Abe, T.; Yamazaki, K.; Murata, T.; Ishizaki, E.; Isobe, C. Increase in oxidized NO products and reduction in oxidized glutathione in cerebrospinal fluid from patients with sporadic form of amyotrophic lateral sclerosis. *Neurosci Lett* **260:**204-206; 1999.
[81] Oteiza, P. I.; Uchitel, O. D.; Carrasquedo, F.; Dubrovski, A. L.; Roma, J. C.; Fraga, C. G. Evaluation of antioxidants, protein, and lipid oxidation products in blood from sporadic amyotrophic lateral sclerosis patients. *Neurochem Res* **22:**535-539; 1997.
[82] Calabrese, V.; Scapagnini, G.; Ravagna, A.; Bella, R.; Foresti, R.; Bates, T. E.; Giuffrida Stella, A. M.; Pennisi, G. Nitric oxide synthase is present in the cerebrospinal fluid of patients with active multiple sclerosis and is associated with increases in cerebrospinal fluid protein nitrotyrosine and S-nitrosothiols and with changes in glutathione levels. *J Neurosci Res* **70:**580-587; 2002.
[83] Roum, J. H.; Buhl, R.; McElvaney, N. G.; Borok, Z.; Crystal, R. G. Systemic deficiency of glutathione in cystic fibrosis. *J Appl Physiol* **75:**2419-2424; 1993.
[84] Valbuena, G. N.; Rizzardini, M.; Cimini, S.; Siskos, A. P.; Bendotti, C.; Cantoni, L.; Keun, H. C. Metabolomic analysis reveals increased aerobic glycolysis and amino acid deficit in a cellular model of amyotrophic lateral sclerosis. *Mol Neurobiol* **53:**2222-2240; 2016.
[85] Smith, E. J.; Shay, K. P.; Thomas, N. O.; Butler, J. A.; Finlay, L. F.; Hagen, T. M. Age-related loss of hepatic Nrf2 protein homeostasis: Potential role for heightened expression of miR-146a. *Free Radic Biol Med* **89:**1184-1191; 2015.
[86] Diaz-Hernandez, J. I.; Almeida, A.; Delgado-Esteban, M.; Fernandez, E.; Bolanos, J. P. Knockdown of glutamate-cysteine ligase by small hairpin RNA reveals that both catalytic and modulatory subunits are essential for the survival of primary neurons. *J Biol Chem* **280:**38992-39001; 2005.
[87] Wild, A. C.; Moinova, H. R.; Mulcahy, R. T. Regulation of gamma-glutamylcysteine synthetase subunit gene expression by the transcription factor Nrf2. *J Biol Chem* **274:**33627-33636; 1999.
[88] Huang, C. S.; Chang, L. S.; Anderson, M. E.; Meister, A. Catalytic and Regulatory Propertiesof the Heavy Subunitof Rat Kidney y-Glutamylcysteine Synthetas. *J Biol Chem* **268:**19675-19680; 1993.

[89] Tartari, S.; D'Alessandro, G.; Babetto, E.; Rizzardini, M.; Conforti, L.; Cantoni, L. Adaptation to G93Asuperoxide dismutase 1 in a motor neuron cell line model of amyotrophic lateral sclerosis: the role of glutathione. *FEBS J* **276:**2861-2874; 2009.
[90] Arai, T.; Hasegawa, M.; Akiyama, H.; Ikeda, K.; Nonaka, T.; Mori, H.; Mann, D.; Tsuchiya, M.; Hashizume, Y.; Oda, T. TDP-43 is a component of ubiquitin-positive tau-negative inclu- sions in frontotemporal lobar degeneration and amyotrophic lateral sclerosis. *Biochem. Biophys. Res. Comm.* **351:**602-611; 2006.
[91] Seyfried, J.; Soldner, F.; Schulz, J. B.; Klockgether, T.; Kovar, K. A.; Wüllner, U. Differential effects of L-buthionine sulfoximine and ethacrynic acid on glutathione levels and mitochondrial function in PC12 cells. *Neursci Lett.* **264:**1-4; 1999.
[92] Iguchi, Y.; Katsuno, M.; Takagi, S.; Ishigaki, S.; Niwa, J.; Hasegawa, M.; Tanaka, F.; Sobue, G. Oxidative stress induced by glutathione depletion reproduces pathological modifications of TDP-43 linked to TDP-43 proteinopathies. *Neurobiol Dis* **45:**862-870; 2012.
[93] Chi, L.; Ke, Y.; Luo, C.; Gozal, D.; Liu, R. Depletion of reduced glutathione enhances motor neuron degeneration in vitro and in vivo. *Neuroscience* **144:**991-1003; 2007.
[94] Vargas, M. R.; Pehar, M.; Cassina, P.; Beckman, J. S.; Barbeito, L. Increased glutathione biosynthesis by Nrf2 activation in astrocytes prevents p75NTR-dependent motor neuron apoptosis. *J Neurochem* **97:**687-696; 2006.
[95] Diaz-Amarilla, P.; Miquel, E.; Trostchansky, A.; Trias, E.; Ferreira, A. M.; Freeman, B. A.; Cassina, P.; Barbeito, L.; Vargas, M. R.; Rubbo, H. Electrophilic nitro-fatty acids prevent astrocyte-mediated toxicity to motor neurons in a cell model of familial amyotrophic lateral sclerosis via nuclear factor erythroid 2-related factor activation. *Free Radic Biol Med* **95:**112-120; 2016.
[96] Grek, C. L.; Zhang, J.; Manevich, Y.; Townsend, D. M.; Tew, K. D. Causes and consequences of cysteine S-glutathionylation. *J Biol Chem* **288:**26497-26504; 2013.
[97] Wilcox, K. C.; Zhou, L.; Jordon, J. K.; Huang, Y.; Yu, Y.; Redler, R. L.; Chen, X.; Caplow, M.; Dokholyan, N. V. Modifications of superoxide dismutase (SOD1) in human erythrocytes: a possible role in amyotrophic lateral sclerosis. *J Biol Chem* **284:**13940-13947; 2009.
[98] Nakanishi, T.; Kishikawa, M.; Miyazaki, A.; Shimizu, A.; Ogawa, Y.; Sakoda, S.; Ohi, T.; Shoji, H. Simple and defined method to detect the SOD-1 mutants from patients with familial amyotrophic lateral sclerosis by mass spectrometry. *J Neurosci Methods* **81:**41-44; 1998.
[99] Marklund, S. L.; Andersen, P. M.; Forsgren, L.; Nilsson, P.; Ohlsson, P. I.; Wikander, G.; Oberg, A. Normal binding and reactivity of copper in mutant superoxide dismutase isolated from amyotrophic lateral sclerosis patients. *J Neurochem* **69:**675-681; 1997.

[100] McAlary, L.; Yerbury, J. J.; Aquilina, J. A. Glutathionylation potentiates benign superoxide dismutase 1 variants to the toxic forms associated with amyotrophic lateral sclerosis. *Sci Rep* **3:**3275; 2013.
[101] Redler, R. L.; Fee, L.; Fay, J. M.; Caplow, M.; Dokholyan, N. V. Non-native soluble oligomers of Cu/Zn superoxide dismutase (SOD1) contain a conformational epitope linked to cytotoxicity in amyotrophic lateral sclerosis (ALS). *Biochemistry* **53:**2423-2432; 2014.
[102] Redler, R. L.; Wilcox, K. C.; Proctor, E. A.; Fee, L.; Caplow, M.; Dokholyan, N. V. Glutathionylation at Cys-111 induces dissociation of wild type and FALS mutant SOD1 dimers. *Biochemistry* **50:**7057-7066; 2011.
[103] Fay, J. M.; Zhu, C.; Proctor, E. A.; Tao, Y.; Cui, W.; Ke, H.; Dokholyan, N. V. A Phosphomimetic Mutation Stabilizes SOD1 and Rescues Cell Viability in the Context of an ALS-Associated Mutation. *Structure* **24:**1898-1906; 2016.
[104] Rhoads, T. W. Measuring Protein Metal Binding via Mass Spectrometry-Copper, Zinc Superoxide Dismutase and Amyotrophic Lateral Sclerosis. *Biochemistry and Biophysics*. Corvallis, OR: Oregon State University; 2012: 156.
[105] Kawamata, H.; Ng, S. K.; Diaz, N.; Burstein, S.; Morel, L.; Osgood, A.; Sider, B.; Higashimori, H.; Haydon, P. G.; Manfredi, G.; Yang, Y. Abnormal intracellular calcium signaling and SNARE-dependent exocytosis contributes to SOD1G93A astrocyte-mediated toxicity in amyotrophic lateral sclerosis. *J Neurosci* **34:**2331-2348; 2014.
[106] Berkholz, D. S.; Faber, H. R.; Savvides, S. N.; Karplus, P. A. Catalytic cycle of human glutathione reductase near 1 A resolution. *J Mol Biol* **382:**371-384; 2008.
[107] Karplus, P. A.; Pai, E. F.; Schulz, G. E. A crystallographic study of the glutathione binding site of glutathione reductase at 0.3-nm resolution. *Eur J Biochem* **178:**693-703; 1989.
[108] Kelner, M. J.; Montoya, M. A. Structural organization of the human glutathione reductase gene: determination of correct cDNA sequence and identification of a mitochondrial leader sequence. *Biochem Biophys Res Commun* **269:**366-368; 2000.
[109] Couto, N.; Wood, J.; Barber, J. The role of glutathione reductase and related enzymes on cellular redox homoeostasis network. *Free Radic Biol Med* **95:**27-42; 2016.
[110] Cova, E.; Bongioanni, P.; Cereda, C.; Metelli, M. R.; Salvaneschi, L.; Bernuzzi, S.; Guareschi, S.; Rossi, B.; Ceroni, M. Time course of oxidant markers and antioxidant defenses in subgroups of amyotrophic lateral sclerosis patients. *Neurochem Int* **56:**687-693; 2010.
[111] Nikolic-Kokic, A.; Stevic, Z.; Blagojevic, D.; Davidovic, B.; Jones, D. R.; Spasic, M. B. Alterations in anti-oxidative defence enzymes in erythrocytes from sporadic amyotrophic lateral sclerosis (SALS) and familial ALS patients. *Clin Chem Lab Med* **44:**589-593; 2006.
[112] Deponte, M. Glutathione catalysis and the reaction mechanisms of glutathione-dependent enzymes. *Biochim Biophys Acta* **1830:**3217-3266; 2013.

[113] Board, P. G.; Menon, D. Glutathione transferases, regulators of cellular metabolism and physiology. *Biochim Biophys Acta* **1830:**3267-3288; 2013.
[114] Habig, W. H.; Pabst, M. J.; Jakoby, W. B. Glutathione S-transferases. *J Biol Chem* **249:**7130-7139; 1974.
[115] van de Giessen, E.; Fogh, I.; Gopinath, S.; Smith, B.; Hu, X.; Powell, J.; Andersen, P.; Nicholson, G.; Al Chalabi, A.; Shaw, C. E. Association study on glutathione S-transferase omega 1 and 2 and familial ALS. *Amyotroph Lateral Scler* **9:**81-84; 2008.
[116] Usarek, E.; Gajewska, B.; Kazmierczak, B.; Kuzma, M.; Dziewulska, D.; Baranczyk-Kuzma, A. A study of glutathione S-transferase pi expression in central nervous system of subjects with amyotrophic lateral sclerosis using RNA extraction from formalin-fixed, paraffin-embedded material. *Neurochem Res* **30:**1003-1007; 2005.
[117] Kuźma, M.; Jamrozik, Z.; Barańczyk-Kuźma, A. Activity and expression of glutathione S-transferase pi in patients with amyotrophic lateral sclerosis. *Clin Chim Acta* **364:**217-221; 2006.
[118] Gajewska, B.; Kaźmierczak, B.; Kuźma-Kozakiewicz, M.; Jamrozik, Z.; Barańczyk-Kuźma, A. *GSTP1* polymorphisms and their association with glutathione transferase and peroxidase activities in patients with motor neuron disease. *CNS & Neurol Disord: Drug Targets* **14**; 2015.
[119] Espinoza, S. E.; Guo, H.; Fedarko, N.; DeZern, A.; Fried, L. P.; Xue, Q. L.; Leng, S.; Beamer, B.; Walston, J. D. Glutathione Peroxidase Enzyme Activity in Aging. *J Gerontol A Biol Sci Med Sci* **63:**505-509; 2008.
[120] Thomas, N. O.; Shay, K. P.; Kelley, A. R.; Butler, J. A.; Hagen, T. M. Glutathione maintenance mitigates age-related susceptibility to redox cycling agents. *Redox Biol* **10:**45-52; 2016.
[121] Fujita, K. Y., M.; Shibayama, K.; Ando, M.; Honda, M.; Nagata, Y. Decreased cytochrome c oxidase activity but unchanged superoxide dismutase activities in the spinal cords of patients with amyotrophic lateral sclerosis. *J Neurosci Res* **45:**276-281; 1996.
[122] Przedborski, S.; Donaldson, D. M.; Murphy, P. L.; Hirsch, O.; Lange, D.; Naini, A. B.; McKenna-Yasek, D.; Brown, R. H., Jr. Blood superoxide dismutase, catalase and glutathione peroxidase activities in familial and sporadic amyotrophic lateral sclerosis. *Neurodegeneration* **5:**57-64; 1996.
[123] Bonnefont-Rousselot, D.; Lacomblez, L.; Jaudon, M.-C.; Lepage, S.; Salachas, F.; Bensimon, G.; Bizard, C.; Doppler, V.; Delattre, J.; Meininger, V. Blood oxidative stress in amyotrophic lateral sclerosis. *J Neurol Sci* **178:**57-62; 2000.
[124] Andersen, P. M.; Nilsson, P.; Forsgren, L.; Marklund, S. L. CuZn-Superoxide dismutase, extracellular superoxide dismutase, and glutathione peroxidase in blood from individuals homozygous for Asp^{90} Ala CuZn-superoxide dismutase mutation. *J Neurochem* **70:**715-720; 1998.
[125] Przedborski, S.; Donaldson, D.; Jakowec, M.; Kish, S. J.; Guttman, M.; Rosoklija, G.; Hays, A. P. Brain Superoxide Dismutase, Cadase, and Glutahone

Peroxidase Activities in Amyotrophc Lateral Sclerosis. *Ann Neurol* **39:**158-165; 1996.
[126] Vargas, M. R.; Pehar, M.; Diaz-Amarilla, P. J.; Beckman, J. S.; Barbeito, L. Transcriptional profile of primary astrocytes expressing ALS-linked mutant SOD1. *J Neurosci Res* **86:**3515-3525; 2008.
[127] Tanaka, H.; Shimazawa, M.; Takata, M.; Kaneko, H.; Tsuruma, K.; Ikeda, T.; Warita, H.; Aoki, M.; Yamada, M.; Takahashi, H.; Hozumi, I.; Minatsu, H.; Inuzuka, T.; Hara, H. ITIH4 and Gpx3 are potential biomarkers for amyotrophic lateral sclerosis. *J Neurosci* **260:**1782-1797; 2013.
[128] Yang, W. S.; SriRamaratnam, R.; Welsch, M. E.; Shimada, K.; Skouta, R.; Viswanathan, V. S.; Cheah, J. H.; Clemons, P. A.; Shamji, A. F.; Clish, C. B.; Brown, L. M.; Girotti, A. W.; Cornish, V. W.; Schreiber, S. L.; Stockwell, B. R. Regulation of ferroptotic cancer cell death by GPX4. *Cell* **156:**317-331; 2014.
[129] Veyrat-Durebex, C.; Corcia, P.; Mucha, A.; Benzimra, S.; Mallet, C.; Gendrot, C.; Moreau, C.; Devos, D.; Piver, E.; Pages, J. C.; Maillot, F.; Andres, C. R.; Vourc'h, P.; Blasco, H. Iron metabolism disturbance in a French cohort of ALS patients. *Biomed Res Int* **2014:**485723; 2014.
[130] Do Van, B.; Gouel, F.; Jonneaux, A.; Timmerman, K.; Gele, P.; Petrault, M.; Bastide, M.; Laloux, C.; Moreau, C.; Bordet, R.; Devos, D.; Devedjian, J. C. Ferroptosis, a newly characterized form of cell death in Parkinson's disease that is regulated by PKC. *Neurobiol Dis* **94:**169-178; 2016.
[131] Dixon, S. J.; Lemberg, K. M.; Lamprecht, M. R.; Skouta, R.; Zaitsev, E. M.; Gleason, C. E.; Patel, D. N.; Bauer, A. J.; Cantley, A. M.; Yang, W. S.; Morrison, B., 3rd; Stockwell, B. R. Ferroptosis: an iron-dependent form of nonapoptotic cell death. *Cell* **149:**1060-1072; 2012.
[132] Liu, R.; Baolin, L.; Flanagan, S. W.; Oberley, L. W.; Gozal, D.; Qiu, M. Increased mitochondrial antioxidative activity or decreased oxygen free radical propagation prevent mutant SOD1-mediated motor neuron cell death and increase amyotrophic lateral sclerosis-like transgenic mouse survival. *J Neurochem* **80:**488-500; 2002.
[133] Cudkowicz, M. E. P., K.A.; Sapp, P.C.; Mathews, R.K.; Leahy, J.; Pasinelli, P.; Francis, J.W.; Jiang, D.; Andersen, J.K.; Brown, R.H., Jr.; . Survival in transgenic ALS mice does not vary with CNS glutathione peroxidase activity. *Neurology* **59:**729-734; 2002.
[134] Chen, L.; Hambright, W. S.; Na, R.; Ran, Q. Ablation of the Ferroptosis Inhibitor Glutathione Peroxidase 4 in Neurons Results in Rapid Motor Neuron Degeneration and Paralysis. *J Biol Chem* **290:**28097-28106; 2015.
[135] Holmgren, A. Thioredoxin and glutaredoxin systems. *J Biol Chem* **264:**13963-13966; 1989.
[136] Fernandes, A. P.; Holmgren, A. Glutaredoxins: glutathione-dependent redox enzymes with functions far beyond a simple thioredoxin backup system. *Antioxid Redox Signal* **6:**63-74; 2004.
[137] Arnér, E. S. J.; Holmgren, A. Physiological functions of thioredoxin and thioredoxin reductase. *Eur J Biochem* **267:**6102-6109; 2000.

[138] Putker, M.; O'Neill, J. S. Reciprocal Control of the Circadian Clock and Cellular Redox State - a Critical Appraisal. *Mol Cells* **39:**6-19; 2016.
[139] Rhee, S. G. Overview on Peroxiredoxin. *Mol Cells* **39:**1-5; 2016.
[140] Knoops, B.; Argyropoulou, V.; Becker, S.; Ferte, L.; Kuznetsova, O. Multiple Roles of Peroxiredoxins in Inflammation. *Mol Cells* **39:**60-64; 2016.
[141] Wood, Z. A.; Schröder, E.; Harris, J. R.; Poole, L. B. Structure, mechanism and regulation
of peroxiredoxins. *Trends Biochem Sci* **28:**32-40; 2003.
[142] Perkins, A.; Poole, L. B.; Karplus, P. A. Tuning of peroxiredoxin catalysis for various physiological roles. *Biochemistry* **52:**7693-7705; 2014.
[143] Perkins, A.; Parsonage, D.; Nelson, K. J.; Ogba, O. M.; Cheong, P. H.; Poole, L. B.; Karplus, P. A. Peroxiredoxin Catalysis at Atomic Resolution. *Structure* **24:**1668-1678; 2016.
[144] Nanou, A.; Higginbottom, A.; Valori, C. F.; Wyles, M.; Ning, K.; Shaw, P.; Azzouz, M. Viral delivery of antioxidant genes as a therapeutic strategy in experimental models of amyotrophic lateral sclerosis. *Mol Ther* **21:**1486-1496; 2013.
[145] Malaspina, A.; Kaushik, N.; de Belleroche, J. Differential expression of 14 genes in amyotrophic lateral sclerosis spinal cord detected using gridded cDNA arrays. *J Neurochem* **77:**132-145; 2001.
[146] Ferri, A.; Fiorenzo, P.; Nencini, M.; Cozzolino, M.; Pesaresi, M. G.; Valle, C.; Sepe, S.; Moreno, S.; Carri, M. T. Glutaredoxin 2 prevents aggregation of mutant SOD1 in mitochondria and abolishes its toxicity. *Hum Mol Genet* **19:**4529-4542; 2010.
[147] Álvarez-Zaldiernas, C.; Lu, J.; Zheng, Y.; Yang, H.; Blasi, J.; Solsona, C.; Holmgren, A. Cellular Redox Systems Impact the Aggregation of Cu,Zn Superoxide Dismutase Linked to Familial Amyotrophic Lateral Sclerosis. *J Biol Chem* **291:**17197-17208; 2016.
[148] Tokuda, E.; Furukawa, Y. Copper Homeostasis as a Therapeutic Target in Amyotrophic Lateral Sclerosis with SOD1 Mutations. *Int J Mol Sci* **17**; 2016.
[149] Tokuda, E.; Okawa, E.; Ono, S. Dysregulation of intracellular copper trafficking pathway in a mouse model of mutant copper/zinc superoxide dismutase-linked familial amyotrophic lateral sclerosis. *J Neurochem* **111:**181-191; 2009.
[150] Trumbull, K. A.; Beckman, J. S. A role for copper in the toxicity of zinc-deficient superoxide dismutase to motor neurons in amyotrophic lateral sclerosis. *Antioxid Redox Signal* **11:**1627-1639; 2009.
[151] Tokuda, E.; Okawa, E.; Watanabe, S.; Ono, S.; Marklund, S. L. Dysregulation of intracellular copper homeostasis is common to transgenic mice expressing human mutant superoxide dismutase-1s regardless of their copper-binding abilities. *Neurobiol Dis* **54:**308-319; 2013.
[152] Son, M.; Puttaparthi, K.; Kawamata, H.; Rajendran, B.; Boyer, P. J.; Manfredi, G.; Elliott, J. L. Overexpression of CCS in G93A-SOD1 mice leads to

acclerated neurological deficits with severe mitochondrial pathology. *Proc Natl Acad Sci U S A* **104:**6072-6077; 2007.
[153] Carroll, M. C.; Girouard, J. B.; Ulloa, J. L.; Subramaniam, J. R.; Wong, P. C.; Valentine, J. S.; Culotta, V. C. Mechanisms for activating Cu- and Zn-containing superoxide dismutase in the absence of the CCS Cu chaperone. *Proc Natl Acad Sci U S A* **101:**5964-5969; 2004.
[154] Mattie, M. D.; Freedman, J. H. Copper-inducible transcription- regulation by metal- and oxidative stress- responsive pathways. *Am J Physiol Cell Physiol* **286:**C293-C301; 2004.
[155] Brose, J.; La Fontaine, S.; Wedd, A. G.; Xiao, Z. Redox sulfur chemistry of the copper chaperone Atox1 is regulated by the enzyme glutaredoxin 1, the reduction potential of the glutathione couple GSSG/2GSH and the availability of Cu(I). *Metallomics* **6:**793-808; 2014.
[156] Hatori, Y.; Clasen, S.; Hasan, N. M.; Barry, A. N.; Lutsenko, S. Functional Partnership of the Copper Export Machinery and Glutathione Balance in Human Cells. *J Biol Chem* **287:**26678-26687; 2012.
[157] Maryon, E. B.; Molloy, S. A.; Kaplan, J. H. Cellular glutathione plays a key role in copper uptake mediated by human copper transporter 1. *Am J Physiol Cell Physiol* **304:**C768-779; 2013.
[158] Chiò, A. C., A.; Terreni, A.A.;Schiffer, D. Reduced glutathione in amyotrophic lateral sclerosis: an open, crossover, randomized trial. *Ital J Neurol Sci* **19:**363-366; 1998.
[159] Anderson, M. E.; Powrie, F.; Puri, R. N.; Meister, A. Glutathione monoethyl ester: preparation, uptake by tissues, and conversion to glutathione. *Arch Biochem Biophys* **239:**538-548; 1985.
[160] Netzahualcoyotzi, C.; Tapia, R. Degeneration of spinal motor neurons by chronic AMPA-induced excitotoxicity in vivo and protection by energy substrates. *Acta Neuropathol Commun* **3:**27; 2015.
[161] Louwerse, E. S.; Weverling, G. J.; Bossuyt, P. M.; Meyjes, F. E.; de Jong, J. M. Randomized, double-blind, controlled trial of acetylcysteine in amyotrophic lateral sclerosis. *Arch Neurol* **52:**559-564; 1995.
[162] Beretta, S.; Sala, G.; Mattavelli, L.; Ceresa, C.; Casciati, A.; Ferri, A.; Carrì, M. T.; Ferrarese, C. Mitochondrial dysfunction due to mutant copper/zinc superoxide dismutase associated with amyotrophic lateral sclerosis is reversed by N-acetylcysteine. *Neurobiology of Disease* **13:**213-221; 2003.
[163] Andreassen, O. A.; Dedeoglu, A.; Klivenyi, P.; Beal, M. F.; Bush, A. I. N-acetyl-L-cysteine improves survival and preserves motor performance in an animal model of familial amyotrophic lateral sclerosis. *Neuroreport* **11:**2491-2493; 2000.
[164] Ross, E. K.; Winter, A. N.; Wilkins, H. M.; Sumner, W. A.; Duval, N.; Patterson, D.; Linseman, D. A. A Cystine-Rich Whey Supplement (Immunocal((R))) Delays Disease Onset and Prevents Spinal Cord Glutathione Depletion in the hSOD1(G93A) Mouse Model of Amyotrophic Lateral Sclerosis. *Antioxidants (Basel)* **3:**843-865; 2014.

[165] Neymotin, A.; Calingasan, N. Y.; Wille, E.; Naseri, N.; Petri, S.; Damiano, M.; Liby, K. T.; Risingsong, R.; Sporn, M.; Beal, M. F.; Kiaei, M. Neuroprotective effect of Nrf2/ARE activators, CDDO ethylamide and CDDO trifluoroethylamide, in a mouse model of amyotrophic lateral sclerosis. *Free Radic Biol Med* **51:**88-96; 2011.
[166] Tanaka, K.; Kanno, T.; Yanagisawa, Y.; Yasutake, K.; Inoue, S.; Hirayama, N.; Ikeda, J. E. A novel acylaminoimidazole derivative, WN1316, alleviates disease progression via suppression of glial inflammation in ALS mouse model. *PLoS One* **9:**e87728; 2014.
[167] Tanaka, K.; Kanno, T.; Yanagisawa, Y.; Yasutake, K.; Hadano, S.; Yoshii, F.; Ikeda, J.-E. Bromocriptine methylate suppresses glial inflammation and moderates disease progression in a mouse model of amyotrophic lateral sclerosis. *Exp Neurol* **232:**41-52; 2011.
[168] Nagata, E.; Ogino, M.; Iwamoto, K.; Kitagawa, Y.; Iwasaki, Y.; Yoshii, F.; Ikeda, J. E.; Investigators, A. L. S. C. Bromocriptine Mesylate Attenuates Amyotrophic Lateral Sclerosis: A Phase 2a, Randomized, Double-Blind, Placebo-Controlled Research in Japanese Patients. *PLoS One* **11:**e0149509; 2016.
[169] Boll, M. C.; Bayliss, L.; Vargas-Cañas, S.; Burgos, J.; Montes, S.; Peñaloza-Solano, G.; Rios, C.; Alcaraz-Zubeldia, M. Clinical and biological changes under treatment with lithium carbonate and valproic acid in sporadic amyotrophic lateral sclerosis. *J Neurol Sci* **340:**103-108; 2014.
[170] Muyderman, H.; Hutson, P. G.; Matusica, D.; Rogers, M. L.; Rush, R. A. The human G93A-superoxide dismutase-1 mutation, mitochondrial glutathione and apoptotic cell death. *Neurochem Res* **34:**1847-1856; 2009.
[171] Booty, L. M.; King, M. S.; Thangaratnarajah, C.; Majd, H.; James, A. M.; Kunji, E. R.; Murphy, M. P. The mitochondrial dicarboxylate and 2-oxoglutarate carriers do not transport glutathione. *FEBS Lett* **589:**621-628; 2015.
[172] Smith, R. A.; Porteous, C. M.; Gane, A. M.; Murphy, M. P. Delivery of bioactive molecules to mitochondria in vivo. *Proc Natl Acad Sci U S A* **100:**5407-5412; 2003.
[173] Ross, M. F.; Prime, T. A.; Abakumova, I.; James, A. M.; Porteous, C. M.; Smith, R. A.; Murphy, M. P. Rapid and extensive uptake and activation of hydrophobic triphenylphosphonium cations within cells. *Biochem J* **411:**633-645; 2008.
[174] Kelso, G. F.; Porteous, C. M.; Coulter, C. V.; Hughes, G.; Porteous, W. K.; Ledgerwood, E. C.; Smith, R. A.; Murphy, M. P. Selective targeting of a redox-active ubiquinone to mitochondria within cells: antioxidant and antiapoptotic properties. *J Biol Chem* **276:**4588-4596; 2001.
[175] Murphy, M. P.; Smith, R. A. Targeting antioxidants to mitochondria by conjugation to lipophilic cations. *Annu Rev Pharmacol Toxicol* **47:**629-656; 2007.
[176] Brown, S. E.; Ross, M. F.; Sanjuan-Pla, A.; Manas, A. R.; Smith, R. A.; Murphy, M. P. Targeting lipoic acid to mitochondria: synthesis and characterization of a triphenylphosphonium-conjugated alpha-lipoyl derivative. *Free Radic Biol Med* **42:**1766-1780; 2007.

[177] Finichiu, P. G.; Larsen, D. S.; Evans, C.; Larsen, L.; Bright, T. P.; Robb, E. L.; Trnka, J.; Prime, T. A.; James, A. M.; Smith, R. A.; Murphy, M. P. A mitochondria-targeted derivative of ascorbate: MitoC. *Free Radic Biol Med* **89:**668-678; 2015.
[178] Jameson, V. J.; Cocheme, H. M.; Logan, A.; Hanton, L. R.; Smith, R. A.; Murphy, M. P. Synthesis of triphenylphosphonium vitamin E derivatives as mitochondria-targeted antioxidants. *Tetrahedron* **71:**8444-8453; 2015.
[179] Lee, Y. C.; Huang, H. Y.; Chang, C. J.; Cheng, C. H.; Chen, Y. T. Mitochondrial GLUT10 facilitates dehydroascorbic acid import and protects cells against oxidative stress: mechanistic insight into arterial tortuosity syndrome. *Hum Mol Genet* **19:**3721-3733; 2010.
[180] Munoz-Montesino, C.; Roa, F. J.; Pena, E.; Gonzalez, M.; Sotomayor, K.; Inostroza, E.; Munoz, C. A.; Gonzalez, I.; Maldonado, M.; Soliz, C.; Reyes, A. M.; Vera, J. C.; Rivas, C. I. Mitochondrial ascorbic acid transport is mediated by a low-affinity form of the sodium-coupled ascorbic acid transporter-2. *Free Radic Biol Med* **70:**241-254; 2014.
[181] Sheu, S. S.; Nauduri, D.; Anders, M. W. Targeting antioxidants to mitochondria: a new therapeutic direction. *Biochim Biophys Acta* **1762:**256-265; 2006.
[182] Parella, T. Pulse Program Catalogue: II. Biomolecular NMR Experiments. In: GmbH, B. B., ed.; 2010: 827.
[183] Gurney ME, P. H., Chiu AY, Dal Canto MC, Polchow CY, Alexander DD, Caliendo J, Hentati A, Kwon YW, Deng H-X, Chen W, Zhai P, Sufit RL, Siddique T. Motor neuron degeneration in mice that express a human Cu,Zn superoxide dismutase mutation. *Science* **264:**1772-1775; 1994.
[184] Aoki M, K. S., Nagai M, Itoyama. Development of a rat model of amyotrophic lateral sclerosis expressing a human *SOD1* transgene. *Neuropathology* **25:**365-370; 2005.
[185] Dimri GP, L. X., Basile G, Acosta M, Scott G, Roskelley C, Medranos EE, Linskens M, Rubeli I, Pereira-Smith O, Peacocke M, Campisi J. A biomarker that identifies senescent human cells in culture and in aging skin *in vivo*. *Proc Natl Acad Sci USA* **92:**9363-9367; 1995.
[186] Bruijn LI, B. M., Lee MK, Anderson KL, Jenkins NA, Copeland NG, Sisodia SS, Rothstein JD, Borchelt DR, Price DL, Cleveland DW. ALS-Linked SOD1 mutant G85R mediates damage to astrocytes and promotes rapidly progressive disease with SOD1-containing inclusions. *Neuron* **18:**327-338; 1997.
[187] Boillée S, Y. K., Lobsiger CS, Copeland NG, Jenkins NA, Kassiotis G, Kollas G, Cleveland DW. Onset and progression in inherited ALS determined by motor neurons and microglia. *Science* **312:**1389-1392; 2006.
[188] Nagai, M.; Re, D. B.; Nagata, T.; Chalazonitis, A.; Jessell, T. M.; Wichterle, H.; Przedborski, S. Astrocytes expressing ALS-linked mutated SOD1 release factors selectively toxic to motor neurons. *Nat Neurosci* **10:**615-622; 2007.

[189] Haidet-Phillips AM, H. M., Miranda CJ, Meyer K, Braun L, Frakes A, Song SW, Likhite S, Murtha MJ, Foust KD, Rao M, Eagle A, Kammesheidt A, Christensen A, Mendell JR, Burghes AHM, Kaspar BK. Astrocytes from familial and sporadic ALS patients are toxic to motor neurons. *Nat Biotechnol* **29:**824-828; 2011.
[190] Trias, E.; Ibarburu, S.; Barreto-Nunez, R.; Barbeito, L. Significance of aberrant glial cell phenotypes in pathophysiology of amyotrophic lateral sclerosis. *Neurosci Lett*; 2016.
[191] Chinta, S. J.; Woods, G.; Rane, A.; Demaria, M.; Campisi, J.; Andersen, J. K. Cellular senescence and the aging brain. *Exp Gerontol* **68:**3-7; 2015.
[192] Turnquist, C.; Horikawa, I.; Foran, E.; Major, E. O.; Vojtesek, B.; Lane, D. P.; Lu, X.; Harris, B. T.; Harris, C. C. p53 isoforms regulate astrocyte-mediated neuroprotection and neurodegeneration. *Cell Death Differ* **23:**1515-1528; 2016.
[193] Streit, W. J. Microglial senescence: does the brain's immune system have an expiration date? *Trends Neurosci* **29:**506-510; 2006.
[194] Streit, W. J.; Miller, K. R.; Lopes, K. O.; Njie, E. G. Microglial degeneration in the aging brain - bad news for neurons? *Front Biosci* **1:**3423-3438; 2008.
[195] Streit, W. J.; Xue, Q. S. Human CNS immune senescence and neurodegeneration. *Curr Opin Immunol* **29:**93-96; 2014.
[196] Njie, E. G.; Boelen, E.; Stassen, F. R.; Steinbusch, H. W.; Borchelt, D. R.; Streit, W. J. Ex vivo cultures of microglia from young and aged rodent brain reveal age-related changes in microglial function. *Neurobiol Aging* **33:**195 e191-112; 2012.
[197] Das, M. M.; Svendsen, C. N. Astrocytes show reduced support of motor neurons with aging that is accelerated in a rodent model of ALS. *Neurobiol Aging* **36:**1130-1139; 2015.
[198] Howland, D. S.; Liu, J.; She, Y.; Goad, B.; Maragakis, N. J.; Kim, B.; Erickson, J.; Kulik, J.; DeVito, L.; Psaltis, G.; DeGennaro, L. J.; Cleveland, D. W.; Rothstein, J. D. Focal loss of the glutamate transporter EAAT2 in a transgenic rat model of SOD1 mutant-mediated amyotrophic lateral sclerosis (ALS). *Proceedings of the National Academy of Sciences of the United States of America* **99:**1604-1609; 2002.
[199] Díaz-Amarilla P, O.-B. S., Trias E, Cragnolini A, Martínez-Palma L, Cassina P, Beckman J, Barbeito L. Phenotypically aberrant astrocytes that promote motoneuron damage in a model of inherited amyotrophic lateral sclerosis. *Proc Natl Acad Sci USA* **108:**18126-18131; 2011.
[200] Debacq-Chainiaux, F.; Erusalimsky, J. D.; Campisi, J.; Toussaint, O. Protocols to detect senescence-associated beta-galactosidase (SA-betagal) activity, a biomarker of senescent cells in culture and in vivo. *Nat Protoc* **4:**1798-1806; 2009.
[201] Van Lint, P.; Libert, C. Chemokine and cytokine processing by matrix metalloproteinases and its effect on leukocyte migration and inflammation. *J Leukoc Biol* **82:**1375-1381; 2007.

[202] Butovsky, O.; Siddiqui, S.; Gabriely, G.; Lanser, A. J.; Dake, B.; Murugaiyan, G.; Doykan, C. E.; Wu, P. M.; Gali, R. R.; Iyer, L. K.; Lawson, R.; Berry, J.; Krichevsky, A. M.; Cudkowicz, M. E.; Weiner, H. L. Modulating inflammatory monocytes with a unique microRNA gene signature ameliorates murine ALS. *J Clin Invest* **122:**3063-3087; 2012.
[203] Kurz DJ, D. S., Hong Y, Erusalimsky JD. Senescence-associated β-galactosidase reflects an increase in lysosomal mass during replicative ageing of human endothelial cells. *J Cell Sci* **113:**3613-3622; 2000.
[204] Young, A. R.; Narita, M.; Ferreira, M.; Kirschner, K.; Sadaie, M.; Darot, J. F.; Tavare, S.; Arakawa, S.; Shimizu, S.; Watt, F. M.; Narita, M. Autophagy mediates the mitotic senescence transition. *Genes Dev* **23:**798-803; 2009.
[205] Li L, Z. X., Le W. Altered macroautophagy in the spinal cord of SOD1 mutant mice. *Autophagy* **4:**290-293; 2008.
[206] Soon, C. P.; Crouch, P. J.; Turner, B. J.; McLean, C. A.; Laughton, K. M.; Atkin, J. D.; Masters, C. L.; White, A. R.; Li, Q. X. Serum matrix metalloproteinase-9 activity is dysregulated with disease progression in the mutant SOD1 transgenic mice. *Neuromuscul Disord* **20:**260-266; 2010.
[207] Kaplan, A.; Spiller, K. J.; Towne, C.; Kanning, K. C.; Choe, G. T.; Geber, A.; Akay, T.; Aebischer, P.; Henderson, C. E. Neuronal matrix metalloproteinase-9 is a determinant of selective neurodegeneration. *Neuron* **81:**333-348; 2014.
[208] Overhoff, M. G.; Garbe, J. C.; Koh, J.; Stampfer, M. R.; Beach, D. H.; Bishop, C. L. Cellular senescence mediated by p16INK4A-coupled miRNA pathways. *Nucleic Acids Res* **42:**1606-1618; 2014.
[209] Campos-Melo D, D. C., He Z, Volkening K, Strong MJ. Altered microRNA expression profile in amyotrophic lateral sclerosis: a role in the regulation of NFL mRNA levels. *Mol Brain* **6:**1-13; 2013.
[210] Parisi, C.; Arisi, I.; D'Ambrosi, N.; Storti, A. E.; Brandi, R.; D'Onofrio, M.; Volonte, C. Dysregulated microRNAs in amyotrophic lateral sclerosis microglia modulate genes linked to neuroinflammation. *Cell Death Dis* **4:**e959; 2013.
[211] D'Ambrosi, N.; Finocchi, P.; Apolloni, S.; Cozzolino, M.; Ferri, A.; Padovano, V.; Pietrini, G.; Carri, M. T.; Volonte, C. The proinflammatory action of microglial P2 receptors is enhanced in SOD1 models for amyotrophic lateral sclerosis. *J Immunol* **183:**4648-4656; 2009.
[212] Franco MC, Y. Y., Refakis CA, Feldman JL, Stokes AL, Basso M, Melero Fernández de Mera RM, Sparrow NA, Calingasan NY, Kiaei M, Rhoads TW, Ma TC, Grumet M, Barnes S, Beal MF, Beckman JS, Mehl R, Estévez AG. Nitration of Hsp90 induces cell death. *PNAS* **110:**E1102-1111; 2013.
[213] Gandelman, M.; Peluffo, H.; Beckman, J. S.; Cassina, P.; Barbeito, L. Extracellular ATP and the P2X7 receptor in astrocyte-mediated motor neuron death: implications for amyotrophic lateral sclerosis. *J Neuroinflammation* **7:**33; 2010.
[214] Bhaumik D, S. G., Schokrpur S, Patil CK, Orjalo AV, Rodier F, Lithgow GJ, and Campisi J. MicroRNAs miRNA-146a/b negatively modulate the

senescence-associated inflammatory mediators IL-6 and IL-8. *Aging* **1:**402-411; 2009.
[215] Freund A, P. C., and Campisi J. p38MAPK is a novel DNA damage response-independent regulator of the senescence-associated secretory phenotype. *EMBO* **30:**1536-1548; 2011.
[216] Raingeuad, J., Gupta, S., Rogers, J.S., Dickens, M., Han, J., Ulevitch, R.J., Davis, R.J. Pro-inflammatory cytokines and environmental stress cause p38 mitogen-activated protein kinase activation by dual phosphorylation on tyrosine and threonine. *J Biol Chem* **270:**7420-7426; 1995.
[217] Alimbetov, D.; Davis, T.; Brook, A. J.; Cox, L. S.; Faragher, R. G.; Nurgozhin, T.; Zhumadilov, Z.; Kipling, D. Suppression of the senescence-associated secretory phenotype (SASP) in human fibroblasts using small molecule inhibitors of p38 MAP kinase and MK2. *Biogerontology*; 2015.
[218] Dewil, M.; dela Cruz, V. F.; Van Den Bosch, L.; Robberecht, W. Inhibition of p38 mitogen activated protein kinase activation and mutant SOD1(G93A)-induced motor neuron death. *Neurobiol Dis* **26:**332-341; 2007.
[219] Sako W, I. H., Yoshida M, Koizumi H, Kamada M, Fujita K, Hashizume Y, Izumi Y, and Kaji R. Nuclear factor κ B expression in patients with sporadic amyotrophic lateral sclerosis and hereditary amyotrophic lateral sclerosis with optineurin mutations. *Clin Neuropathol* **31:**418-423; 2012.
[220] Crosio, C.; Valle, C.; Casciati, A.; Iaccarino, C.; Carri, M. T. Astroglial inhibition of NF-kappaB does not ameliorate disease onset and progression in a mouse model for amyotrophic lateral sclerosis (ALS). *PLoS One* **6:**e17187; 2011.
[221] Taganov KD, B. M., Chang K-J, and Baltimore D. NF-κB-dependent induction of microRNA miR-146, an inhibitor targeted to signaling proteins of innate immune responses. *PNAS* **103:**12481-12486; 2006.
[222] Zhao, W.; Beers, D. R.; Appel, S. H. Immune-mediated mechanisms in the pathoprogression of amyotrophic lateral sclerosis. *J Neuroimmune Pharmacol* **8:**888-899; 2013.
[223] Sargsyan, S. A.; Blackburn, D. J.; Barber, S. C.; Monk, P. N.; Shaw, P. J. Mutant SOD1 G93A microglia have an inflammatory phenotype and elevated production of MCP-1. *Neuroreport* **20:**1450-1455; 2009.
[224] Kurz, D. J.; Decary, S.; Hong, Y.; Trivier, E.; Akhmedov, A.; Erusalimsky, J. D. Chronic oxidative stress compromises telomere integrity and accelerates the onset of senescence in human endothelial cells. *J Cell Sci* **117:**2417-2426; 2004.
[225] Apolloni, S.; Parisi, C.; Pesaresi, M. G.; Rossi, S.; Carri, M. T.; Cozzolino, M.; Volonte, C.; D'Ambrosi, N. The NADPH oxidase pathway is dysregulated by the P2X7 receptor in the SOD1-G93A microglia model of amyotrophic lateral sclerosis. *J Immunol* **190:**5187-5195; 2013.
[226] Cassina, P.; Peluffo, H.; Pehar, M.; Martinez-Palma, L.; Ressia, A.; Beckman, J. S.; Estévez, A. G.; Barbeito, L. Peroxynitrite triggers a phenotypic transformation in spinal cord astrocytes that induces motor neuron apoptosis. *Journal of Neuroscience Research* **67:**21-29; 2002.

[227] Boland, M. L.; Chourasia, A. H.; Macleod, K. F. Mitochondrial dysfunction in cancer. *Front Oncol* **3:**292; 2013.
[228] Sivitz, W. a. Y., MA. Mitochondrial dysfunction in diabetes: from molecular mechnisms to functional significance and therapeutic opportunities. *Antioxid Redox Signal* **12:**537-577; 2010.
[229] Manfredi, G.; Xu, Z. Mitochondrial dysfunction and its role in motor neuron degeneration in ALS. *Mitochondrion* **5:**77-87; 2005.
[230] Shi, P.; Gal, J.; Kwinter, D. M.; Liu, X.; Zhu, H. Mitochondrial dysfunction in amyotrophic lateral sclerosis. *Biochim Biophys Acta* **1802:**45-51; 2010.
[231] Wang, X.; Wang, W.; Li, L.; Perry, G.; Lee, H. G.; Zhu, X. Oxidative stress and mitochondrial dysfunction in Alzheimer's disease. *Biochim Biophys Acta* **1842:**1240-1247; 2014.
[232] Exner, N., Lutz, AK, Haass, C, and Winklhofer, KF. Mitochondrial dysfunction in Parkinson's disease: molecular mechanisms and pathophysiological consequences. *EMBO J* **31:**3038-3062; 2012.
[233] Cocco, T.; Sgobbo, P.; Clemente, M.; Lopriore, B.; Grattagliano, I.; Di Paola, M.; Villani, G. Tissue-specific changes of mitochondrial functions in aged rats: effect of a long-term dietary treatment with N-acetylcysteine. *Free Radic Biol Med* **38:**796-805; 2005.
[234] Levy, E. J.; Anderson, M. E.; Meister, A. Transport of glutathione diethyl ester into human cells. *Proc Natl Acad Sci U S A* **90:**9171-9175; 1993.
[235] Meerwein, H.; Borner, P.; Fuchs, O.; Sasse, H. J.; Schrodt, H.; Spille, J. Reaktionen mit Alkylkationen. *Chem. Ber.* **89:**2060-2079; 1956.
[236] Raber, D. J.; Gariano, J., P.; Brod, A. O.; Gariano, A.; Guida, W. C.; Herbst, M. D. Esterification of carboxylic acids with trialkyloxonium salts. *J. Org. Chem.* **44:**1149-1154; 1979.
[237] Hamada, T.; Yonemitsu, O. Esterification of model peptides in aqueous solution. *Chem. Pharm. Bull.* **19:**1444-1449; 1971.
[238] Vogel, E. R.; Jackson, W.; Masterson, D. S. Efficient Esterification of Oxidized l-Glutathione and Other Small Peptides. *Molecules* **20:**10487-10495; 2015.
[239] MacMillan, D. S.; Murray, J.; Sneddon, H. F.; Jamieson, C.; Watson, A. J. B. Evaluation of alternative solvents in common amide coupling reactions: replacement of dichloromethane and N,N-dimethylformamide. *Green Chemistry* **15:**596; 2013.
[240] Asin-Cayuela, J.; Manas, A. R.; James, A. M.; Smith, R. A.; Murphy, M. P. Fine-tuning the hydrophobicity of a mitochondria-targeted antioxidant. *FEBS Lett* **571:**9-16; 2004.
[241] Alcalde, E.; Dinares, I.; Ibanez, A.; Mesquida, N. A simple halide-to-anion exchange method for heteroaromatic salts and ionic liquids. *Molecules* **17:**4007-4027; 2012.
[242] Beilby, P. R.; Thomas, N. O.; Hagen, T. M.; Beckman, J. S. Design and Synthesis of Mitochondrially-Targeted Glutathione. *In preparation*; 2017.

[243] Rossi, C.; Donati, A.; Ulgiati, S.; Sansoni, M. R. Dynamic behaviour of oxidized glutathione in solution investigated by nuclear magnetic resonance. *Can J Chem* **71:**506-511; 1993.
[244] Hatori, Y.; Yan, Y.; Schmidt, K.; Furukawa, E.; Hasan, N. M.; Yang, N.; Liu, C. N.; Sockanathan, S.; Lutsenko, S. Neuronal differentiation is associated with a redox-regulated increase of copper flow to the secretory pathway. *Nat Commun* **7:**10640; 2016.
[245] Aquilano, K.; Baldelli, S.; Ciriolo, M. R. Glutathione: new roles in redox signaling for an old antioxidant. *Front Pharmacol* **5:**196; 2014.
[246] Marzullo, G.; Friedhoff, A. J. An inhibitor of opiate receptor binding from human erythrocytes identified as a glutathione-copper complex. *Life Sci.* **21:**1559-1567; 1977.
[247] Karplus, P. A.; Pai, E. F.; Schulz, G. E. A crystallographic study of the glutathione binding site of glutathione reductase at o.3-nm resolution. *Eur J Biochem* **178:**693-703; 1989.
[248] Barbeito, L. H.; Pehar, M.; Cassina, P.; Vargas, M. R.; Peluffo, H.; Viera, L.; Estevez, A. G.; Beckman, J. S. A role for astrocytes in motor neuron loss in amyotrophic lateral sclerosis. *Brain Res Brain Res Rev* **47:**263-274; 2004.
[249] Lowry, K. S.; Murray, S. S.; McLean, C. A.; Talman, P.; Mathers, S.; Lopes, E. C.; Cheema, S. S. A potential role for the p75 low- affinity neurotrophin receptor in spinal motor neuron degeneration in murine and human amyotrophic lateral sclerosis. *Amyotroph Lateral Scler Other Motor Neuron Disord.* **2:**127-134; 2001.
[250] Lu, S. C. Glutathione synthesis. *Biochim Biophys Acta* **1830:**3143-3153; 2013.
[251] Yang, Y.; Dieter, M. Z.; Chen, Y.; Shertzer, H. G.; Nebert, D. W.; Dalton, T. P. Initial characterization of the glutamate-cysteine ligase modifier subunit Gclm(-/-) knockout mouse. Novel model system for a severely compromised oxidative stress response. *J Biol Chem* **277:**49446-49452; 2002.
[252] Beckman, J. S.; Beilby, P. R.; Hagen, T. M. Compounds for delivering glutathione to a target and methods of making and using the same. United States of America: Oregon State University; 2016.
[253] Ziegler, D. V.; Wiley, C. D.; Velarde, C. Mitochondrial effectors of cellular senescence: beyond the free radical theory of aging. *Aging Cell* **14:**1-7; 2014.
[254] Zheng, L.; Cardaci, S.; Jerby, L.; MacKenzie, E. D.; Sciacovelli, M.; Johnson, T. I.; Gaude, E.; King, A.; Leach, J. D.; Edrada-Ebel, R.; Hedley, A.; Morrice, N. A.; Kalna, G.; Blyth, K.; Ruppin, E.; Frezza, C.; Gottlieb, E. Fumarate induces redox-dependent senescence by modifying glutathione metabolism. *Nat Commun* **6:**6001; 2015.
[255] Volonte, D.; Liu, Z.; Musille, P. M.; Stoppani, E.; Wakabayashi, N.; Di, Y. P.; Lisanti, M. P.; Kensler, T. W.; CGalbiati, F. Inhibition of nuclear factor-erythroid 2–related factor (Nrf2) by caveolin-1 promotes stress- induced premature senescence. *Mol Biol Cell* **24:**1852-1862; 2013.

[256] Gao, F. H.; Liu, F.; Wei, W.; Liu, L. B.; Xu, M. H.; Guo, Z. Y.; Li, W.; Jiang, B.; Wu, Y. L. Oridonin induces apoptosis and senescence by increasing hydrogen peroxide and glutathione depletion in colorectal cancer cells. *Int J Mol Med* **29:**549-555; 2012.